DOCTORAL (Ph.D) DISSERTATION

ROJESH KHANGEMBAM

DEBRECEN

2023

UNIVERSITY OF DEBRECEN
DOCTORAL SCHOOL OF ANIMAL SCIENCE

Head of the Doctoral School:
Dr. István Komlósi, D.Sc.
professor

Supervisor:
Dr. Nóra Pálfyné Vass, DVM, Ph.D.
assistant professor

QUALITATIVE ASSESSMENT OF *Haemonchus contortus* INFECTION IN SMALL RUMINANT FLOCKS IN HUNGARY: PREVALENCE AND DIAGNOSTIC STUDY

Prepared by:
Rojesh Khangembam
Ph.D. candidate

DEBRECEN

2023

QUALITATIVE ASSESSMENT OF *Haemonchus contortus* INFECTION IN SMALL RUMINANT FLOCKS IN HUNGARY: PREVALENCE AND DIAGNOSTIC STUDY

Dissertation submitted in partial fulfilment of requirements of the doctoral (PhD) degree in Animal Husbandry

Written by: **Rojesh Khangembam**
certified Master of Veterinary Science (Vet. Parasitology)

Prepared in the framework of the Doctoral School of Animal Science, University of Debrecen
(Animal genetics – gene conservation, animal ecology Programme)

Dissertation Supervisor: **Dr. Nóra Pálfyné Vass,** DVM, Ph.D**.**

The official opponents of the dissertation:

	Name	Sc. Degree	Signature
	_____	_____	_____
	_____	_____	_____

The evaluation board:

	Name	Sc. Degree	Signature
Chairman:	_____	_____	_____
Member:	_____	_____	_____
Secretary:	_____	_____	_____

Date and venue of the dissertation defence:

Debrecen, 2023/……/……

Table of Contents

ABBREVIATIONS AND ACRONYMS

ATP	Adenosine Triphosphate
BIO	Biotin
BIP	Backward Inner Primer
BLAST	Basic Local Alignment Search Tool
BLP	Backward Loop Primer
COI	Cytochrome c Oxidase Subunit I
COWP	Copper Oxide Wire Particle
CRISPR-Cas	Clustered Regularly Interspaced Short Palindromic Repeats - CRISPR Associated (protein)
DNA	Deoxyribonucleic Acid
ddPCR	Digital Droplet PCR
dNTP	Deoxynucleoside Triphosphate
EPG	Eggs Per Gram
EtBr	Ethidium bromide
ETS	External Transcribed Spacers
FAMACHA	Faffa Malan Chart
FASTA	Fast Alignment
FEC	Faecal Egg Count
FECRT	Faecal Egg Count Reduction Test
FIP	Forward Inner Primer
FITC	Fluorescein Isothiocyanate
FLP	Forward Loop Primer
gDNA	Genomic DNA
GIN	Gastrointestinal Nematode
HNB	Hydroxy Naphthol Blue
IA	Isothermal Amplification
ITS	Internal Transcribed Spacers
IU	Internation Unit
L1,L2,L3,L4	1^{st} – 4th Larval stage
LAMP	Loop-mediated Isothermal Amplification
LF	Lateral Flow
LAMP-LF	LAMP- Lateral Flow

MEGA	Molecular Evolutionary Genetics Analysis
MUSCLE	Multiple Sequence Comparison by Log-expectation
NASBA	Nucleic Acid Sequence-based Amplification
Nad4	Nicotinamide Dehydrogenase subunit gene 4
NGS	Next-generation Sequencing
NTC	Non-Template Control
NTS	Non-transcribed Spacers
PBS	Phosphate-buffered Saline
PCR	Polymerase Chain Reaction
PCV	Packed Cell Volume
PNA	Peanut Agglutinin
POC	Point-of-care
qLAMP	Quantitative LAMP
qPCR	Quantitative PCR
RCA	Rolling Circle Amplification
RFLP-PCR	Restriction Fragment Length Polymorphism PCR
RNA	Ribonucleic Acid
RPA	Recombinase Polymerase Amplification
rRNA	ribosomal RNA
SARS-Cov-2	Severe acute respiratory syndrome coronavirus 2
SDA	Strand Displacement Amplification
SNP	Single Nucleotide Polymorphism
SSB	Single-strand DNA Binding protein
TT	Targeted Treatment
TST	Targeted Selective Treatment
UDG	Uracil-DNA Glycosylases
WAAVP	World Association for the Advancement of Veterinary Parasitology

bp	Base-pair
cm	Centimeter
g	Gram
fg	Femtogram
mg	Milligram

mm	Millimetre
mM	Micromolar
ml	Milliliter
µg	Microgram
µl	Microliter
µm	Micrometer

1. INTRODUCTION

Out of the many parasitic diseases plaguing sheep husbandry, haemonchosis is one of the most clinically as well as economically significant parasitic diseases (BESIER et al., 2016b; SHEN et al., 2017). It is caused by a gastrointestinal nematode (GIN) namely *Haemonchus contortus*, which is also commonly known as "Barber's Pole Worm". The classification of the parasite is as follows: Kingdom: Animalia; Phylum: Nematoda; Class: Secernentea; Order: Strongylida; Superfamily: Trichostrongyloidea; Family: Trichostrongylidae; Subfamily: Haemonchinae; Genus: *Haemonchus*; Species: *H. contortus* (ANGULO-CUBILLÁN et al., 2007; GOUŸ DE BELLOCQ et al., 2001; URQUHART et al., 1996).

The origin of *H. contortus* is considered to be from Africa and then evolved and later propagated elsewhere in the world due to the movement of the host animals and other human interventions. The problem of climate change, drug resistance and the fast adaptability of the parasite to environmental changes also greatly influenced the diversity and distribution of the parasite (ROSE et al., 2016; SALLÉ et al., 2019). Nowadays, the parasite occurs almost globally and its impact in the European region is also quite significant. There are reports of increasing incidences in the European continent as far as in the colder Scandinavian countries. This is thought to be due to hypobiosis, a phenomenon of reduced larval development to escape unfavourable environmental conditions, of the fourth stage (L4) larvae (O'CONNOR et al., 2006; BESIER et al., 2016b). Yet, there are only very few published reports on the occurrence of haemonchosis in the sheep farming sector in Hungary.

This abomasum residing worm is arguably considered the most pathogenic GIN species infecting small ruminants across the world due to its voracious blood-sucking nature and also its high fecundity. The parasite is notorious for causing severe anaemia owing to its blood-feeding behaviour ultimately killing heavily infected animals. Mortality is also common in young ones due to an underdeveloped immune system as well as in pregnant animals due to reduced immunity during pregnancy (VERÍSSIMO et al., 2012; BESIER et al., 2016b). The treatment and control of the disease incur huge economic losses to the farmers to the tune of about 436 million Australian Dollars (EMERY et al., 2016), 103 million USD and 46 million USD annually in India and South Africa.

To date, the most common control and treatment method for this parasite is based on anthelmintic drugs. Anthelminthic treatment can kill or get rid of those drug-

susceptible parasites while those whose genotype makes them resistant will survive the treatment. With the uncontrolled and rampant use of these drugs, drug resistance is also becoming a concern (PRICHARD, 2001) as there has been no newly developed class of drugs (since Monapantel) which has no resistance. Thus, for an effective control and treatment program, an accurate diagnosis is being sought, considering the occurrence of mixed infection at the field level. Yet, the accurate differential diagnosis of the parasite is difficult with the commonly employed laboratory microscopy techniques. Moreover, the molecular-based techniques are sophisticated, labour-consuming and not suitable for farm-site diagnosis. Hence, experts are now recommending treating only those animals that need it and leaving the healthier flocks untreated to minimise anthelmintic resistance. Thus, the importance of this parasite can be rightfully acknowledged with regular updates on this parasite, especially on its prevalence and specific diagnosis aspects as per its changing behaviours.

Aims of the study

Most of the diagnostic approaches in parasitology are still based on conventional faecal egg examination (FEC) and larval culture and morphological examination. Although there are advances in molecular-based techniques, they are still primarily based in high-end laboratories, time-consuming and often expensive (ZARLENGA et al., 2016). This is a hindrance to tackling the issue of increasing drug resistance as accurate diagnosis is being advised for sustainable control measures (NAEEM et al., 2021). Moreover, these are not benefitted in middle and low-income countries where farmers have little to no access to sophisticated laboratory-based diagnoses.

This gap in accurate diagnosis by the molecular technique can be filled to some extent with the introduction of isothermal amplification (IA) techniques. Among them, the most promising ones are the loop-mediated isothermal amplification (LAMP) and recombinase polymerase amplification (RPA) techniques. There are already available reports of these techniques adopted for the detection of major diseases of plants, humans and animals (OLIVEIRA et al., 2021), either at the research or commercial level. This is also demonstrated in the increase of such isothermal amplification-based test kits for the covid-19 diagnosis. Yet, most of the point-of-care (POC)/farm-site friendly diagnostics being developed for parasitic diseases are mainly concentrated in the area of parasitoses of humans. Keeping in view the importance of *H. contortus* in terms of its diagnosis and the very limited data on its prevalence in Hungary, this study has adopted to pursue the following aims:

- Screening of small ruminant farms in and around Eastern and Central Hungary for *H. contortus* parasitism by using faecal egg examination techniques
- Proof of concept development of qualitative LAMP technique for *H. contortus* diagnosis
- Proof of concept development of qualitative and farm-site friendly LAMP-LF technique for *H. contortus* diagnosis
- Proof of concept development of a qualitative and farm-site-friendly RPA technique for *H. contortus* diagnosis

2. LITERATURE REVIEW

2.1. General morphology of adult worms

H. contortus is a unisexual nematode. The adults are easily obtained at post-mortem examination because of their predilection site in the abomasum. Freshly collected specimens of adult females are usually red-white striped colouration due to the winding of ovaries and uteri around the blood-filled intestines. Whereas, freshly collected males are usually uniformly red or reddish-brown. Adult females are usually 2–3 cm in length while the males are 1-2 cm (LOVE and HUTCHINSON, 2003; GAREH et al., 2021). The outer covering of this parasitic worm is called the 'Cuticle', which usually presents longitudinal striations known as 'Synlophe'. At its anterior end, the adult worm has a poorly developed oral cavity with a lancet (or tooth) on the dorsal side and also the parasite bears a pair of spinous cuticular expansions known as 'Cervical papilla'. At its posterior end, the cuticle of the males is flattened and modified into a copulatory organ called the 'Copulatory bursa'. Another structure that helps in identification is the 'Spicules', which are chitinous spine-like projections near the bursa. In *H. contortus* males, the spicules are barbed at the tip. The female usually has a tongue-shaped 'Vulval flap', which is a typical modification of its cuticle. It opens to the vulva, which is located in the posterior third of the body. These features in each of the sexes are key points in the identification of the parasite. The eggs can be visualized under a microscope as non-operculated oval-shaped with a chitinous shell having dark brown blastomeres with an average length of 70 ± 10 μm and width of 45 ± 5 μm (SOULSBY, 1968; TAYLOR et al., 2015; LJUNGSTRÖM et al., 2018; BOWMAN, 2020; GAREH et al., 2021).

2.2. Life-cycle

The life cycle of this parasite is depicted in Figure 1**.** This blood-feeding parasitic nematode matures and reproduces in the abomasum, the main predilection organ, where it feeds on the host's blood. Adults mate and produce eggs that are voided in faeces. Usually, the egg output is very high (5,000 – 15,000 eggs/day) and so there is always a risk of severe contamination of pastures. The pre-patency period is about 2-3 weeks (EMERY et al., 2016; FÁVERO et al., 2016). In favourable environmental conditions, the eggs hatch in 1-2 days and develop into the first (L1) and second (L2) larval stages in the faeces (CLARK et al., 1962; TAYLOR et al., 2015; EMERY et al., 2016). These larval stages feed only on bacteria in the faeces and are considered free-living stages. The L2 then moults to the third larval stage (L3) and comes out from the faecal pads

(ROEBER et al., 2013). The L3 is protected by a sheath to prevent itself from desiccation and so they are non-feeding and they crawl up the grass blades to be ingested by grazing animals. After ingestion, the L3 lose the protective cuticle in the rumen of the host animal and migrates to the abomasum and moults to the fourth (L4) and even up to the fifth (L5) larval stages. The exsheathment is influenced by rumen pH and also by carbon-dioxide concentration and it is an important step in the transformation from the free-living phase to the parasitic phase in its life cycle (HERTZBERG et al., 2002). Finally, it matures into adult worms by sucking blood in the abomasum and starts shedding eggs (ROEBER et al., 2013).

It is to be noted that under unfavourable environmental conditions, there is a pause in the development of the L4 stage to the adults inside the hosts. This occurs as a mechanism for the parasite to survive harsh conditions. This phenomenon is known as "hypobiosis". This was earlier described to be mainly due to the immunity of the host, but further research has proven that environmental factors play a huge part. Hypobiosis is found to occur both in temperate and tropical climates, in the winter and dry seasons, respectively. The arrested larva continues to develop into an adult once the environmental conditions are favourable (BLITZ and GIBBS., 1972; FAKAE, 1990; GATONGI et al., 1998; FALZON et al., 2014).

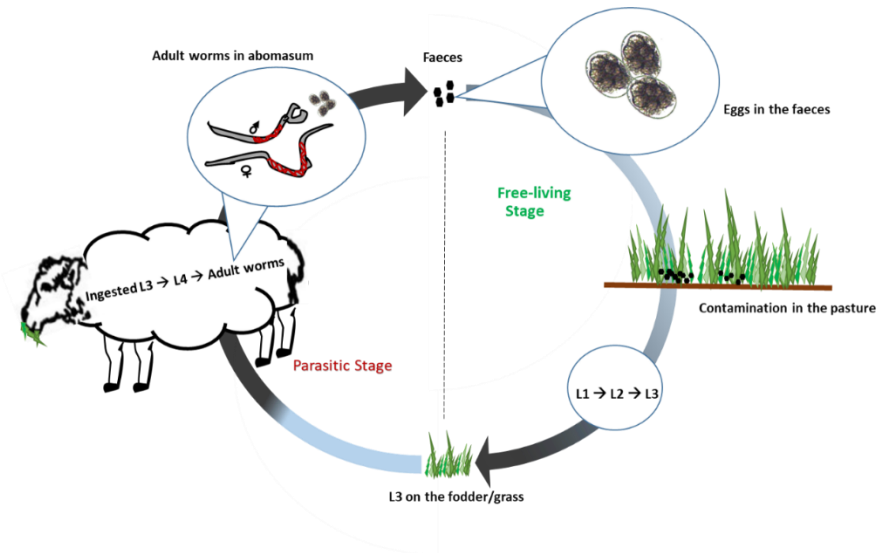

Figure 1: Schematic life-cycle of *H. contortus*. Adult worms reside in the abomasum and start laying eggs which are voided in the faeces of the host animal. The eggs contaminate the pastures. Free-living stages are L1 to L3, where L3 crawls up the grass blades. Grazing animals consume them and the cycle is completed. L1-L4: 1st to 4th larval stages.

2.3. Pathogenesis and Clinical Signs

The pathophysiology of haemonchosis and its clinical signs are mainly linked to the anaemia that develops as a consequence of the blood-feeding nature of the parasite. Both the adult and from the L4 stages onwards, the parasite sucks blood and can leave haemorrhagic wounds in the abomasum (SOULSBY, 1968; BESIER et al., 2016b). Anaemic conditions can be detectable by 10-12 days post-infection. Individual adult worms can remove up to 30-50 µl of blood per day (DARGIE and ALLONBY, 1975; BESIER et al., 2016b). In severe cases, a sheep parasitised by up to 5000 *H. contortus* may lose 250 ml of blood daily and this obviously proves fatal. The severity of disease in the host is closely related to the number of *H. contortus*, as evidence has shown a significant correlation between blood loss and the number of adult worms (LE JAMBRE, 1995). Diarrhoea is not commonly observed in haemonchosis and faeces are usually less and dark-coloured due to blood in it. If there is concurrent infection with other GIN, bloody diarrhoea may be observed (TAYLOR et al., 2015). Although not a pathognomonic symptom of this disease, a commonly observed symptom is the "bottle-jaw" (Figure 2) condition which is due to oedema in the inter-mandibular space as a result of hypoproteinaemia. Recent research findings have also shown that the immunity level and nutritional status of the host are also equally important in the establishment of the infection (NNADI et al., 2009; SACCAREAU et al., 2017; NAEEM et al., 2021). Haemonchosis can be categorised into three forms: hyperacute, acute and chronic and these are briefly discussed below. Figure 2 shows the main clinically observable signs and symptoms of the disease.

Figure 2: Clinical signs of haemonchosis showing 'bottle-jaw' condition, pale mucous membrane and weakness. Adapted from GAREH et al., (2021)

Hyperacute haemonchosis is uncommon comparatively and this form is mainly observed when highly susceptible animals are exposed to a sudden massive infection of up to 30,000 parasites at a time, especially in young animals. This can lead to massive haemorrhagic gastritis/abomasitis leading to severe anaemia and ultimately death within a few days. Although not fully understood, the pathogenesis of sudden death observed in this form of haemonchosis is considered mainly due to hypovolemic shock (ARSENOPOULOS et al., 2021; FLAY et al., 2022). The affected animal usually has very reduced erythropoiesis and may even die before compensatory erythropoiesis sets in. Those animals that survive are usually severely anaemic (SOULSBY, 1968; ROEBER et al., 2013; BESIER et al., 2016b).

Acute-haemonchosis is mainly observed when young and susceptible animals become infected over time, usually harbouring about 2000-20,000 larvae per individual animal (SOULSBY, 1968; FLAY et al., 2022). The degree of anaemia can be described in three stages (DARGIE and ALLONBY, 1975). First-stage anaemia becomes apparent about 2-6 weeks after infection and is characterised by a progressive decrease in the packed red cell volume (PCV). If the affected animal survives, the haematocrit usually becomes stable at a low level but at the cost of a 2-fold to a 3-fold compensatory expansion of erythropoiesis (second-stage anaemia). However, due to the persistent loss of iron and protein into the gastrointestinal tract and increasing inappetence, the bone

marrow subsequently becomes fatigued and the PCV value diminishes further eventually causing death (third-stage anaemia).

Chronic haemonchosis is caused by a smaller but persistent *H. contortus* burden (100-1000 parasites per animal). Anaemia and hypoproteinaemia may or may not be seen. Affected animals are greatly malnourished and emaciated. Owing to these poor body conditions, the production capacity of these animals is reduced. The chronic form of haemonchosis may also occur in seasonally endemic regions as well as when outbreaks are common but half-effective control and treatment measures prevent the emergence of acute haemonchosis.

The clinical signs and symptoms are briefly described in Table 1. The clinical manifestation of *H. contortus* can occur in both adults and young sheep. When lactating sheep are affected, there can be a marked reduction in milk production. This in turn leads to lamb deaths and poor growth rates. Pasture contamination by the grazing-affected sheep, mainly those with chronic haemonchosis, can further perpetuate the disease.

Table 1: Summary of clinical signs and symptoms of haemonchosis

Forms	**Parasite burden per animal**	**Clinical Signs and Symptoms**	**Remarks**
Hyper-acute haemonchosis	● 30,000 or more	● Sudden death ● Very lethargic; may even collapse while grazing ● 'Bottle-jaw' condition; (rare) ● Melaena	● Sudden death is most commonly observed
Acute haemonchosis	● 2000-20,000	● 'Bottle-jaw' condition is very common ● Persistent anaemia ● Very pale mucous membrane	● Post-mortem findings include watery blood, ascites
Chronic haemonchosis	● 100-1000	● Malnourished ● Low body condition score ● Reduction in meat, milk, and wool production	● 100% morbidity but very low mortality

2.4. Treatment and Control

The use of anthelmintic drugs is the most commonly employed method of control of GIN parasites. Although there are few vaccines (NEWTON and MEEUSEN, 2003) against some major classes of parasites, these are at the moment confined to only certain geographical regions of the globe. Moreover, biological controls and other plant derivatives remain largely at the research level, expensive for large-scale implementation and/or require detailed planning (DE CLERCQ et al., 2011; STENBERG et al., 2021). Thus, at the moment, regular deworming and other chemotherapeutics are the major preventive and therapeutic measures adopted worldwide. Yet, indiscriminate use of these drugs has led to another problem in the form of 'anthelmintic resistance'. This evolution of drug-resistant strains and problems related to drug residues in animal products and by-products have immensely put pressure on this method (GETACHEW et al., 2007). One common practice in this anthelmintic treatment is periodical deworming of all the animals on the farm with anthelmintics. This is often costly, offers minimum capacity in the development of immune response in the growing animals, and also increases the risk of parasite's resistance to the administered drugs.

Keeping in view the ever-rising drug resistance problem, consumers as well as some livestock farmers are encouraging a "green ruminant production system" (WALLER and THAMSBORG, 2004) that could lead to a more organic and less chemical dependant system of livestock farming. Experts and veterinarians are now more focused on treating only those animals that are heavily affected and pose a threat to the susceptible 'refugia' population of the parasites (KENYON et al., 2009; KEARNEY et al., 2016). Unfortunately**,** there is already an alarming increase in the reports of *H. contortus* showing resistance to almost all classes of anthelmintic drugs individually or as multi-drug resistance (KOTZE et al., 2012; ROSE VINEER et al., 2020; ARSENOPOULOS et al., 2021; ANTONOPOULOS et al., 2022). To mitigate this problem, two alternate approaches are being proposed: i) the targeted treatment (TT) method where a targeted group is dosed with anthelmintics and others are allowed to graze on infected pastures; ii) targeted selective treatment (TST) in which only selected animals are treated leaving others as presumably being healthy or harbouring less resistant worms (NAEEM et al., 2021).

These targeted strategies are based on clinical signs and symptoms of haemonchosis and the estimated worm burdens (KEARNEY et al., 2016). One of the most popular methods for gauging the intensity of the infection is using the FAMACHA (abbreviated

as Faffa Malan Chart). This method is based on the idea that the degree of conjunctival mucous membrane paleness can be used to score the degree of anaemia caused by haemonchosis (VAN WYK et al., 2006; BESIER et al., 2016a; ARSENOPOULOS et al., 2021). The colourimetric evaluation of the mucous membrane is done by using a colour chart score, where it ranges from 1= normal to 5 = severe anaemia (as shown in Figure 3). Only animals showing a score of 3 or higher are selectively dewormed. By following this simple, farm-site-friendly anaemia assessment tool, treatment is done strategically and hence, contributes to slowing down the rate of drug resistance (KEARNEY et al., 2016). Figure 3 shows the scoring of anaemia using a FAMACHA card and the commonly used anthelmintics are listed in Table 2.

Figure 3: Application of FAMACHA card to assess the anaemia. (Source:https://events.udel.edu/event/online_famacha_certification_for_sheep_and_goat_producers#.Y9bOCnbMKMo . Dated 01-29-2023)

Table 2: Common anthelmintic drugs

Drug Class	Drug Example	Remarks
Avermectin	Ivermectin, Moxidectin	Broad spectrum
Amino-acetonitrile	Monepantel	Newest class
Benzimidazoles	Albendazole, Fenbendazole,	Broad spectrum
Imidazothiazoles	Levamisole	Can be used for prophylaxis also
Salicylanilides	Closantel	Narrow spectrum

Given the rising anthelmintic resistance, other non-anthelmintic control measures are being advised nowadays. This usually involves an integrated control mechanism in terms of breeding and selection programmes; feeding and nutrition management; pasture management and vaccination programmes (BESIER et al., 2016a; KEARNEY et al., 2016; NAEEM et al., 2021). Yet, each of these also has its fallacy. For instance, breeding programs are usually laborious and a long-term strategy (BENAVIDES et al., 2015; NAEEM et al., 2021) and the only effective vaccine against *H. contortus* is commercially available only in Australia and South Africa (marketed as Barbervax and Wirevax, respectively) and requires an intensive vaccination schedule (BASSETTO and AMARANTE, 2015; BESIER et al., 2016a; TEIXEIRA et al., 2019). Biological controls using certain species of nematophagous fungi like *Duddingtonia flagrans*, rotational grazing, nutritional supplementation in the form of copper oxide wire particle (COWP) and many other plant extracts (tannin in particular) are all proven effective in many studies (BURKE and MILLER, 2006; KEARNEY et al., 2016; LIU et al., 2020; ARSENOPOULOS et al., 2021) although the questions remain about the integrity of these methods at widescale farming scenarios. Thus, more research on its adaptability and application protocols needs to be done.

2.5. Genetic diversity and genome of *H. contortus*

H. contortus is now globally recognised as a nematode parasite of veterinary importance, especially in the small ruminant industry. Its origin is considered to be from sub-Saharan wild ungulates (GILLEARD and REDMAN, 2016; HOBERG and ZARLENGA, 2016) and gradually spread out globally due to human intervention and climatic change (SALLÉ et al., 2019). Several factors are responsible for the diversity of the genetic structure of *Haemonchus* populations. These include drug resistance selection pressure, geographical limitations, population sizes, host movement and host species

(LAING et al., 2013; GILLEARD and REDMAN, 2016; PITAKSAKULRAT et al., 2021) A detailed analysis of the origin and diversification of the parasite by HOBERG and ZARLENGA (2016) asserted the complexity of the history of *H. contortus.* Although recognised globally as a dominant nematode pathogen of domestic small ruminants, the origin of this parasite species is linked to a congregation of antelopes in Africa during the late Tertiary period. Eventually, the cosmopolitan distribution happened due to recurrent anthropogenic invasion, the establishment of trade routes for domestic ruminants and thus, gradually leading to the development of complex assorted worm populations (HOBERG et al., 2004; HOBERG and ZARLENGA, 2016; SALLÉ et al., 2019). Human factors contributing to this are mainly colonisation and migration, and also to some extent the increase in sheep domestication.

The parasite started to spread out from the original population to West Africa, the Mediterranean, and South West Asia. Isolates sampled from Brazil were reported to have been derived from West African isolates spread to the Americas, presumably due to the transatlantic slave trade (SALLÉ et al., 2019). Caribbean isolates (SPANGLER et al., 2017) were most likely due to the Spanish colonisation, giving a West African and a Mediterranean lineage. Similarly, the Australian isolates showed a Mediterranean lineage while the Greek isolate was more closely related to that of the Australian isolate and not that of any European isolate (GILLEARD and REDMAN, 2016; SALLÉ et al., 2019). When it comes to regional diversity within countries, *H. contortus* has a lower yet detectable diversity. For instance, the parasite populations from southern India, Thailand and Tunisia (AKKARI et al., 2013; CHAUDHRY et al., 2015; PITAKSAKULRAT et al., 2021) are reportedly more closely related to each other than that in the United Kingdom. This could be explained by the overwintering and hypobiotic nature of the parasite inside the host. This stage in the life cycle creates a "population bottleneck" in the parasite especially when the affected host is dewormed regularly and the pasture larval population is also low (GILLEARD and REDMAN, 2016).

H. contortus has both parasitic and free-living phases during its life cycle (Figure 1), and these stages are affected by various environmental influences (GILLEARD and REDMAN, 2016). The free-living stages can be exposed to a wide range of temperature and moisture conditions, depending on the geographical location and season. Contrastingly, the host environment is more stable and can shelter them effectively from the harsh environment. This ability to survive inside the host during unfavourable environmental conditions has allowed this parasite species to spread and

thrive even in much colder regions than its origin climate of sub-Saharan Africa (BESIER et al., 2016b; GILLEARD and REDMAN, 2016). It has been reported in recent studies on its genome (LAING et al., 2013; DOYLE et al., 2020) that there are distinct groups of genes expressed in each specific life cycle phase and another category of sex-linked and differentially expressed gene clusters in the adult stage. For instance, during development from egg to early larval stages, genes involved in larval morphogenesis, motor ability function and other related enzymatic functions are up-regulated. Similarly in adult stages, the sex-linked gene clusters in adult males are responsible for spermatogenesis while in adult females, these clusters are related to oocyte formation, meiosis and vulval development (LAING et al., 2013).

Whole genome sequencing of various laboratory strains has reported levels of genome-wide variation present in this nematode parasite. DOYLE et al. (2020) have reported a highly contiguous 283.4 Mbp genome assembly for the MHco3(ISE).N1 laboratory isolates at chromosome scale. LAING et al. (2013) published the first genome of the parasite, reporting a final draft assembly consisting of 67,687 contigs linked into 26,044 scaffolds of a total length of 370 Mb. Later on, SCHWARZ et al., (2013) reported a study of a draft genome of the parasite that is 320 Mb in size and encoded 23,610 protein-coding genes. Both of these genome sequencing studies have found a significantly high level of sequence polymorphism in the raw sequence reads used to derive the consensus reference genome sequences (GILLEARD and REDMAN, 2016). *H. contortus* has also been found to have high levels of genetic diversity within populations. Certain studies using microsatellite markers have proved this (REDMAN et al., 2008; GILLEARD and REDMAN, 2016). SALLÉ et al. (2019) have also reported some degree of single nucleotide polymorphism (SNP) with estimates derived from whole genome sequencing of nineteen global isolates spanning five continents relative to the reference MHco3(ISE) isolate. As discussed earlier, *H. contortus* is a unisexual nematode and a single female can mate with multiple males. This mating behaviour gives a higher level of genetic variation to those offspring produced by a single female mating with multiple males comparatively to that of a single pair mating (REDMAN et al., 2008). In summary, it can be concluded that high levels of genetic variation can exist in both inter and intra-isolates.

2.6. Epidemiology

As described above, *H. contortus* evolved to spread globally through the movement of host animals naturally and through anthropogenic involvement. Although haemonchosis was more commonly seen in known high-risk areas with hot and humid conditions, climate change and the rise in global temperatures have increasingly allowed the parasite to survive and even flourish in previously low-risk zones and more intensive distribution in small ruminants (ROSE et al., 2016; F. YIN et al., 2016). Keeping in the scope of this study, a brief discussion of haemonchosis in the world in general and Europe is presented below.

2.6.1 *Global*

Although the parasite occurrence is now worldwide, the epidemiology of the parasite can be discussed under tropical-subtropical and temperate regions as these two regions are relatively more important (TAYLOR et al., 2015).

The tropical and sub-tropical region encompasses the climatic regions of Africa, South America, the Caribbean, the Pacific tropical islands, Southern and South-East Asia, the Southern USA and Northern Australia (ARSENOPOULOS et al., 2021). Haemonchosis is mainly a disease of sheep in warm climates. This is explained due to the fact that larval development of the parasite occurs optimally at relatively warmer temperatures. Also, contrary to other helminth infections, there is little evidence that sheep in endemic areas develop an effective acquired immunity to the parasite. This results in the continuous contamination of the pasture and a source of infection. Yet, it should be noted that the frequency and the severity of the disease could also largely be dependent on the rainfall conditions of the area as humidity plays an important role in the microclimate of the faeces and herbage. For instance, in Cameroon, Ethiopia and Ghana where annual dry seasons occur, L3 larvae reach peak numbers seasonally, depending on rainfall/humidity conditions (NDAMUKONG and NGONE, 1996; SISSAY et al., 2007; BLACKIE, 2014; ARSENOPOULOS et al., 2021). The survival of the parasite is also associated with the ability of the larvae to undergo hypobiosis. Evidence of this had been reported from certain tropical and subtropical regions in Australia, Brazil, the Middle East and Nigeria. Despite the initiation of this phenomenon still unclear, hypobiosis occurs at the start of an extended dry season and helps the parasite to survive in the host as arrested L4. The resumption of development occurs just before the beginning of seasonal rains. However, in areas of endemic haemonchosis after the advent of a period of heavy rain, the FEC of infected sheep could be observed to drop sharply, even up to near zero levels.

This is due to the expulsion of the majority of the adult worm burden. This phenomenon is commonly termed “Self-cure”. This is considered to be the consequence of an immediate-type hypersensitivity reaction to the parasitic antigens derived from the developing larvae. Self-cure was observed to happen to those animals which have experienced a suitable amount of larva exposure at definite intervals than those which carry an initial infection. Also, a transient increase in blood histamine level and intense mucosal oedema of the abomasum could be observed (SOULSBY, 1968; TAYLOR et al., 2015).

The temperate regions can be subdivided into cool temperate regions and warm temperate regions. Cool-cold temperate regions include areas in northern Europe, the Scandinavian countries, the United Kingdom, Canada and some parts of Northern USA, south-east Australia and New Zealand (TAYLOR et al., 2015; ARSENOPOULOS et al., 2021). The mechanism of infection and other ecological parameters is quite different from that of the tropical and subtropical regions. The most common is the single annual cycle in the propagation of the larvae. Infective larvae usually develop from eggs shed by ewes in the spring, which contaminate the grazing lands. These larvae are ingested by ewes and lambs in early summer. Yet, the majority of them become arrested in the abomasum hypobiotic larvae until the following spring. During the period of maturation of these hypobiotic larvae, clinical signs of acute haemonchosis may occur and in the ewe, this often coincides with lambing (TAYLOR et al., 2015). In the warm temperate regions, depending on the rainfall and humidity, haemonchosis is a significant threat during the warmer months while in those areas with mild temperatures during winter, haemonchosis outbreaks can be seasonal. In warm temperate and summer rainfall regions, hypobiosis is predominant only during the cold winter season. Contrary to this, the risk of haemonchosis is considerably lower in colder temperate regions. This is because the low temperature that limits larval development until warmer favourable conditions set in (TAYLOR et al., 2015). Keeping in the scope of this study, a brief discussion of haemonchosis in Europe in general and Hungary, in particular, is presented below.

2.6.2 *Europe*

Despite strong evidence that the parasite favours strongly with tropical climates and its spatial distribution is influenced greatly by climatic limitations (KAO et al., 2000; RINALDI et al., 2015; ROSE et al., 2016), the parasitic range of occurrence for *H. contortus* has recently expanded in Europe too. Considerable cases have already been reported and are also increasing in countries such as Ireland, and Scotland and even

reaching up to colder countries like Sweden and Norway (HÖGLUND et al., 2009; KENYON et al., 2009; BURGESS et al., 2012; DOMKE et al., 2013; RINALDI et al., 2015). With the advent of more sophisticated molecular techniques like next-generation sequencing (NGS), digital droplet PCR (ddPCR), pyrosequencing etc, many reports on the parasite occurrence along with resistance to the commonly used drugs are increasing. For instance, there are already reports of the occurrence of haemonchosis along with resistance to common anthelmintics in Austria (UNTERSWEG et al., 2021), the Czech Republic (VADLEJCH et al., 2021), Denmark (PENA-ESPINOZA et al., 2014), France (CAZAJOUS et al., 2018; BORDES et al., 2020), Ireland, Italy, Switzerland (RAMÜNKE et al., 2016), Poland (KOWAL et al., 2016; MICKIEWICZ et al., 2020), Slovakia (BABJÁK et al., 2017) and Sweden (BALTRUŠIS et al., 2020). This points to the fact that the parasite has gradually taken root in the continent and it would not be over speculation to say more reports on the prevalence, as well as the resistance to the drugs, will keep on increasing. Yet, there are very few published reports and studies of haemonchosis in Hungary. This should not be taken lightly considering the geographical context of the country as well as the livestock movement among its neighbouring countries, many of which have already established *H. contortus* epidemiology. At the time of writing this, the most recent report available stated the detection of the parasite in some farms in and around eastern Hungary (KHANGEMBAM et al., 2021). Other available reports on the parasite in the country presented evidence of benzimidazole resistance in red deer farms and a few neighbouring sheep farms (NAGY et al., 2016, 2017; CSIVINCSIK et al., 2017). Apart from these, the only other report is an early study conducted to research the haematological parameters of Merino sheep experimentally infected by the parasite (KASSAI et al., 1990).

2.7. Diagnosis

The diagnosis of *H. contortus* infection can be done through various means. Depending on the circumstances and the availability of equipment and expertise, the means of diagnosis can be post-mortem examination; clinical signs and haematological evidence; morphological identification of the parasite and its egg; and molecular techniques (D. ZARLENGA et al., 2016; NAEEM et al., 2021). To be able to shift to a more targeted and effective treatment and control regime, accurate diagnosis is highly indispensable. Keeping in the context of the dissertation, some of these techniques are briefly discussed in the following paragraphs.

2.7.1 *Conventional Diagnosis*

Conventional diagnosis usually relies on observation of signs and symptoms of suspected animals, post-mortem examination if a carcass is available and to some extent laboratory examination of parasites and eggs.

2.7.1.1 *Post-mortem*

This method is best done if cadavers are of animals that died due to suspected acute or hyperacute haemonchosis. This method can provide rapid confirmation if the cadavers are examined promptly. Upon dissection of the abomasum, the main predilection site, numerous worms could be visibly attached to the abomasal mucosa. As discussed earlier, the female worms have the typical "barber's pole" appearance (Appendix Figure 1-A) in fresh specimens (BESIER et al., 2016a) and this feature can aid in the identification of the worms (Appendix Figure 1-A). The abomasum mucosa can be oedematous with pin-point haemorrhage and even bleeding. In acute haemonchosis, the worm burden could range from 2000-20,000 while in hyperacute cases can record more than 30,000 (BESIER et al., 2016b). Other secondary findings are closely related to anaemic symptoms such as pale mucous membrane, bottle-jaw condition and watery blood clots in the abomasum. It should be noted that post-mortem findings should be associated with history and clinical symptoms with credible suspicion of the disease in the flock too as this method is not indicative in chronic cases, which generally give low worm burden (ARSENOPOULOS et al., 2021).

2.7.1.2 *Clinical signs, haematological changes and FAMACHA system*

The clinical signs and symptoms (Table 1) of this disease are mainly due to the blood-feeding behaviour of both the adult and L4 stage larvae. The main manifestation of this includes anaemia, lethargy and exercise intolerance in varying degrees, oedema and even sudden death (BESIER et al., 2016a; BOWMAN, 2020). The degree of anaemia depends on the worm burden and the subsequent immunity of the host animal.

In hyperacute haemonchosis, apparently healthy sheep could die suddenly. Infected sheep, which could harbour up to 30,000 worms, could lose blood at the rate of 500-600ml per day. This amounts to a loss of haemoglobin equivalent at the rate of 18–54g/day (JACKSON and COCKCROFT, 2002; TAYLOR et al., 2015; FLAY et al., 2022).

In the case of acute haemonchosis, young and immune-compromised animals are usually the victim. The anaemia develops rapidly and this is often accompanied by the characteristic "bottle jaw" appearance due to submandibular oedema. This is the result of

hypoproteinaemia, mainly albumin, which is due to many mechanisms including the blood-sucking activity of the parasite, leakage of protein in the abomasal lumen as well as a reduction in protein absorption. This eventually creates an imbalance in the osmotic pressure and fluids leak out of the vascular space, thus causing oedema (SIMPSON, 2000; BOWMAN, 2020; FLAY et al., 2022). Nevertheless, some animal can die before the onset of oedema (BESIER et al., 2016a) or some can even recover up to some extent when the compensatory erythropoiesis mechanism give some relief in conjunction with timely treatment (DARGIE and ALLONBY, 1975; TAYLOR et al., 2015).

Chronic cases of haemonchosis manifest as victims of malnourishment. There is a significant loss in milk, meat and wool yield (BARGER and COX, 1984; ARSENOPOULOS et al., 2021). Besides these, many studies on pregnant animals, as well as the young ones of small ruminants (COBON and O'SULLIVAN, 1992; HOWLADER et al., 1997; GITHIGIA et al., 2001; COPEMAN, 2006), have found the debilitating effect of the disease in terms of reduction in average weight gains, lactation and overall body condition scores.

2.7.1.3 *Microscopy and morphological examination of parasite eggs*

The simplest and most commonly used method to detect gastrointestinal parasites, including the trichostrongyle, is the microscopic examination and identification of parasite eggs voided in faecal samples (RINALDI et al., 2022) and it is termed "copro-microscopy". The clinical diagnosis of GIN parasites in small ruminants as well as even in humans still relies on this as a routine laboratory procedure (COLES et al., 1992; NDAO, 2009). Although it has been more than a century (NIELSEN, 2021) since the basic principle of this was laid down by C.J. Devaine, the technique still proves to be an important tool despite its limitations. Also, many improvements, derivations and even automation of this technique and FEC has been happening over the years. Copromicroscopic examination can give qualitative information (as positive or negative for parasite presence). It can also give quantitative information through the faecal egg count reduction test (FECRT) that can make useful decisions for deworming the flock as well as the efficacy of the anthelmintic in use.

Almost all the conventional FEC examination techniques adopt a counting chamber, a suitable floatation medium and a microscope. A classic technique using an egg-counting chamber is the McMaster method (GORDON and WHITLOCK, 1939) which is widely regarded as an industry standard even to this day (COLES et al., 1992; PARAS et al., 2018; NIELSEN, 2021). The McMaster technique utilises a special glass

slide, having two “counting chambers”. Each of these chambers has a 10mm x 10mm grid etched permanently on the top cover. In principle, each counting chamber can accommodate a fixed volume of faecal suspension (0.15ml x 2 chambers) to be examined microscopically. When a known weight of faeces (usually 4g) and a known volume of a suitable flotation liquid medium (usually 56ml) are used to prepare the suspension, then the number of eggs per gram (EPG) of faeces. The final FEC is then obtained by multiplying the EPG with a factor of 50 (*McMaster Egg Counting Technique: Principle*, n.d.; Coles et al., 1992). Modified versions may include filtration of the faecal suspension and centrifugation to improve egg yield in it. Subsequently, many other techniques based on this principle have been developed with modifications unique to their own including the automated and semi-automated capability of the egg count and identification. Some of these newer techniques are FECPAK (PRESLAND et al., 2005), FECPAK^{G2} device (BOELOW et al., 2022; FRANCIS and ŠLAPETA, 2022), FLOTAC® and its successor Mini-FLOTAC® (CRINGOLI et al., 2017), Kubic FLOTAC® (CRINGOLI et al., 2021), out of which FECPAK and Kubic-FLOTAC microscopy are semi-automated. Besides these, there are also paid services available for artificial intelligence-based computerised detection and counting of the eggs via digital analysis of images (ELGHRYANI et al., 2020; NAGAMORI et al., 2021; SLUSAREWICZ et al., 2021) that are uploaded to their systems (NIELSEN, 2021) and a few of these services are Parasight (Parasight Sytem Inc, USA), Telenostic (Telenostic Ltd, Ireland), VETSCAN IMAGYST (Zoetis, USA). Keeping in context with my work, the mechanism of only the Mini-FLOTAC® is being discussed below.

The Mini-FLOTAC® system (CRINGOLI et al., 2017) is an improved version and the successor of the FLOTAC® (CRINGOLI et al., 2010) protocol. It consists of the base and reading disk, an accessory key and a microscope adaptor (Figure 4). The reading disk has two 1ml flotation chambers with etched grids for egg counting (Figure 4 D - F). The floatation medium (concentrated sodium chloride solution in this study) is filled in the Fill-FLOTAC® (Figure 4 A-B), which is a plastic device that can be used to homogenise, sieve and pour the faecal sample solution in the flotation chambers. The sieve is attached underneath the lid while a conical tube is attached over it that can accommodate up to 5g of faeces sample (Figure 4 – C). After charging the facial solution to the reading disk (Figure 4 E), the eggs inside the counting chambers are allowed to float for about 10mins (Figure 4 F), and they are counted under a microscope.

Results are obtained by multiplying the egg counts with a factor of 5 (for livestock) and expressed as eggs per gram (EPG) of faeces. The analytical sensitivity of this technique is reported to be 5 EPG sensitivity (CRINGOLI et al., 2017). This Mini-FLOTAC® offers certain advantages considering that the whole protocol does not involve a centrifugation step, both fresh and fixed faecal samples (pooled or individual) can be used and takes about 10–12 min of preparation before microscopy examination (BARDA et al., 2013; KENYON et al., 2016; RINALDI et al., 2019). Moreover, the technique can also be performed at the farm site itself using a portable microscope (CRINGOLI et al., 2017) and thus, it is also suitable for a point of care (POC) examination.

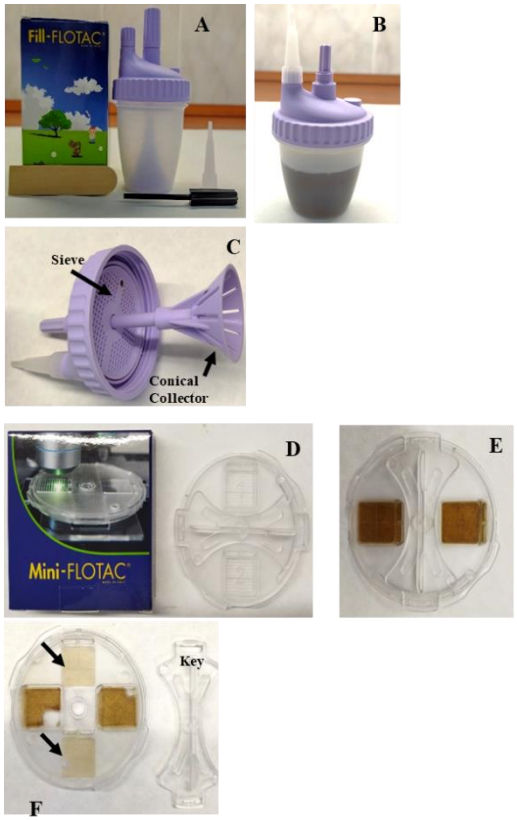

Figure 4: The Mini-FLOTAC system. A: The Fill-FLOTAC along with a wooden spatula, charging tube and dissembling rod; B: Fill-FLOTAC with a faecal suspension; C: Parts of the lid/cap of Fill-FLOTAC; D: Mini-FLOTAC before the suspension is charged into its counting chamber; E: Mini-FLOTAC after charging with the faecal suspension; F: counting chamber ready for observation (solid arrows).

At present, standardised protocols and recommendations have also been laid down by the World Association for the Advancement of Veterinary Parasitology (WAAVP) for the general guidelines for the evaluation of the efficacy of anthelmintics for livestock

animals (RINALDI et al., 2022), which indirectly can be done effectively if accurate diagnosis is made through the faecal egg examination(FEC) techniques. For these reasons, the importance of faecal egg diagnosis has increased significantly and several diagnostic parameters have been scrutinised to evaluate the diagnostic integrity of these techniques (NIELSEN, 2021; RINALDI et al., 2022). Despite the stringent criteria and guidelines, FEC still possesses certain demerits such as worm burden and egg outputs co-relation, sample distribution, the fecundity of the parasite species and the general personnel expertise and capability of the diagnostic centre (LEVECKE et al., 2012; GHAFAR et al., 2021; RINALDI et al., 2022). For instance, traditional quantification protocols like that of the McMaster technique are often incompatible with the standardized processing of large sample numbers (MES et al., 2007) and the FLOTAC® technique has a disadvantage in farm settings owing to its necessity of a powerful centrifuge machine (CRINGOLI et al., 2010). Moreover, each technique presents its diagnostic sensitivity and this analytical sensitivity will principally determine whether a technique is capable of detecting true egg counts below 50 EPG (NIELSEN, 2021). In general, the ‘modified and further improved’ McMaster technique has an analytical sensitivity of 50 EPG while the 'special modification’ McMaster method has only up to 10 EPG. This shows that even the most sensitive McMaster method would be insufficient for a demanding parasitic egg diagnosis (MES et al., 2007; CRINGOLI et al., 2010). Nevertheless, FEC presents a merit of a lower cost and simpler compared to the more sophisticated molecular diagnosis methods as long as sufficient animals from a group are sampled, the laboratory protocols are appropriate (including that of the identification of eggs) and minimising other variables such as correct choice of floatation medium (BESIER et al., 2016a).

While parasitic gastroenteritis is a disease complex with many parasite species involved in causing it, the genera most commonly associated with this complex are *Haemonchus*, *Ostertagia*, *Teladorsagia*, and *Trichostrongylus* (abomasum); *Cooperia*, *Nematodirus* and *Trichostrongylus* in the small intestine; and *Oesophagostomum* in the large intestine (SOULSBY, 1968; TAYLOR et al., 2015; BESIER et al., 2016a). However, the eggs of these genera are thin-shelled, segmented and cannot be readily differentiated except for *Nematodirus* spp., which has a distinctive large oval-shaped egg (BESIER et al., 2016a). Also, as mentioned above, the number of eggs can affect the faecal egg count and examination. Fortunately, FEC is higher for *H. contortus* compared to other trichostrongyle nematodes, because there is a relatively strong relationship

between the worm burden and the worm egg output (COADWELL and WARD, 1982; BESIER et al., 2016a). Besides, females of *H. contortus* have very high fecundity, capable of laying up to 15,000 eggs/day (TAYLOR et al., 2015; EMERY et al., 2016) in acute haemonchosis. Along with clinical signs, an appropriate FEC examination can somehow allow haemonchosis to be distinguished from other diseases (BESIER et al., 2016a). Also, to make species-specific differentiation of *H. contortus* more accurate, a fluorescence microscopy technique has been already established and this is being discussed briefly below.

2.7.1.4 *Peanut agglutinin (PNA) fluorescence microscopy*

Due to the difficulties in accurately differentiating eggs of the trichostrongyle nematode parasites, the culture of eggs in faecal samples to obtain the infective larval stage is another method for diagnosis. This identification is usually performed based on the dimensions and morphology criteria of various structures of the larva (VAN WYK and MAYHEW, 2013). Yet, this morphological identification is time-consuming as the recovery of the cultured larva takes about a week and is also an expertise-intensive method (BESIER et al., 2016a). Luckily for *H. contortus* identification, this larval culture need not be performed and the eggs in the faeces can be differentiated by allowing it to bind to a lectin and observing under an appropriate fluorescence filter. This method of *H. contortus* egg identification was first reported by PALMER and McCOMBE, (1996) which proved that peanut agglutinin (PNA) can specifically bind to *H. contortus* eggs.

Lectins are carbohydrate-binding proteins that are highly specific for monosaccharides or groups of sugars within a large carbohydrate molecule. This property of binding by specific lectins to carbohydrates on the surface of eggs has been exploited to identify parasites of plants and animals (CHEN et al., 2001; COLDITZ et al., 2002). PNA is a lectin derived from *Arachis hypogaea* which was shown to specifically bind to *H. contortus* eggs. When eggs are treated with PNA conjugated to fluorescein isothiocyanate (FITC) and observed under appropriate filters of a fluorescence microscope, the eggs can be visualised by the glowing green and stained outline. The technique has been refined further by many others in terms of nematode specificity, sample storage conditions, and fluorescence filter type (HILLRICHS et al., 2012; UMAIR et al., 2016; ABBAS and HILDRETH, 2019) and there are reports that even larvated *H. contortus* eggs also stained positive (JURASEK et al., 2010). This method has also been proven to compare well with the larval identification method in mixed-field infection scenarios (COLDITZ et al., 2002; ZARLENGA et al., 2016). HILLRICHS et

al., (2012) experimented with derivatives of various lectins to distinguish various life cycle stages (eggs, adult worms, L3 stages) of *H. contortus* and *T. circumcincta* and concluded that other lectins that interacted with different stages were less specific and affected by the age of the worm. Despite this specificity, the main demerits of this method are the difficulty to concentrate and harvest eggs from the faecal sample, the long duration of sample preparation, difficulty in making a standard egg count (JURASEK et al., 2010; D. ZARLENGA et al., 2016) and the requirement of a sophisticated fluorescence microscope.

2.7.2 *Molecular techniques*

ZARLENGA et al., (2016) remarked in their detailed review of haemonchosis diagnosis that some of the 'first-generation' molecular and biochemical methods developed in the early '90s for *H. contortus* identification and examination of drug resistance were: restriction enzyme digestion followed by agarose gel electrophoresis, Southern blotting techniques and profiles of isoenzyme bands (BEH et al., 1989; ECHEVARRIA et al., 1992; ZARLENGA et al., 1994). Unfortunately, issues with the sensitivity and specificity of these earlier tests stimulated the transition to other forms of molecular assays. Nowadays, there are plenty of options for more sensitive molecular-based diagnosis techniques for *H. contortus*. They range from conventional polymerase chain reaction (PCR) based methods to more advanced nemabiome sequencing (REDMAN et al., 2019; BORKOWSKI et al., 2020; QUEIROZ et al., 2020; COSTA-JUNIOR et al., 2021) techniques. Keeping in context with the aim of the dissertation, PCR-based technology and two isothermal-amplification based techniques are discussed briefly in the following paragraphs.

2.7.2.1 *PCR-based techniques for the detection of H. contortus*

PCR (MULLIS et al., 1986) revolutionised biological science with its varied applications. The basic principle of this technique is based on the use of the DNA polymerase enzyme for an *in vitro* replication of target DNA sequences through a thermocycler device. The result is the exponential amplificon of the DNA fragment. This has also been exploited for the diagnosis of many parasitic diseases, including *H. contortus.* The earliest gene sequence of *H. contortus* was made available in the 1990s, and since then, the PCR-based methodology in the diagnosis of this parasite increased manifold (RINALDI et al., 2022). Subsequently, several genes (CAMPBELL et al., 2008; BESIER et al., 2016a; ARSENOPOULOS et al., 2021; PITAKSAKULRAT et al.,

2021; RINALDI et al., 2022) have been targeted for this method. They include β-tubulin genes or 16S rRNA genes, internal transcribed spacers (ITS), external transcribed spacers (ETS) and non-transcribed spacers (NTS) and a few mitochondrial genes, especially the nicotinamide dehydrogenase subunit gene 4 (*nad4*), cytochrome c oxidase subunit I (COI). Out of these regions, the ITS region of the ribosomal DNA is of particular interest in the PCR detection of *H. contortus*.

ITS region, designated as ITS1 and ITS2 according to their locations, is the non-coding DNA (spacer DNA) located between the small-subunit ribosomal RNA (rRNA) and large-subunit rRNA genes in the chromosome (LAFONTAINE and TOLLERVEY, 2001). These spacer regions, particularly ITS2, are popular for PCR targets because of their tandemly repeated arrangements, often in hundreds of repeats and they tend to evolve faster. Thus, there is reduced sequence variation of individuals within and between populations but increased similarity within species, including those of trichostrongyle worms (GASSER et al., 1994, 2008; RINALDI et al., 2022). GASSER et al., (2008) have reported that the degree of variation of both the ITS1 and ITS2 sequences within a species is significantly less (<1.5%). Simply put, the ITS2 region is highly conserved among the trichostrongyles and can be used as PCR targets for differentiating at the species level. Many reports for PCR-based diagnosis and other detailed studies of *H. contortus* are now available targeting this gene region since STEVENSON et al., (1995) first published their findings. For example, earlier studies using this gene target have been done to differentiate between eight species of the Trichonstrongylidae family (HEISE et al., 1999) and two species in the same family (ZARLENGA et al., 1994) while REDMAN et al., (2008) studied and reported the marked genetic variation among different laboratory isolates of *H. contortus*. Hence, this study also employed this PCR target region to confirm the presence of this parasite.

It should also be noted here that different forms of PCR have also been explored in the diagnosis of *H. contortus* and numerous reports are already available. The restriction fragment length polymorphism PCR (RFLP-PCR), which exploits the digestion of PCR amplicons with endonucleases resulting in specific cutting of nucleotide sequence, have been used for differentiation (GASSER et al., 1994) as well as benzimidazole resistance study (NABAVI et al., 2011). There are also reports from multiplexing PCR to diagnose the parasite from mixed species samples (ZARLENGA et al., 2001; MCNALLY et al., 2013; LEHRTER et al., 2016; RESLOVA et al., 2021) although RINALDI et al., (2022) remarked that these multiplexing techniques are usually more of qualitative and at the

most a semi-quantitative approach. For quantitative results, numerous quantitative PCR (qPCR) studies on *H. contortus* detection and its association with drug resistance are available and have been extensively reviewed by ZARLENGA et al., (2016) and RINALDI et al., (2022). However, this method is more equipment intensive and often cost-prohibitive due to the special dyes and probes needed for the detection of end-result (ZARLENGA et al., 2016). The latest technology based on the PCR-based method is the ddPCR. This is based on the combination of probe-based PCR with a microfluidics analysis system allowing the detection of the target template in individual droplets of amplicons by special equipment (RINALDI et al., 2022). At the time of writing this, limited reports on species-specific detection using ddPCR are available with ELMAHALAWY et al., (2018) being the pioneer and a few on benzimidazole resistance studies, for instance as reported by BALTRUŠIS et al., (2020).

PCR techniques have also limitations despite it being recognised as the gold standard of molecular techniques. Although the DNA of the parasite can be obtained from all the stages of the parasite, DNA templates extracted from the eggs voided in faeces are most commonly used (ZARLENGA et al., 2016; ARSENOPOULOS et al., 2021; RINALDI et al., 2022). This DNA extraction is often a rate-limiting step in the sense that it is prone to PCR inhibitors present in the faeces sample, parasite egg amount variations and subsequently low amount of extracted DNA (ARSENOPOULOS et al., 2021; FLAY et al., 2022). In addition, the requirement of sophisticated types of equipment and the long duration from sample processing to result are also major drawbacks.

2.7.2.2 *Isothermal-amplification based techniques: LAMP and RPA*

As mentioned above, PCR still holds the reputation as the "gold standard" technique for DNA amplification (GARG et al., 2022). However, the prerequisite for different working temperatures leads to the need for a thermocycler device, which is usually expensive and confined to laboratories with trained technicians operating it. Also, it is time-consuming and often hinders its application in innovative integrated devices for a single workflow and is usually unsuitable for farm-site applications (OLIVEIRA et al., 2021; GARG et al., 2022). This gap in nucleic acid amplification technique has been greatly filled up by the introduction of various IA techniques. As the name suggests, the basic principle of this novel technique is the exponential amplification of the target nucleic acid template under a constant temperature (meaning isothermal conditions). With this, the need for expensive thermocycler devices is nullified and there are various methods to detect the end-result, which are often farm-site friendly and thus suitable for

a POC diagnosis (OLIVEIRA et al., 2021). The research and development into this new area of nucleic acid amplification have been steady and productive that there are already many available, namely nucleic acid sequence-based amplification (NASBA), loop-mediated isothermal amplification (LAMP), strand displacement amplification (SDA), recombinase polymerase amplification (RPA) and rolling circle amplification (RCA). Keeping in context with the objective of the dissertation, only LAMP and RPA are briefly discussed.

LAMP technique

The LAMP technique was first developed by NOTOMI et al., (2000) and since its inception, it is considered one of the most widely adopted IA techniques for pathogen diagnosis including *H. contortus* (RINALDI et al., 2022). As there is no denaturing of DNA in high temperatures, the amplification of non-denatured DNA is facilitated by *Bst* DNA polymerase enzyme. The *Bst* polymerase displays strand displacement activity as it extends annealed primer sequence without exonuclease activity at the 5'-3' direction (MORI et al., 2013; ABDULLAHI et al., 2015;). LAMP is a one-step amplification technique with high sensitivity and specificity under isothermal conditions, usually ranging from 60-65°C (NOTOMI et al., 2000; MORI et al., 2013; ABDULLAHI et al., 2015). LAMP utilises two pairs of compulsory primers, namely: i) a forward inner primer (FIP) and a backward inner primer (BIP); ii) two outer primers termed as a forward outer primer (designated as 'F3') and a backward outer primer (designated as 'B3'). There is also an optional "loop primer", designated as forward loop primer (FLP) and backward loop primer (BLP) All these can recognise six separate regions within a target DNA. Thus, the LAMP assay has high specificity, because the exponential amplification executes when all six regions (or four regions if no loop primers are used) bind to the respective complementary sequences within a target DNA (NOTOMI et al., 2000; MORI et al., 2013). The mechanism of LAMP amplification is briefly explained below and shown in Figure 5.

On the targeted region of the DNA, primers target six distinct sections designated as 'F1', 'F2', and 'F3' (for the forward strand) and 'B1', 'B2', and 'B3' (for the backward strand) as shown in Step-I in Figure 5. Sequences complementary to each of these sections are designated as 'F1c, F2c, F3c' and 'B1c, B2c and B3c'. It should also be noted that F3 is also known as the Forward Outer Primer; B3 is the Backward Outer Primer; F1c-F2 is the FIP and B1c-B2 is the BIP. The LAMP amplification occurs in two phases, non-cyclical and cyclical.

The non-cyclical phase of LAMP begins with the binding of the FIP to its complementary sequence at the 5' end of the double-stranded DNA. *Bst* polymerase then facilitates the extension with its strand displacing property resulting in a full length of a complimentary strand (orange arrow, Step IIa Figure 5) to the target DNA. At the same time, F3 also binds to the F3c region external to the FIP initiating displacement of the newly formed DNA strand. This results in the single-stranded DNA with a dumbbell shape at the 5' end as F1-F1c forms a self-hybridising loop (orange strand, Step II Figure 5). The same thing happens with the BIP on the other strand, subsequently forming a new (green strand, Step II Figure 5) self-hybridising loop strand. Now, the BIP (and FIP on the other hand) uses the newly displaced single-stranded DNA with loop-shape at the 5' end as a template and the same mechanism above takes place (shown in orange dotted line, Step II Figure 5). This time, the self-hybridising loop occurs in two ends of both the newly formed strands (orange and green strands). Finally, the non-cyclical step ends with the formation of dumb-bell-shaped DNA (Step III Figure 5). The cyclical phase starts with strand displacement by *Bst* polymerase, the binding of the outer primers (complementary segments are F3c and B3c this time) and inner primers (complementary to F2c and B2c this time). The final result is the exponential amplification of complex cauliflower-shaped structures (Step-IV Figure 5), which are very specific (NOTOMI et al., 2000; MORI et al., 2013; ABDULLAHI et al., 2015).

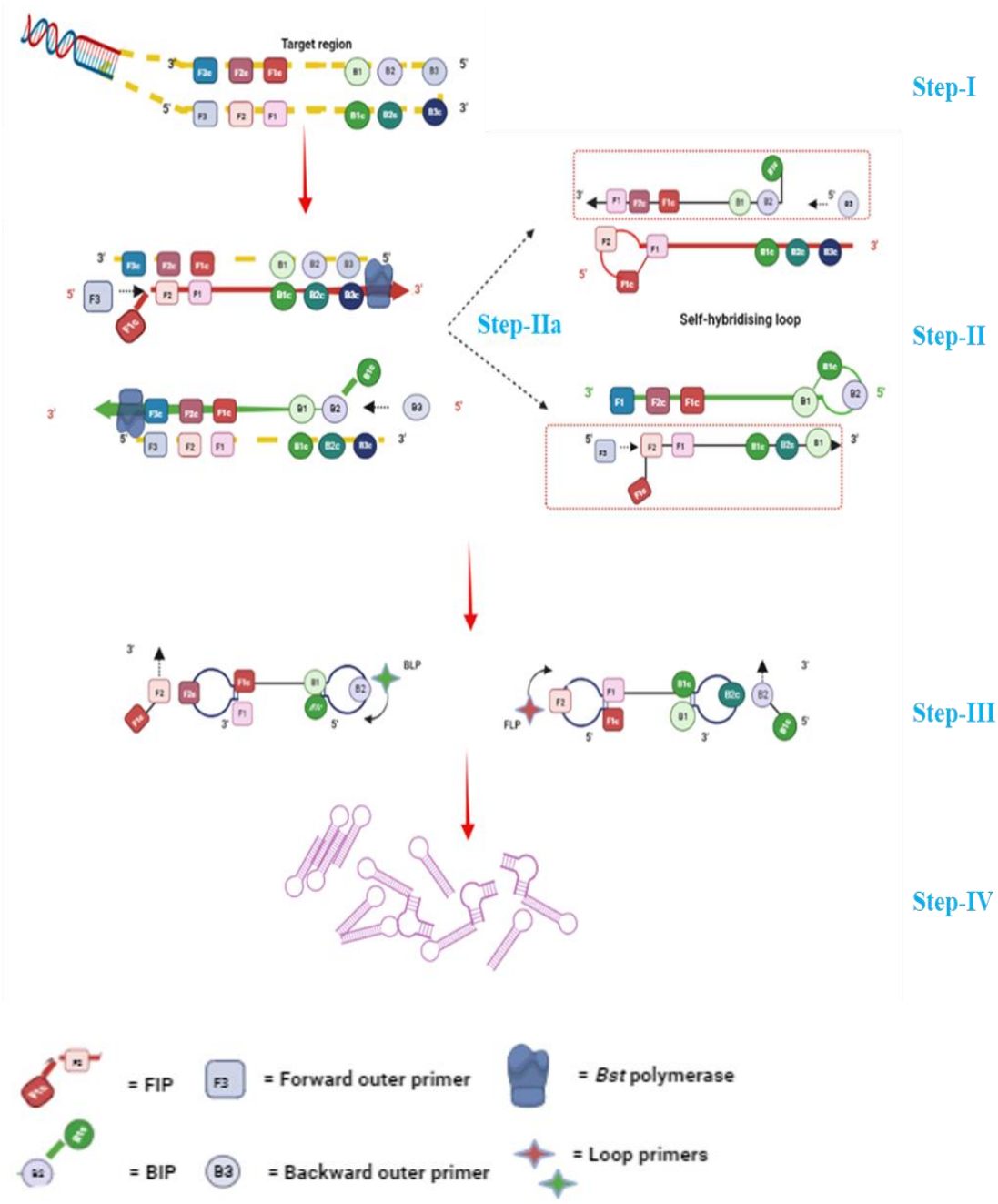

Figure 5: Schematic flow diagram of LAMP assay. Step-I: initial binding of the complementary segments; Step-IIa: non-cyclical phase- annealing and extension by the collective action of the inner and outer primers and strand displacement of *Bst* polymerase; Step-II: formation of a self-hybridising loop to the newly formed strands; Step-III: cyclical phase begins, formation of self-hybridising loops on both ends of 5'-3' and further annealing, extension and subsequent amplification; Step-IV: exponential amplification of complex cauliflower-shaped amplicons.

The result can be visualised with many methods such as a change in turbidity, laminar flow paper-based, colourimetric and even via a smartphone application of which numerous reports are already available and reviewed in detail by ABDULLAHI et al., (2015) and GARG et al., (2022). Out of these methods, the colourimetric detection and lateral flow (LF) paper-based are of context to the dissertation study. For colourimetric observations, several types of fluorescent dyes have been used for the detection of colour change, usually through a fluorescence device. Moreover, metal ion indicators like hydroxy naphthol blue (HNB) and other pH-sensitive dyes like cresol red, phenol red, and neutral red are also utilised for visual colour change (GARG et al., 2022). The study here adopted the phenol red-based colourimetric detection using a commercial kit. The LF assay detection uses a special strip having an absorbent pad, containing an antibody specific to a target analyte. When tagged amplicons (as described in the Materials and Methods section) are introduced to this absorbent pad, those target amplicons bind and show a positive reaction (ABDULLAHI et al., 2015) visualisation similar to that of the commonly available pregnancy test kit.

The LAMP technique has also been employed in the detection of various pathogens (MORI et al., 2013; ABDULLAHI et al., 2015) including the recent pandemic virus, SARS-Cov-2 (CHAOUCH, 2021; GARG et al., 2022). This is also being employed in the field of parasitology (RINALDI et al., 2022) of which the first of its application in *H. contortus* detection was reported by MELVILLE et al., (2014) and ZARLENGA et al., (2016) claimed a 'calculated detection of upto 2 EPG'. Despite its many advantages, one of the major drawbacks of this technique is the difficulty in designing the three pairs of primers to which there is a limited number of software dedicated to it. Also, owing to the high stability of the amplicons, there can be some degree of cross-contamination and false positives although good laboratory practice can minimise this to a great extent.

RPA technique

RPA is another isothermal amplification technique capable of operating at a much lower temperature range, usually between 37°C and 42°C (LOBATO and O'SULLIVAN, 2018; OLIVEIRA et al., 2021; TAN et al., 2022) although there are claims of an operational temperature of 25°C (DAHER et al., 2016). The technique was first reported by PIEPENBURG et al., (2006) and has been emerging to be one of the most widely used isothermal amplification techniques besides LAMP.

This technique employs the activity of two main enzymes as a replacement for the usual heat denaturation step in PCR: i) the recombinase (*Escherichia coli* RecA or uvsX from T4-like bacteriophages); ii) single-strand DNA binding protein (SSB). The replication is facilitated by a DNA polymerase (from *Bacillus subtilis* Pol 1, *Bsu*) having strand-displacement activity necessary to extend the primer (DAHER et al., 2016; TAN et al., 2022). Other necessary reagents involved are a crowding agent (Polyethylene glycol, Carbowax20M); an adenosine triphosphate (ATP) source like phosphocreatine through creatine kinase (DAHER et al., 2016). The mechanism of action of RPA is shown in Figure 6. In brief, the process initiates when the recombinase protein binds to primers in the presence of ATP and a crowding agent resulting in a recombinase-primer complex. The complex then scans double-stranded DNA looking for a homologous sequence and stimulates strand invasion by the primer at the cognate site. The displaced DNA strand is stabilised by the SSB protein. Finally, the recombinase disassembles and a strand displacing DNA polymerase, such as *Bsu* polymerase, attaches to the 3' end of the primer and elongates it in the presence of dNTPs. Ultimately, the cyclic replication of this process leads to an exponential amplification of the target template (PIEPENBURG et al., 2006; LOBATO and O'SULLIVAN, 2018).

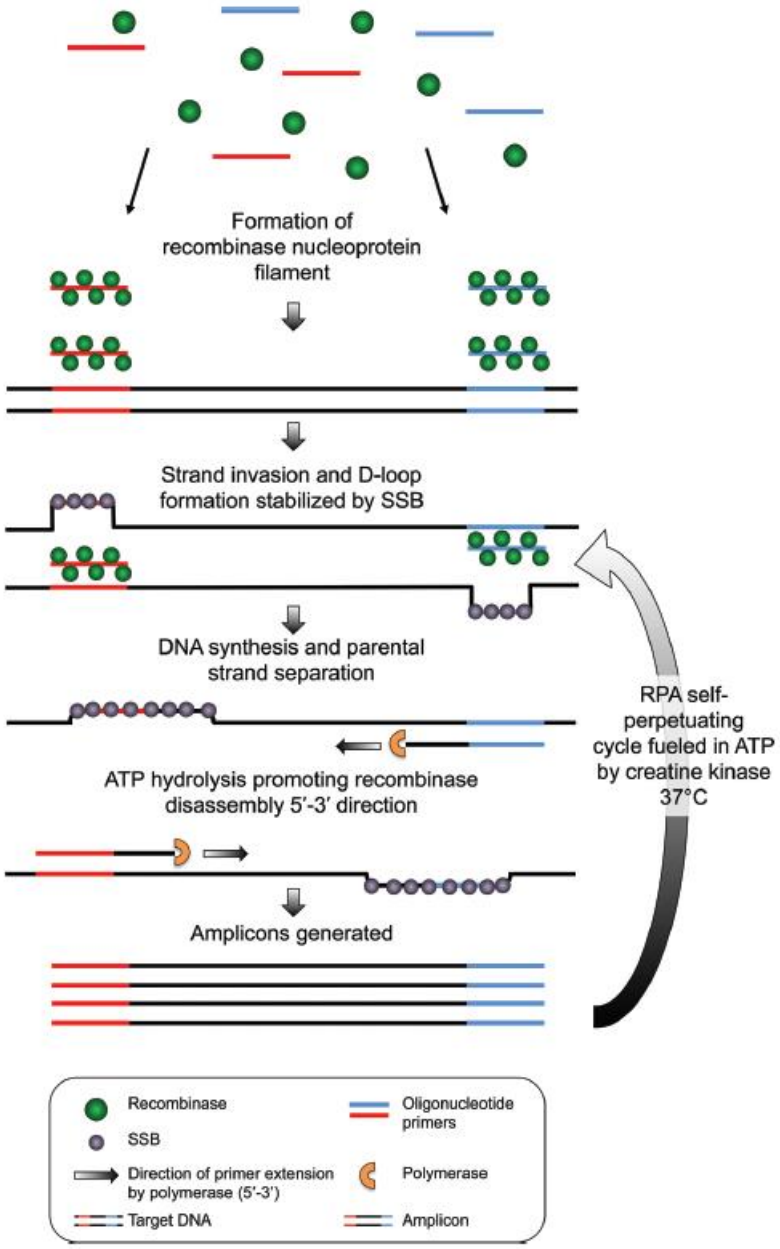

Figure 6: Schematic flow diagram of RPA mechanism as adapted from from DAHER et al., (2016). In the presence of a crowding agent, dNTP and ATP, the recombinase, SSB, and strand-displacing DNA polymerase facilitate exponential DNA amplification eliminating thermal cycling.

The advantage of this reaction is mainly its minimal sample preparation, the capability of amplifying as low as 1-10 DNA target copies (LOBATO and O'SULLIVAN, 2018) and the quickest reaction time range of 10-20 min (DAHER et al., 2016; KUNZE et al., 2016; LOBATO and O'SULLIVAN, 2018; OLIVEIRA et al., 2021). This gives an extra edge in designing a farm-site-friendly diagnostic tool. The end-result detection methods vary from conventional gel electrophoresis to real-time

CRISPR-Cas assisted detection and smart-phone based detection (DAHER et al., 2016; LOBATO and O'SULLIVAN, 2018; OLIVEIRA et al., 2021; PARK et al., 2021). The disadvantages of this method are mainly the lack of dedicated primer designing tools, expensive reagents and a single kit supplier. Currently, there is only one commercially available kit manufacturer, the TwistDx kits (TwistDx Ltd., UK) with various end-results detection methods (like agarose gel electrophoresis, lateral flow, and probe-based real-time detection). Varied pathogens have also been detected by this assay, ranging from SARS-cov-2 (PARK et al., 2021) to food-borne pathogens (BHUNIA et al., 2020). The assay also finds its application in the field of parasitology, although much of it is for protozoal parasites of humans (CASTELLANOS-GONZALEZ et al., 2018). At the time of writing this, the only report of RPA detection of *H. contortus* was reported by WU et al., (2021).

3. MATERIALS AND METHODS

3.1. Sample location, ethics and sources of positive control specimens

The faecal samples used were collected from the animals as per the Hungarian Animal Protection and Welfare Act (Act XXVIII of 1998, 3.§) from farms (n = 14) in six counties in and around Eastern and South-Eastern Hungary between 2019 and 2022 (excluding covid-19 lockdown period in 2020-2021) as shown in Figure 7. Additionally, suspected adult *H. contortus* obtained from farmed roe deer (*Capreolus capreolus*) abomasums and also a pooled goat faecal sample were also utilised (assigned as Farm FD and Farm FG, respectively) in the course of the optimised assay trials. It should be noted here that the samples were obtained as part of a separate larger study (Toth, unpublished) that dealt with the epidemiology of trichostrongylidae worms. Thus, detailed FEC of the individual animals was outside the scope of this study and hence, only the average FEC of the farms were utilised. The faecal samples from the individual animals were collected as per COLES et al., (1992) with slight modifications. For each farm, a minimum of n= 20 animals were sampled. Each sample was packed in a labelled ZipLock bag and transported with ice packs/cooler to the laboratory. If individual sampling was not possible, a representative pooled sample was collected by pooling freshly voided faeces (min n=10 faeces pad) from the ground (KENYON et al., 2016).

A positive control specimen of *H. contortus* eggs (designated herein as 'KS'), obtained from the abomasal contents of lambs infected orally with approximately 5000 L3 infective larvae of susceptible isolate, MHCo3(ISE), was also kindly supplied by the Institute of Parasitology, Košice, Slovakia. For this, the necessary ethical permissions were granted by the Ethics Committee of the Institute of Parasitology of the Slovak Academy of Sciences under European Union guidelines (EU Directive 2010/63/EU for animal experiments). Another nine species of trichostrongyle worms (*Cooperia curticei, Haemonchus contortus, Nematodirus battus, Oesophagostomum venulosum, Teladorsagia circumcincta, Trichostrongylus axei, Trichostrongylus colubriformis, Trichostrongylus vitrinus* and *Trichuris ovis*) and a batch of pure *H. contortus* eggs were also obtained courtesy of Dr Lynsey Melville, Moredun Research Institute, Scotland. The meteorological data of the above locations were obtained from the Centre for Precision Farming, R&D Services, FAFSEM, University of Debrecen.

All the laboratory experiments were performed at the molecular laboratory of the Doctoral School of Animal Science, Institute of Animal Science, University of Debrecen,

Hungary. Another positive control gDNA sample (designated herein as BP) was also kindly provided by the Department of Parasitology and Zoology, University of Veterinary Medicine, Budapest. Some methodological and data analysis parts of the study were also done in collaboration with the School of Veterinary Medicine, University of Glasgow, Scotland.

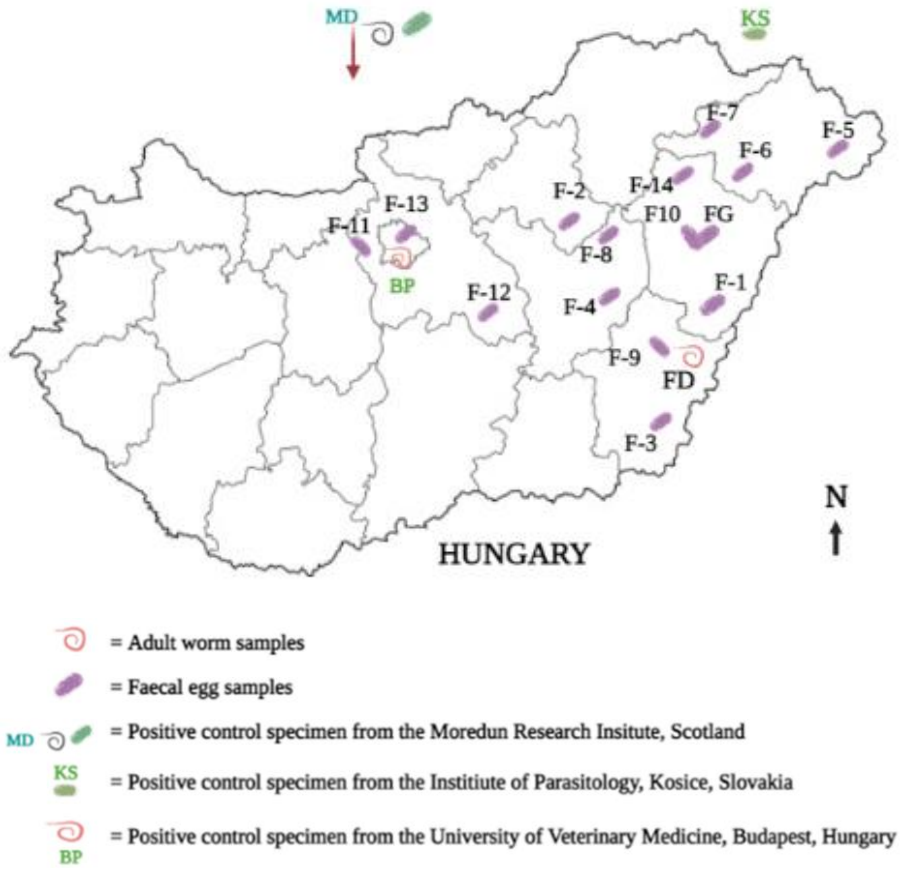

Figure 7: Location of farms covered in the study. F-1 to F-14: sheep farms; FD: roe deer farm; FG: goat farm; MD, BP and KS were sources of positive control specimens.

3.2. Faecal egg examination by Mini-FLOTAC

FEC was performed using saturated sodium chloride solution (specific gravity of 1.200; dilution ratio of 1:10) as the floatation medium, using the Mini- FLOTAC® and Fill- FLOTAC® system as per the protocols laid down by CRINGOLI et al., (2010). Briefly, 5g of the faecal sample was loaded using the conical collector and 45 ml of the saturated salt solution was filled in the Fill- FLOTAC®. Then, a faecal suspension was

prepared by homogenising the loaded faecal sample with a pumping action of the conical collector inside the Fill- FLOTAC®. The Fill- FLOTAC® was inverted/shaken for up to 5 times and the faecal suspension was charged into both the chambers in the Mini-FLOTAC®. After allowing the eggs to be floated for 10 min, the reading disk was turned with the key provided and the eggs were counted using an Olympus BX51 microscope under 10x. The EPG was calculated by multiplying the counted eggs by a factor of 5. All photographic records were taken using the cellSense software using a DP70 digital camera (Olympus) mounted on the microscope. Wherever applicable, the faecal suspension from the Fill- FLOTAC® device was also utilised as described in the following texts. Statistical analysis (of FEC comparison to meteorological data) was done using GraphPad Prism 8.4.3 (GraphPad Software Inc. USA).

3.3. PNA fluorescence microscopy

For successful and efficient staining, the parasite eggs needed to be harvested/recovered as much as possible. This was done in the following two manners.

3.3.1 *Faecal egg harvesting/concentration with centrifugation*

The eggs were harvested from the faecal solution described above with a slight modification from the protocols reported by ABBAS and HILDRETH et al. (2019) and JURASEK et al., (2010). Briefly, the remaining suspension, after charging in the Mini-FLOTAC, was sieved through a 250µm filter sieve (Thermo-Scientific) into a Falcon tube (VWR International) and centrifuged at 1000 x *g* for 2 min. Then, 5 ml of the supernatant was aspirated carefully and transferred to a new Falcon tube. The volume was adjusted to 45ml by adding distilled water. After the final centrifugation at 2000 x *g* for 5 min, the supernatant was discarded carefully not to disturb the faecal pellets at the bottom of the tube. The above steps were replicated twice with the pooled faecal samples of each farm and finally, the pellets were collected in a 2ml tube. A replicate of the pellet was verified for eggs under 10x microscopy and either proceeded to PNA staining or stored in PBS at 4ºC overnight if the staining could not be done on the same day.

3.3.2 *Faecal egg harvesting/concentration without centrifugation*

Keeping in view the farm-site proof of concept assay design, another centrifuge-free egg concentration method was carried out as described by FRANCIS and ŠLAPETA, (2022) with a modification for Fill- FLOTAC® faecal suspension. This procedure is shown in Figure 8.

Briefly, the faecal suspension after being sieved through the 250µm filter, was divided into four batches of 10ml each in a test tube (TT-1). After allowing a floatation

of 10 min, about 2ml of the upper fluid meniscus was aspirated into a new 2ml tube (designated as TT-2) for each of the TT-1. Then, a clean 200µl pipette tip was inverted allowing again the fluid meniscus from the TT-2 tube to be aspirated into it by capillary action, with the aim of harvesting/concentrating as many eggs as possible. The final aspirated suspension was transferred to another 2ml tubes containing 1ml of 1x PBS. The egg presence was verified by checking one of the replicates under 10x microscopy.

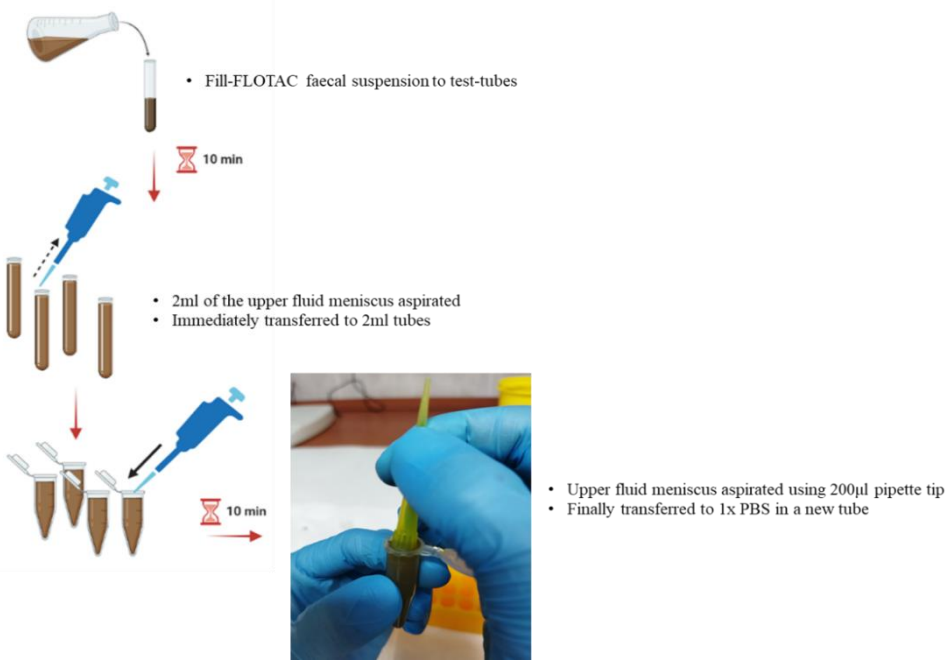

Figure 8: Schematic diagram of egg concentration from Fill-FLOTAC suspension without a centrifugation step. The top fluid meniscus of the faecal suspension was collected in 2ml tubes and allowed floatation. The floated eggs were recovered by an inverted 200µl pipette tip.

3.3.3 *PNA fluorescence microscopy*

This was performed according to the protocols reported by JURASEK et al. (2010) with some modifications. The PNA-FITC (Sigma-Aldrich, Cat. No. L-7381) was reconstituted at 5µg/ml and aliquoted into individual working 1ml solutions. The concentrated eggs in 1x PBS, collected as described above, were centrifuged at 280 x *g* for 5 min and the supernatant was discarded. Then, the reconstituted PNA-FITC aliquot was transferred to the tube containing the egg pellet and incubated for 1 hour under constant agitation at room temperature using a benchtop vortexer in the dark. Then, 15-20µl of the egg sediment was transferred onto a clean glass slide, covered with a coverslip. The stained samples were examined with a fluorescence microscope using FITC filters (480-490nm excitation filter, Olympus BX51 microscope mounted) in a dimly lit

laboratory. The same staining was also performed for the pure *H. contortus* egg culture. Each sample was examined and stained eggs were counted in two technical replicates. Partially stained and unstained eggs were counted as negative results. Again, the photographic records were taken using the Olympus cellSens software through an Olympus DP70 camera mounted to the Olympus BX51 microscope. Two fields of vision were recorded for each photograph: first in the fluorescence mode and then in the bright field for the same field of view. The eggs were counted as stained and partially-stained eggs which were interpreted as positive and negative results respectively under the fluorescence field.

3.4. DNA extraction

In line with developing a molecular-based technique, those individual faecal samples having EPG <100 were separately stored in Ziplock bags at 4°C for downstream DNA extraction processes. Two farms (F-6 and F-14) that recorded a low FEC and no visually detected trichostrongyle eggs were adopted as 'negative control farm samples'. This DNA extraction was done from both the individual as well as pooled faecal samples (respective to each farm). It should be noted here that for the pooled sample DNA extraction, a minimum of n =5 individual animals were considered. DNA from all the faecal samples was extracted using a QIAamp Fast DNA Stool Mini Kit (Qiagen), following the manufacturer's instructions, and DNA from the adult worms was extracted using an E.Z.N.A.Tissue DNA Kit (Omega Bio-Tek Inc.). All the DNA quantifications (A260nm absorbance) and purity analysis (A260/A280nm absorbance ratio) were accomplished using the Synergy HTX Multi-Mode Microplate Reader (BioTek) installed with Gen5 Software (version 3.03, BioTek).

3.4.1 *Crude DNA extraction trials*

It is to be noted here that the following crude DNA extraction methods were also trialled keeping in line with the POC assays. Wherever centrifugation was necessary, the low *g* centrifuge machine (FVL-2400 Combi-Spin Centrifuge/Vortex (BioSan, Latvia) was used. This portable centrifuge machine provided a maximum of 700 x *g* centrifugation and medium-strength vortexing. All the experiments were performed in three technical replicates unless stated otherwise.

Magnetic beads-based method: This was conducted using the commercially available magnetic beads-based genesigEasy DNA/RNA Extraction Kit (Primerdesign Ltd, UK). The positive control samples used here were the KS. Extraction was performed following the protocols described by the kit manual. To test the applicability of the Fill-

FLOTAC® suspension, both the direct faecal samples and the suspension from the Fill-FLOTAC® were used as the starting material for the DNA extraction. The farms were arbitrarily chosen for this trail and done in technically replicated.

Glass-bead beating lysis method: This was done as described in MELVILLE et al., (2014) with a slight modification. To execute the bead-beating effect, the glass beads from the E.Z.N.A Stool DNA Kit (Omega Bio-Tek, Inc.) were utilised. To each 2 ml tube containing the egg pellets, 200 mg of the glass beads were added and vortexed for 5 min. Again, to check the applicability of the Fill- FLOTAC®, the bead-beating lysis was also done using directly the Fill- FLOTAC®faecal suspension and without the egg concentration steps described above. Finally, the lysate from each replicate was diluted 1:5 with double-distilled water and used as the template per LAMP reaction.

Chelex reagent-based methods: Three sub-trials were performed using Chelex 100 (BioRad) solution-based crude DNA extractions following a few protocols and studies using this chemical for crude DNA extraction (AWAWDEH et al., 2019; GUEVARA et al., 2018). These modified protocols are briefly described in Figure 9. The Proteinase K and the glass beads used were obtained from the E.Z.N.A Stool DNA Kit (Omega Bio-Tek, Inc.).

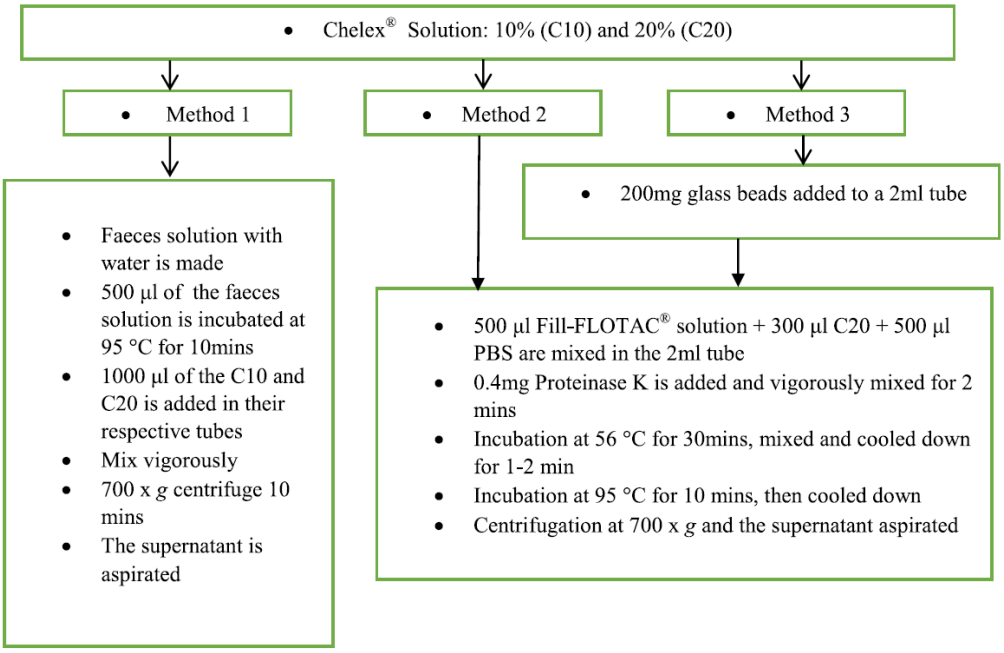

Figure 9: Chelex reagent-based crude DNA extraction steps (Source: KHANGEMBAM et al., 2021)

Motorised micropestle method: For this, the eggs were harvested as described in section 3.3.2. Briefly, the eggs from the topmost film of the faecal suspension were collected in the 1.5ml tube. A battery-operated motorised and micro-pestle compatible Kimble Handheld Homogeniser (VWR, catalogue SCERSP749540-0000) was used to homogenise thoroughly the egg pellets for about 3-5 min. Each sample was done in replicates and care was taken to change the micro-pestle grinder tip for each replicate. After the homogenisation, a small volume of the suspension was observed under the microscope to verify the egg lysis. Then, this suspension was used as the starting material for the DNA extraction using the genesigEasy DNA/RNA Extraction Kit (Primerdesign Ltd, UK) following the manufacturer's protocol.

3.5. Species-species ITS2 PCR

Species-specific ITS2 PCR for *H. contortus* was performed using a GoTaq Flexi Polymerase PCR kit (Promega), according to the kit manual. The parasite-specific ITS2 primer set used in this study was originally described by REDMAN et al. (2008) and ordered from Eurofins Genomics. The PCR was set up in 12.5 µl total reaction volume consisting of: 2.5 µl 5x GoTaq Green Buffer, 1.25 µl $MgCl_2$ 25mM, 0.25µl dNTPs of 10mM each (VWR International), 0.25µl (100 pmol) each of the primers, 0.06µl GoTaq Flexi polymerase 5IU/µl (Promega), 6.94µl of molecular grade water (AccuGene) and 1 µl of DNA template. The thermal profile of the PCR was as set: 94 ºC for 2 min for initial denaturation; 35 cycles each of 94 ºC for 30 sec for denaturation; the annealing temperature of 50 ºC for 30 sec and 72 ºC extension for 30 sec, with a final extension step of 72 ºC 10 min. Results were analysed and the records were maintained by using ChemiDoc XRS+ System and Image Lab software (BioRad) after 2% agarose gel electrophoresis with ethidium bromide (Etbr) staining. The amplicon size was 320 bp as per REDMAN et al., (2008). All three positive control template DNA were used together or individually in the PCR as per required. The primer sequence is given in Table 3.

3.6. Colourimetric LAMP

A validated primer set (as given in Table 3) published by MELVILLE et al. (2014) was adopted for the LAMP assay in this study but the method of the end result detection was different from the original study. To facilitate a naked eye detection of the results, a WarmStart Colorimetric LAMP 2X Master Mix (DNA & RNA) with UDG kit (New England Biolabs Ltd, UK) was utilised. The working 10x LAMP reaction primer mix contained: 1.6µM of each FIP and BIP primer, 0.8µM of each Loop Forward and Loop Backward primer and 0.2µM of each F3 and B3 primer. The LAMP assay was carried

out as defined by the kit manual in a total of 25µl reaction volume that consisted of 12.5µl of WarmStart Colorimetric LAMP 2X MasterMix with UDG; 2.5µl of the working primer mix prepared above, 1µl of template DNA and 9µl of molecular grade water (AccuGene).

For initial optimisation, the reaction was run using an Alpha Cycler 1 (PCRmax, UK) at temperature-time conditions of 60 ºC to 63 ºC for 30–45 min using the positive control DNA (either BP or KS or both) as well as a non-template control using the molecular grade water during optimisation. All reactions were done in technical replicates. Whenever a visually detectable colourimetric change of orange-yellow happened in the reaction mix, the result was said to be a positive result while the negative result was interpreted by the pink-red colour of the reaction mixture.

Once this initial optimisation was established, the assay was replicated successfully using the VWR Advanced Mini Dry Block Heaters (VWR International). A time-temperature condition of 30 min for 62ºC was adopted. The colour change was also scored among a minimum of n=2 individual observers to determine any differences in the colourimetric change. To determine the analytical sensitivity of the assay, a 10-fold serial dilution of the positive control DNA was prepared out of which 1µl each of the dilutions was used for the LAMP reaction at 62ºC for 30 min.

Table 3: Primer sequences used in the study. **: primers custom tagged with FITC and Biotin (BIO) respectively at FIP and BIP for the LAMP-LF assay

Assay	Primer ID	Sequence (5'- 3')
LAMP and LAMP-LF	FIP**	AACAATCACAGCCGCCACTAAGCTCTATTACATGAGGT GTC
	BIP**	TCATTGATGGTTGAGCTTGAGACTTGTTCGTACTTAAC CACCATCA
	F3	GGTTCCATTGATCACGAGAA
	B3	CAGTACACCACATACTCAAGAA
	FLP	AAGCGGCTCATGTCATACAT
	BLP	CTATAATACTGCCTCGCCGTT
ITS2 PCR	Forward	GTTACAATTTCATAACATCACGT
	Backward	TTTACAGTTTGCAGAACTTA
RPA	R_HC-1	Forward : ATATCATTCAGGAATGTTACAATTTCATAA Backward: AACATTCATTTTTACAGTTTGCAGAACTTA
	R_HC-2	Forward : GTTACAATTTCATAACATCACGTTGCATGT Backward: TTACAGTTTGCAGAACTTAGTGTTCACATTC
	R_HC-3	Forward: GTTACAATTTCATAACATCACGT Reverse: TTTACAGTTTGCAGAACTTA

3.6.1 *LAMP-LF assay*

The HybriDetect-Universal Lateral Flow Assay Kit (Milenia Biotec, Germany) was utilised for the detection of dual-tagged LAMP amplicons. At the 5' ends of FIP and BIP primers, the LAMP primers described above were tagged with FITC and biotin (BIO) respectively (Table 3). The LAMP primer concentration and reaction conditions are the same as previously described. The assay optimisation was performed according to the kit manual. During this optimisation, only the positive control and NTC were used in three technical replicates. However, the concentration of the amplicon mixed with the kit-supplied LF hybridisation buffer solution was adjusted to avoid false positives. Briefly, the LAMP-LF assay was carried out as follows: each kit-supplied dipstick was charged with each of the single test concentrations of the amplicons on the sample loading pad and dipped vertically into the buffer solutions. 100µl of the kit-supplied buffer solution was loaded into the wells of a 96-well microplate. The results were recorded after

incubation at room temperature at two intervals of 5 and 10 min. The positive result was interpreted only when both the Control and Test bands were stained and the negative result was interpreted if only the Control band was stained as shown in Figure 10. Any deviation from these two staining patterns was regarded as a faulty result.

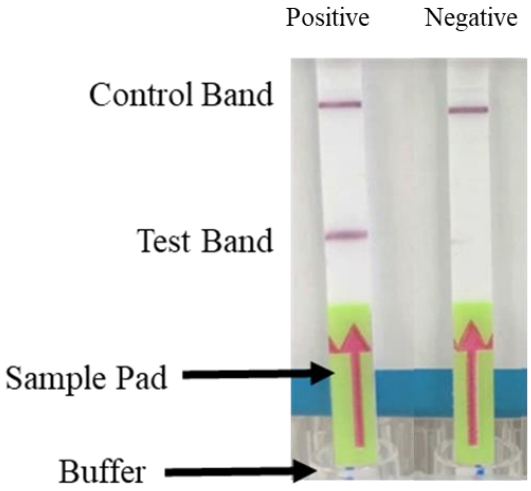

Figure 10: Lateral flow dipstick setup and how to interpret the correct results. Positive results were interpreted as and when both the Control band and the Test band showed colour while a negative result was interpreted only when the Control band showed colour. Any deviation from this was regarded as invalid.

3.7. RPA assay

3.7.1 *RPA primer design and primer screening*

At the time of writing there, there is no dedicated primer designing tool for RPA reaction but the Geneious software version 11.1.5 (Biomatters Ltd., New Zealand) was utilised to construct the primer. Briefly, ITS2 nucleotide sequences of *H. contortus* were obtained from the Genbank (https://www.ncbi.nlm.nih.gov/genbank/) and pairwise aligned adopting the MUSCLE alignment algorithm (with a minimum of 8 iterations). Then, the PCR primer sequences as described earlier were annotated to the aligned consensus sequence. The annotated sequence was modified to increase the length of the primer as per the conditions as stated by the TwistDx manual for RPA primers. Finally, two pairs of custom-designed RPA primers were selected and ordered for production from Eurofins (Eurofins Genomics, Germany).

3.7.2 *RPA reaction and optimisation*

The RPA assay was done with each single reaction volume of 50µl utilising the TwistAmp™ Basic kit (TwistDx, UK) as per the kit manual. Briefly, each reaction tube contained forward and reverse primer (10µM) at 2.5µl each, 29.5µl of primer-free rehydration buffer, 8µl of 0.8M betaine, 4µl molecular grade water, 1µl of DNA template and 2.5µl of 280mM magnesium acetate. Betaine (Thermo Scientific) was added in the reaction, as a modification from the manual, to reduce non-specific amplification as per LUO et al., (2019). The tubes were shaken vigorously at the beginning and the fourth minute as per the manual. Finally, the tubes were incubated at 85ºC for 5min to stop the amplification. The incubation conditions were achieved using the same portable heat block (VWR™ Advanced Mini Dry Block Heater). For the optimisation, the RPA amplicons were cleaned using either EXOCleanUp FAST kit (VWR) or ChargeSwitch™ PCR Clean-Up kit (Thermo Scientific) according to the respective kit protocols although results were also analysed without this post-amplification clean-up. Analytical sensitivity was calculated by performing the reaction using a 10-fold serial dilution of the MD positive control DNA template.

3.7.3 *Visualisation of RPA reaction by agarose gel electrophoresis*

The visualisation of the results of RPA was done by 2.5% agarose gel electrophoresis stained with EtBr using the ChemiDoc XRS+ System and Image Lab software (BioRad). For comparison purposes, the amplicons were also analysed without the recommended post-amplification clean-up step. The expected amplicon band size for the *H. contortus* RPA reaction is 320 bp.

3.7.4 *RPA end-point detection using a UV lamp and DNA intercalating dye*

This was done as per the protocol initially described by SRISRATTAKARN et al., (2020) with some slight modifications, especially the use of different dyes and the mode of visualisation. Briefly, the RPA amplicon tubes were mixed with 5x EvaGreen® Dye (Biotium) at a 4:1 ratio in technical triplicates. Then, to visualise and interpret the result, the reaction tubes were illuminated by UV rays using the ChemiDoc XRS+ System (BioRad). Similarly, various dye: amplicon concentrations (6:1; 4:1; 2:1) were tested using the 10000x GelRed™ (Biotium) at different working concentrations of 10x, 100x, 200x and 300x and in technical triplicates. Finally, for comparison purposes, SYBR Green I Dye at 300x, 400x and 500x concentrations were also tested for naked-eye detection as well as under UV illumination.

3.8. Gene sequencing through Eurofins

This was performed as an additional task besides the main aims of this study as a preliminary trial. Three PCR amplicons of *H. contortus* isolates in three locations (F10, F11 and F13) were submitted to TubeSeq gene sanger-sequencing service (Eurofins Genomics). The results obtained were analysed using the Molecular Evolutionary Genetics Analysis (MEGA) version X software as per described by KUMAR et al., (2018). Briefly, the nucleotide sequence of the gene sequencing was subjected to a BLAST search (https://blast.ncbi.nlm.nih.gov/Blast.cgi) and n=14 of the genome sequence result was chosen. All the sequences were aligned using the ClustalW alignment algorithm and a phylogenetic tree was constructed using the recommended Neighbour-Joining method with the bootstrap value set at 1000.

4. RESULTS and DISCUSSION

4.1. Microscopy Results

4.1.1 *Microscopy: adult worms and eggs*

Initially, all the faecal samples were examined under microscopy and those farms with high FEC and with suspected *H. contortus* eggs were kept for further downstream analysis (both PNA microscopy and optimisation of the two IA techniques). The adult worm specimens obtained from the abomasum of farm FD was also observed under microscopy and identified to be *H. contortus* following the criteria laid down in TAYLOR et al., (2015) which were also subsequently confirmed by molecular-based techniques. As suspected, none of the remaining worms found in the abomasum and small intestines (that did not visually strike as the typical "Barber's pole worm" feature) were found to be *H. contortus* adults.

The microscopy photographic records of the morphological identification of the adult worms are presented in Figure 11. Grossly, the suspected worm specimen presented either reddish or red-white striped and thread-like. The length of the identified adult males ranged from 9-18 mm while those of identified adult females ranged from 15-27mm. The nematode body was observed to be filiform and tapered from the anterior end (Figure 11-A) with the posterior ends modified as described later depending on the sex of the worm. The anterior end presented a buccal capsule with a noticeable tooth or 'lancet' protruding from the dorsal wall (Figure 11- B). Another striking morphological observation was the longitudinal striations on the body which is termed 'synlophe', which are technically a system of cuticular ridges (AMARANTE, 2011) and this can be seen in Figure 11 - C. The synlophe can also add to species differentiation as AMARANTE (2011) noted that these structures could extend significantly beyond the midbody in *H. contortus* while they could terminate near the midbody in *H. placei* for both sexes.

As seen in Figure 11-A, the black arrow shows the cervical papillae, observed at two different magnifications. These cuticular modifications are very prominent in the case of *H. contortus* and positioned from the anterior end about thrice the diameter between papillae. The cervical papillae are often spinous in nature (SOULSBY, 1968; TAYLOR et al., 2015). Trichostrongyle nematodes are unisexual and so male and female worms are usually presented with distinguishing morphological features. Typically, the adult *H. contortus* females have a vulval flap which is linguiform in shape (Figure 11-B). While in males, a well-developed bursa that serves copulatory functions is typically unequal in

shape and size (SOULSBY, 1968) and also possesses a pair of barbed spicules (Figure 11-C).

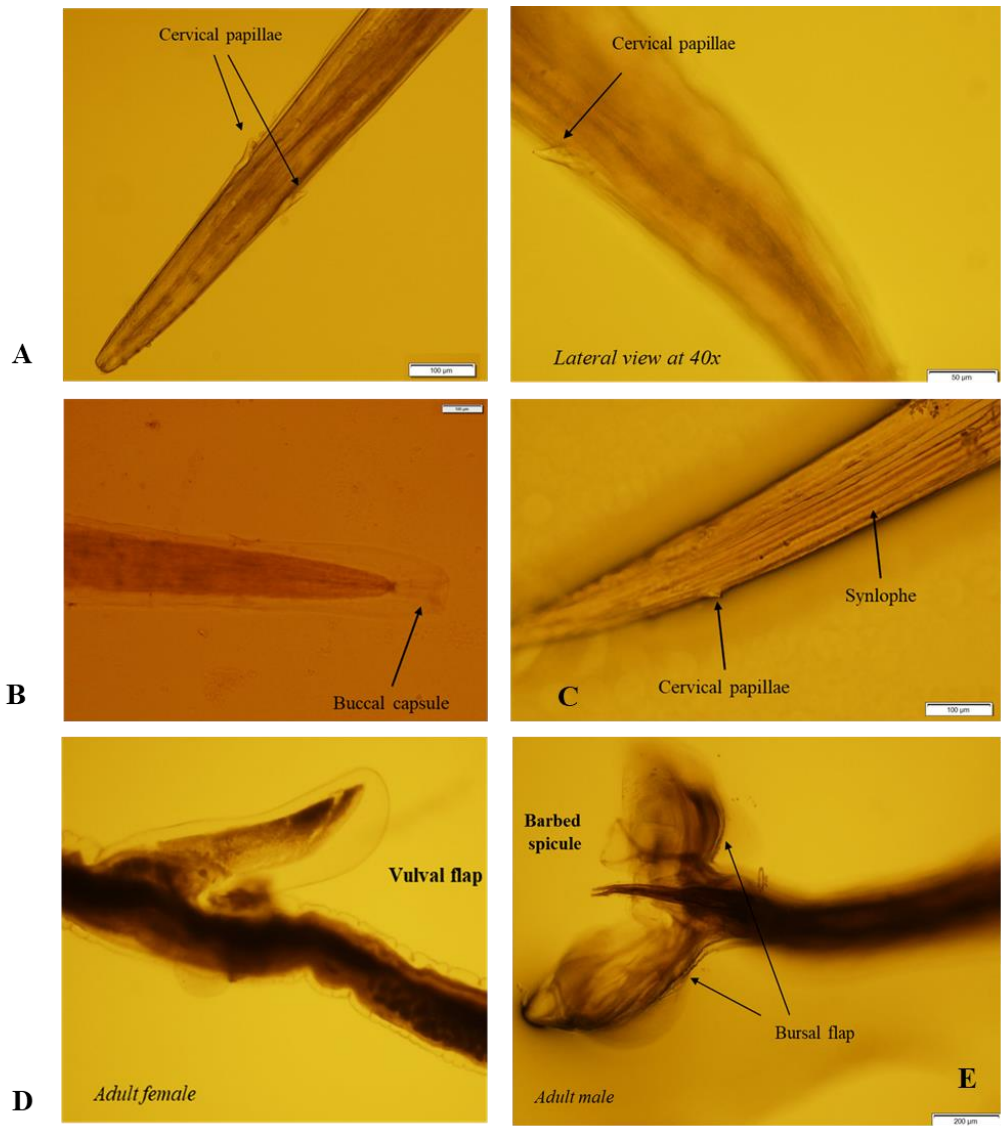

Figure 11: Light microscopy result of adult *H. contortus*. A: anterior end showing the cervical papillae at different magnifications; B: anterior end showing the buccal capsule; C: longitudinal striations called 'synlophe'; D: vulval flap in females; D: bursal in males

Some selected photographic records of the commonly encountered parasite eggs in the routine FEC examination are shown in Figure 12 while a photo panel of commonly occurring nematode eggs for small ruminants are shown in Appendix Figure 1-B (for comparative purposes). As discussed earlier, only the eggs of *N. battus* can be easily identified due to their reasonably large size and oval-shaped egg with an embryo

inside (Figure 12-B). The other most commonly encountered parasite in the study was the Strongyloides worm, which could be observed as larvated eggs (Figure 12-A). Interestingly, a certain number of individual samples (n=84) presented suspected tapeworm species (Figure 12-A, denoted as 'TW') as well as suspected coccidian ova (Figure 12-E, denoted as 'CX'). The tapeworm species is highly suspected to be of *Moniezia* spp, characterised by its distinctive triangular-shaped egg with thick walls and the slightly visible pyriform apparatus inside it. Basic morphometric measurement of the positive control *H. contortus* eggs from the MD sample was also performed and the result is shown in Figure 12- C.

The average dimension of all the samples analysed ranged from 39-43μm in width and 68-89μm in length. The eggshell was observed to be thin, ovoid, slightly yellowish and contained blastomeres inside it. The blastomeres could be either distinctively organised as well as observed to be distributed fully inside the egg (Figure 12 D-E). It should also be noted that certain artefacts (Figure 12-E) were also observed in many of the samples. These artefacts could consist of pollen materials, undigested/semi-digested feed particles and even tiny air bubbles.

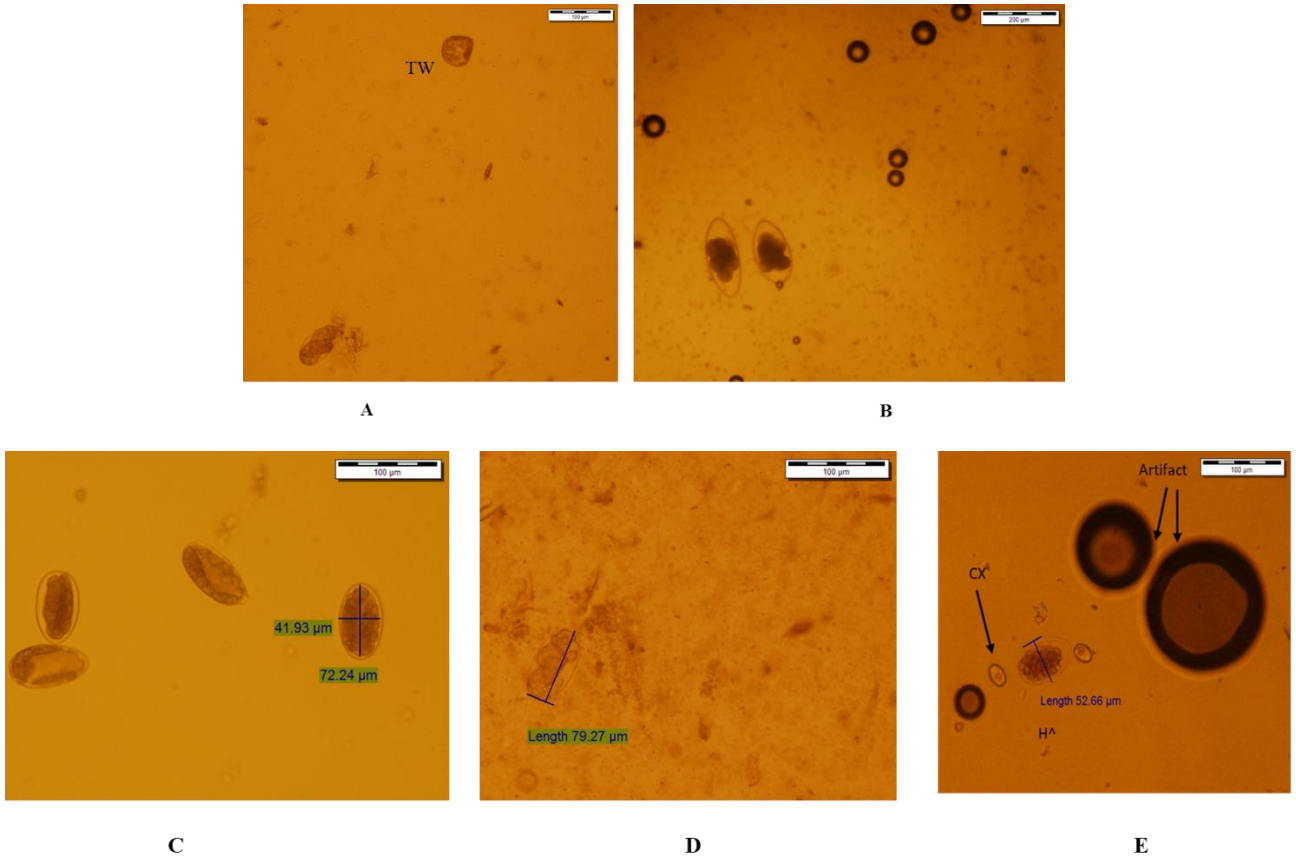

Figure 12: Light microscopy result of parasite eggs observed in routine FEC examination. A: suspected tapeworm (TW) and a Strongyloides; B: *N. battus* egg; C: morphometry of *H. contortus* eggs from MD sample; D: *H. contortus* from a farm sample; E: artefacts and mixed parasite eggs from a farm sample.

4.1.2 *PNA fluorescence microscopy*

Those samples suspected to have *H. contortus* from the initial FEC examination were processed for PNA fluorescence microscopy of which the result is shown in Figure 13 (for positive control specimens) and Figure 14 (for farm samples). Positive *H. contortus* eggs were visualised as bright-green stained outlines with some degree of fluorescence stain inside the eggs also (PALMER and McCOMBE, 1996). Figures 13-A and B show UV-illuminated and normal light modes of the same field of view of the positive control eggs with the blastomeres well-filled inside the eggs while Figures 13-C and D show an egg with a clearly defined blastomere. In both these panels, the outline of the eggs was stained in bright green and the blastomeres/embryo also took up the stain. Notably, under the normal light field of view, Figure 13-D could have been 'easier' to be scored as more *H. contortus* egg-like as per many literature and images available for *H. contortus* egg. For instance, SOULSBY (1968) noted that *H. contortus* eggs generally have 16-32 cell stage embryos. This is just a thumb rule and not all eggs of this parasite can be easily differentiated based on the number of cells. The finding of this study also confirmed this, as shown in Figures 13-A and Figures 13-E and F. Here, the embryos also took up the stain slightly but the number of cells could not be counted as easily. The normal light field of view of the same specimen could have been at best identified as 'trichostrongyle/strongylid- eggs' but PNA fluorescence confirmed this as *H. contortus* eggs. The finding reported here is also consistent with that of other PNA fluorescence studies (JURASEK et al., 2010; DOUANNE et al., 2019).

The results of this technique for eggs recovered from farm samples are presented in Figure 14. Interestingly, several eggs that could be marked as *H. contortus* based on the forms/shapes of the blastomeres under normal light were non-*Haemonchus* actually, as seen in Figures 14 - A and B. Also, farm samples were usually found with mixed infections. Yet, PNA can effectively discriminate against this. For example, a suspected tapeworm (TW) egg and another trichostrongylid egg (red arrow) are shown in Figure 14- C and D. Although COLDITZ et al., (2002) noted that *Moniezia* spp could take up a slight stain, the suspected tapeworm of *Moniezia* spp (TW) did not take up any stain while the trichostrongylid egg took up a faint stain with an unclear outline (Figure 14 - C). At times, larvated/embryonated *H. contortus* eggs could also be detected (Figure 14 - G and H) and could be misdiagnosed as a *Strongyloides* spp egg (Figure 14 E-F). Figure 14 – I (at 10x magnification) shows a field of view of a mixed infection presenting two *H. contortus* eggs as well as another strongylid egg (red circle).

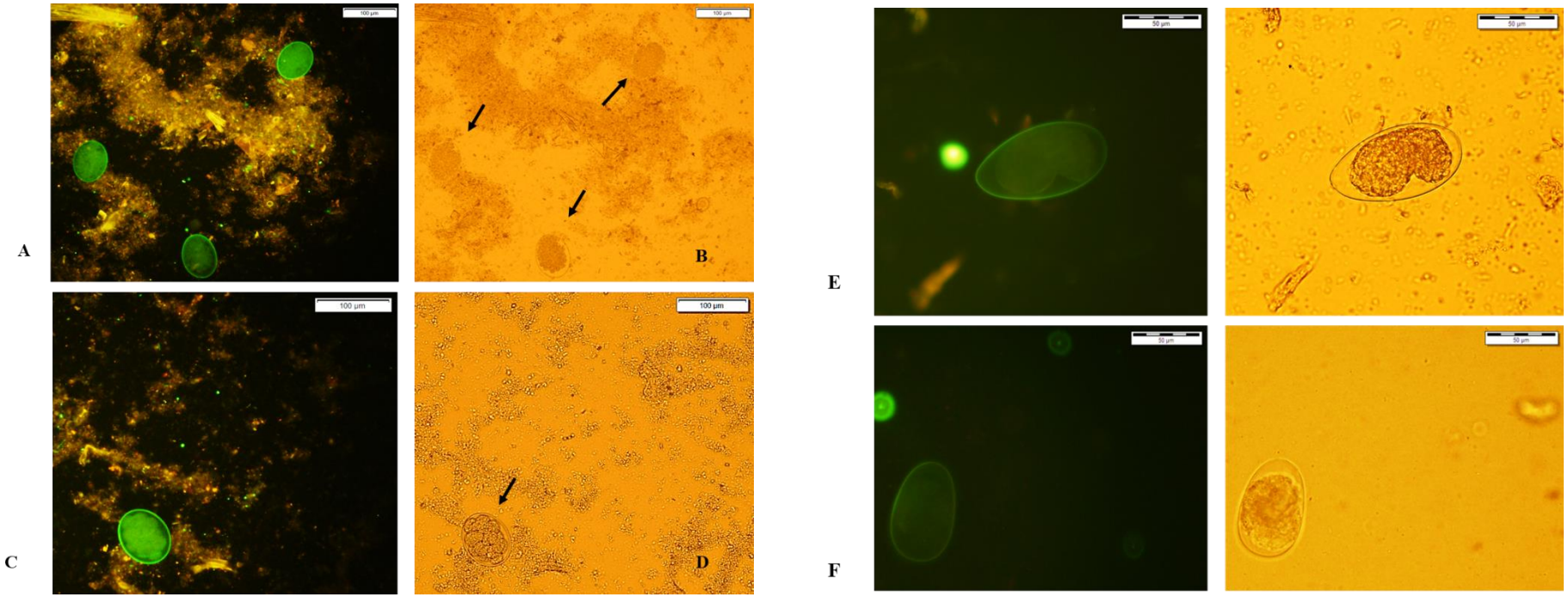

Figure 13: PNA fluorescence microscopy results of the positive control *H. contortus* eggs. The positive result is characterised by a bright green and clearly stained outline of the eggs. Left-side of each panel shows the UV-illuminated field of view while the right side shows the normal light field of view of the same specimen. Magnification of A-D is 20x while E-F is at 40x; A-B: blastomeres can be seen filling up inside the egg; C-D: very well-defined blastomeres with visibly countable dividing cells; E-F: 40x magnified view of *H.contortus* egg stained with PNA; Black arrows show the egg positions

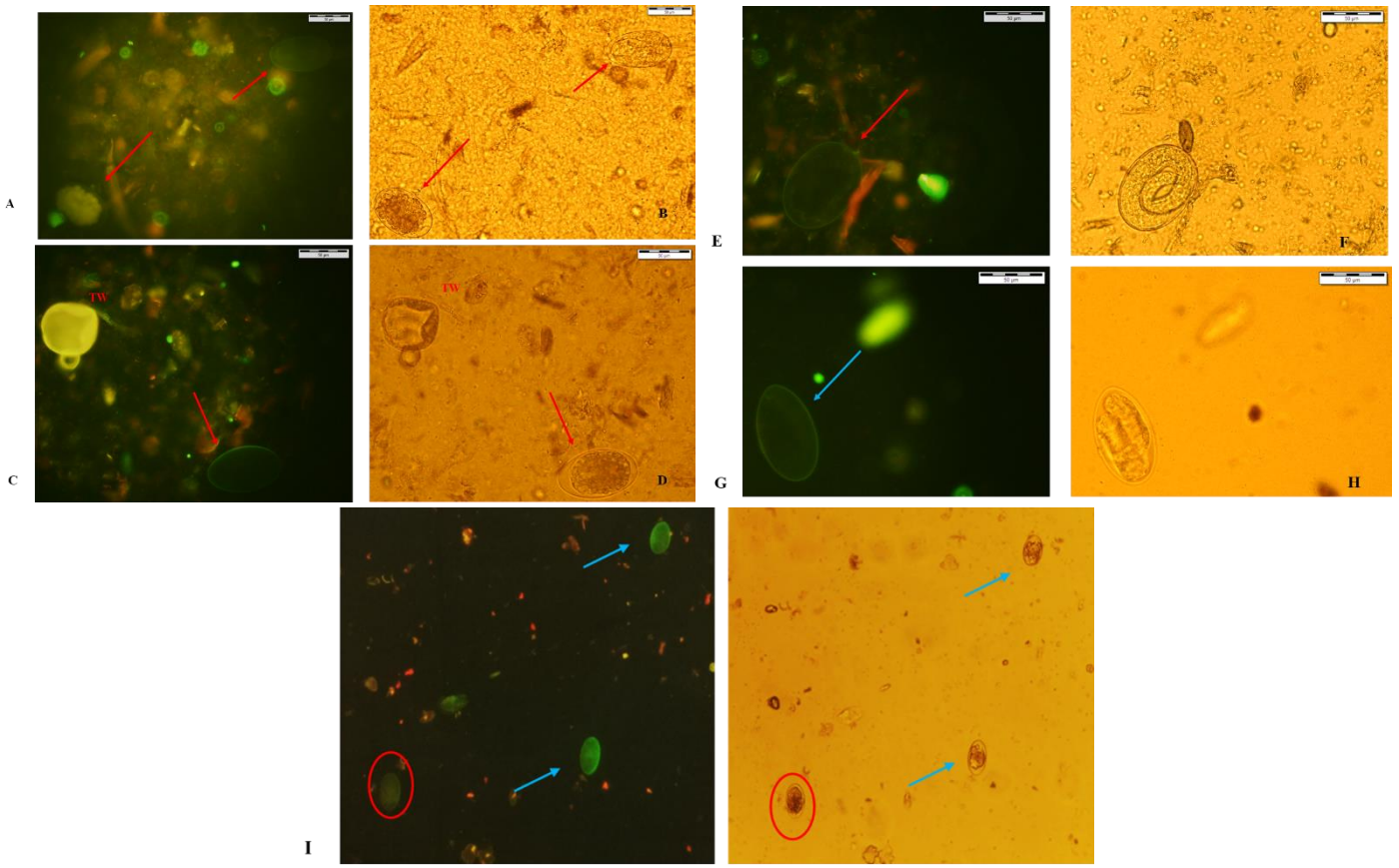

Figure 14: PNA fluorescence microscopy results of the eggs obtained from farm samples. Magnification for A-H is at 40x while 10x for I. The positive result is characterised by a bright green and clearly stained outline of the eggs. Left-side of each panel shows the UV-illuminated field of view while the right side shows the normal light field of view of the same specimen. A-B: suspected *H. contortus* eggs under normal light but found to be negative under PNA fluorescence microscopy; C-D: a tapeworm (TW) egg and a trichostrongyle-egg; E-F: *Strongyloides* spp egg that did not stain; G-H: a 'larvated' *H. contortus* egg taking up the stain; Blue arrow = larvated eggs; Red-arrow and red-circle= negative eggs

4.2. Farm location, meteorological data and brief prevalence report

The sheep farms involved in this study are shown above in Figure 7 and designated as F-1 to F-14, and a pooled faecal sample from a goat farm (FG) and adult worms from the abomasum of roe deers (*Capreolus capreolus*) from location FD were also collected. The positive control specimens were obtained from three sources, namely the Department of Zoology and Parasitology, University of Veterinary Medicine, Budapest, Hungary; Institute of Parasitology, Kosice, Slovakia and the Moredun Research Institute, Scotland (designated as BP, KS and MD respectively).

As mentioned earlier, only the average FEC data of the farms are shown in Table 4. The detailed species-wise FEC is not under the purview of the study as this is part of a concurrent study that deals with the epidemiological study of trichostrongylid nematode worms in Hungary. Nevertheless, microscopic analysis as discussed above showed the detection of the parasite in question. It should be noted that the sampling of farms F-1 to F-9 were done from Autumn-Winter 2018 and in Spring 2019 while F-10 to F-14 were done during the Spring and Autumn of 2021-2022.

Among the fourteen farms covered in the study for FEC examination, F-5 registered the highest average of FEC (= 1750 EPG) and F-6 recorded the lowest average FEC (= 5.7 EPG). It should be noted that F-1 already had a confirmatory diagnosis of haemonchosis by an independent veterinary laboratory as reported by the farmer. On the sampling visit, our team could also notice the poor health condition score of many animals (data not shown; Toth unpublished). As expected, the farm had a positive result in our subsequent assays as well as above discussed microscopic analysis of this study. F-6 and F-14 (FEC = 22.2 EPG) did not detect any *H. contortus* eggs. Interestingly, F-5, F-8 and F-12 all detected a high number of other parasite species eggs, especially tapeworm (and *Coccidia* spp. up to some extent). Also, the degree of intensity of the farms is shown in Table 4 as per the intensity of FEC interpretation criteria laid down by TAYLOR et al., (2015) for mixed infection in small ruminants.

The study also attempted to analyse if the climatic conditions of the farms have any relation with the FEC output, especially of *H. contortus* eggs. For this, only the farms F-1 to F-9 were utilised as the data collection was done more uniformly within two seasons while the other farms could not be uniformly collected due to the covid-19 pandemic. The meteorological data of the farms are shown in Appendix Table 2, where the FEC was compared against the average temperature, cumulative rainfall and average relative humidity. It was found that there was no significant correlation between the average

temperature and the mean FEC vs average temperature (p=0.20), FEC vs relative humidity(p=0.26) and FEC vs Rainfall (p=0.86).

Table 4: Average FEC of the sheep farms involved in the study and degree of infestation as per TAYLOR et al., (2015); Light: <250 EPG; Moderate: 1000 EPG; Heavy: +2000 EPG.

Farm ID	Average FEC (in EPG)	Degree of Infestation	Remarks
F-1	600	Moderate+	The farmer already reported positive haemonchosis
F-2	150	Light	
F-3	276.4	Moderate	
F-4	982.2	Moderate+	
F-5	1750	Moderate++	Mixed infection with other parasite families
F-6	5.7	Light	Negative for *H. contortus*
F-7	113.7	Light	
F-8	767.2	Moderate+	Mixed infection with other parasite families
F-9	168.0	Light	
F-10	159.7	Light	
F-11	577.1	Moderate	
F-12	754.2	Moderate+	Mixed infection with other parasite families
F-13	70.9	Light	
F-14	22.2	Light	Negative for *H. contortus*

It can be seen that there could be a wide gap/range in the FEC among the 'Moderate' groups, for instance. Thus, FEC might not reflect the reality of the worm burden. This is because the FEC and worm burden could not be definitively proven to be correlated as various factors can affect this (RINALDI, 2014). For instance, the host's immunity to the parasites and the age at infection; hypobiosis, and fecundity of the parasite could all contribute to the egg-shedding variations (MCKENNA, 1987; TAYLOR, 2010; RINALDI, 2014). Thus, this interpretation of the intensity should not be treated as an absolute clinical measure but only an indication of the infection load and

a piece of supportive evidence to diagnose alongside other clinical findings (TAYLOR et al., 2015) of the animal affected.

4.2.1 *Recapitulation of microscopic examination and FEC results*

Morphological examination of the recovered worms at the time of necropsy still proves to be a very important piece of evidence for the identification of the causative parasite. The only main demerit in this is the expertise requirement and time consumption. Yet, a detailed study of morphology and morphometry using sophisticated microscopy could shed light on the importance of minute morphological differences that might differentiate the parasite even at the species level. For instance, a recent study by GAREH et al., (2021) that utilised both light microscopies, as well as scanning electron microscopy, revealed the importance of this. The study reported the identification of three *Haemonchus* species from goats in Egypt, namely *H. contortus, H. placei* and *H. longistipes*. This is important and noteworthy in light of claims from reputable sources that *H. contortus* and *H. placei* are only strain variations of the same parasite depending on the host animal (AMARANTE, 2011; TAYLOR et al., 2015). As such, the morphological results reported in this study were also consistent with that of the recognised literature on the subject as SOULSBY, (1968) as well as with other studies on morphology (AMARANTE, 2011; WIDIARSO et al., 2018; GAREH et al., 2021). Except for a few female specimens (n=4), all of them presented the characteristic linguiform vulval flap although SOULSBY (1968) and AMARANTE (2011) claimed there are variations like a knob-like vulval flap. Moreover, the male spicule is regarded as more significant evidence as well as the easiest in discriminating species (AMARANTE, 2011; GAREH et al., 2021). This study also reported consistency in the spicule morphology of all the analysed male specimens.

Regarding the routine FEC examination, it has been over a century since the first parasite faecal egg counting techniques were designed and adopted. Yet, this technique for enumeration and identification continues to be valid and a requirement in routine parasitology research and clinical examination. The technique has been advancing with time and more refined and even automated tools are being developed to reduce the cost, time and expertise requirements. The results obtained in this study also aligned with the literature as well as many studies (BARDA et al., 2013; DOMKE et al., 2013; TAYLOR et al., 2015; LJUNGSTRÖM et al., 2018) and the data obtained from this study can be used to contribute to a general screening tool to detect the presence of the important GIN parasites in Hungary. For large sample sizes, the composite method of FEC using pooled

sampling also offers substantial advantages without compromising on the result accuracy (NICHOLLS and OBENDORF, 1994; KENYON et al., 2016; RINALDI et al., 2019). Extreme caution was taken so that the artefacts were not confused/misdiagnosed as parasitic eggs. It should also be noted that mixed infections are quite common in field cases (BESIER et al., 2016a; ZARLENGA et al., 2016) and this can affect the clinical diagnosis and the subsequent treatment plan of the flock also, such as in TST (KENYON et al., 2009). Hence, a more detailed and species-specific diagnosis for an elaborate epidemiological study and an effective treatment plan could be done once FEC is established.

Lectin staining properties are varied between eggs of various genera of GIT nematode worms and *H. contortus* has been proven to be strongly PNA positive (PALMER and McCOMBE, 1996; HILLRICHS et al., 2012; UMAIR et al., 2016; ABBAS and HILDRETH, 2019). The PNA staining pattern could vary depending on the egg stage, such as larvated and/or embryonated as previous studies (COLDITZ et al., 2002; DOUANNE et al., 2019) have also reported that even larvated *H. contortus* eggs could take up stains and this could aid in reducing false negatives. The PNA staining pattern was also reported effective at differentiating *Haemonchus* from *Trichostrongylus* spp eggs during field infection (ABBAS and HILDRETH, 2019) with no significant biases in the examiner's interpretation of the result (JURASEK et al., 2010) and can be adapted for quantification using a fluorescence plate reader (DOUANNE et al., 2019). The results of this study also proved to be consistent with these findings. However, the quantitative analysis of this technique is beyond the scope of this study but a per cent of *H. contortus* eggs detected for the farms is presented in Appendix Table 1.

Temperature and moisture conditions are the prevailing factors which impact the free-living stages of *H. contortus, T. circumcincta* and *T. colubriformis*. In general, *H. contortus* is most susceptible and least by *T. circumcincta*. Also, the duration of the life cycle is reliant on temperature, with the developmental rate growing at warmer temperatures. Also, the phenomenon of hypobiosis during unfavourable environmental conditions also greatly affects the maturating and subsequent faecal egg shedding (O'CONNOR et al., 2006; TAYLOR et al., 2015; BESIER et al., 2016b). The finding of this study showed no significant correlation between the analysed meteorological data and the FEC. This could be due to hypobiosis and the small sample size. Also, it is worth noting that regional variation might be possible considering that certain farms shared very similar climatic conditions but showed no significant difference (Appendix Table 2).

Thus, further in-depth meteorological analysis along with the spatial distribution pattern study is warranted.

4.3. LAMP assay

4.3.1 *Optimisation, analytical sensitivity analytical specificity*

Initial optimisation of the LAMP assay was performed to define the optimal temperature for the reaction using the WarmStart® Colorimetric LAMP 2x Master Mix (New England Biolabs, UK) and the result is shown in Figure 15. Although amplification was detected in all the temperature ranges (Figure 15-A) during optimisation, subsequent analysis was adopted at 62ºC arbitrarily. Also, the assay was initially run for a maximum of 45 min although subsequently, a 30 min reaction time was determined to be acceptable. The two positive control templates (BP and KS) utilised used during this initial stage did not show any false results, thus confirming the integrity of the optimisation process. For visual detection, the positive result was interpreted as a colourimetric change from pink/purple to yellow/orange as specified in the kit manual (Figure 15).

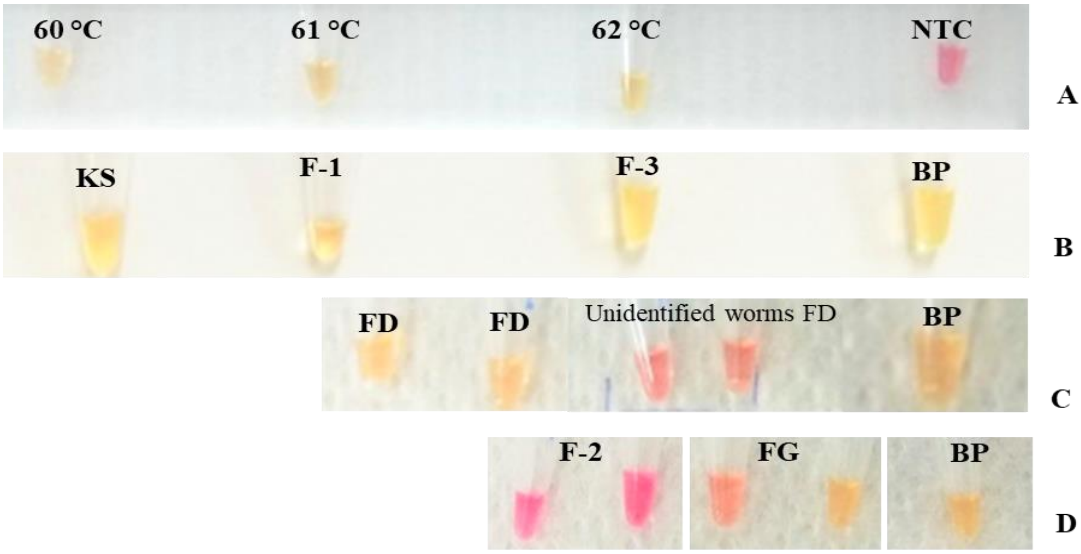

Figure 15: Optimisation of LAMP assay. A: optimised temperature; B: farm DNA isolate tested with optimised time-temperature; C: DNA templates from adult worms; D: optimised time-temperature with goat farm and non-trichostrongyle detected farm; NTC: non-template control; BP: positive control template from Budapest; KS: positive control template from Kosice; F1-F3 and FD-FG: farm sample gDNA. NTC: Non-template control; Pink/Purple = Negative; Yellow/Orange = Positive

To verify the result of the arbitrarily chosen temperature-time combination described above, LAMP assay was also performed using farm samples F-1 and F3 and a positive result was detected (Figure 15-B). These two farms were randomly selected and

had a history of suspected haemonchosis with already detected trichostrongyle eggs. Furthermore, gDNA extracted from the suspected *H. contortus* adult worms, obtained from the abomasum at post-mortem from a hunted roe deer (Farm FD), showed positive results while the gDNA samples of a few unidentified worms collected from the same FD were found to be negative during this optimisation stage (Figure 15-C). Similarly, gDNA isolated from faecal samples from goats (Farm FG) were also tested and found positive for *H. contortus* (Figure 15-C). However, pooled faecal samples (Farm F-2) of individual sheep with no trichostrongyle egg counts observed during FEC gave negative LAMP results (Figure 15-D), although subsequent LAMP trials of pooled samples from the same farm inclusive of all individual samples were found to give a positive result.

The detection range of the assay was found to be 2.5 x 10^{-1} ng/µl to 2.5 x 10^{-4} ng/µl based on the 10-fold serially diluted BP positive control template LAMP assay (Figure 16). The sensitivity of our assay was also found to be close to that of MELVILLE et al., (2014) which reported a minimum detection limit of '10^{-5} ng/µl' of serially diluted positive control gDNA. The minor decrease in the sensitivity of LAMP in this study compared to that of the original study (MELVILLE et al., 2014) could be justified by the difference in the end-result detection system. Whereas the original study employed the UV illumination technique, this study LAMP assay simply relied on naked-eye detection of colourimetric change. Yet, this colourimetric detection offers the advantage of minimal equipment usage for a POC diagnosis system.

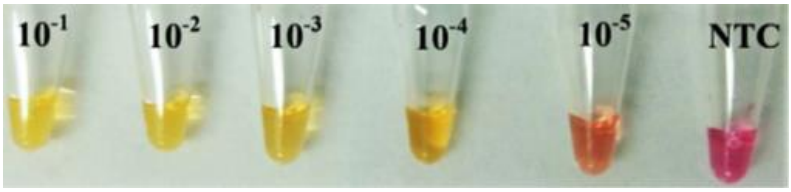

Figure 7: Analytical sensitivity of the colourimetric LAMP assay in this study performed using a 10-fold serially diluted positive control gDNA. NTC: non-template control. NTC: Non-template control; Pink/Purple = Negative; Yellow/Orange = Positive

For specificity analysis, nine positive control specimen worms of the trichostrongylidae family were used as the template gDNA for the LAMP assay and the result is shown in Figure 17. As anticipated, only the gDNA of the *H. contortus* showed a colour change to yellow-orange meaning a positive result (Figure 17-B lower panel).

Whereas, the other eight species showed shades of pink-purple that are nevertheless significantly differentiated from the positive result colourimetric value (Figure 17-B upper panel). To further prove this, the single-species ITS2-PCR showed the same result (Figure 17-A). Besides, it should be noted that the primer set in use had already been tested for *H. contortus* specificity by MELVILE et al., (2014). This study expanded the scope of this original study by utilising a commercially available colourimetric kit adaptable for a naked eye detection system. This was done with the aim of a proof-of-concept diagnostic kit that can be adapted at the POC level.

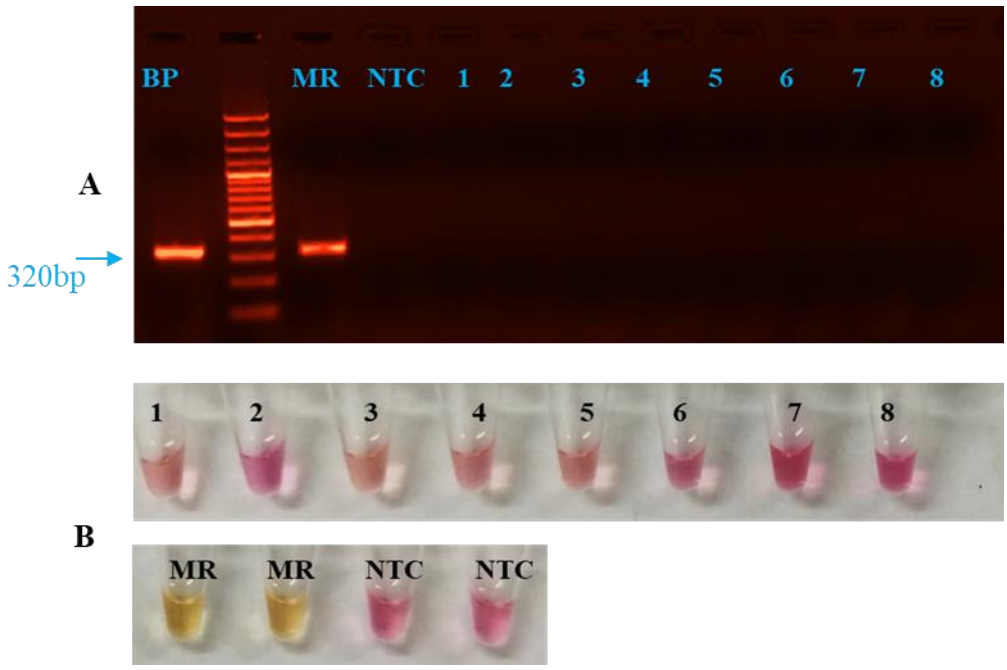

Figure 8: Specificity validation of the LAMP assay using the nine positive control parasite specimen from the Moredun Research Institute. A: ITS2 PCR result. 100bp ladder; B: LAMP assay using the same gDNA from the worm specimen. 1 = *N. battus*, 2 = *T. axei;* 3 = *T. vitrinus;* 4 = *T. colubriformis;* 5 = *T. circumcincta;* 6 = *O. venulosum;*7 = *T. ovis;* 8 = *C. curticei*; MR: *H.contortus* positive control from Moredun; NTC: Non-template control; Pink/Purple = Negative; Yellow/Orange = Positive

Thus, after adequate optimisation, the LAMP assay was adopted for the subsequent validation with ITS2 PCR and further farm sample trials as described later on. Later on, the assay was performed using the WarmStart® Colorimetric LAMP 2x Master Mix with UDG (catalogue number M1804S). Using this kit containing uracil-DNA glycosylase (UDG) reduced any carryover contamination (KIM et al., 2016) and subsequently

minimised the risk of false positive results as LAMP amplicons are highly stable and difficult to decontaminate.

4.3.2 *Individual and pooled sample LAMP assay*

After the optimisation, the assay was tested more by expanding the sample size and also including samples from individual sheep as well as pooled samples. This was done with the objective to verify the assay's diagnostic sensitivity for individuals as well as flocks. The result of this is shown in Figure 18. It should be noted that there are already reports validating the necessity as well as the advantage of pooled faecal sampling for parasitic disease detection (NICHOLLS and OBENDORF, 1994; KENYON et al., 2016; PARAS et al., 2018; RINALDI et al., 2019).

Farm F-4 faecal samples recorded a very high trichostrongyle FEC (Table 4) with some individual samples suspected of having *H. contortus* eggs. LAMP assay using these individual samples as well as pooled samples detected positive results (Figure 18A-B). Faecal samples from Farm F-6 were already found to have a very low average egg count (EPG = 5.96) and no detectable trichostrongyle eggs by microscopic analysis (Toth et al., unpublished). The LAMP analysis of randomly selected individual samples of F-6 was found to have negative results (Figure 18-C). Similarly, pooled and individual samples were examined from Farm F-8 and also tested positive (Figure 18-D).

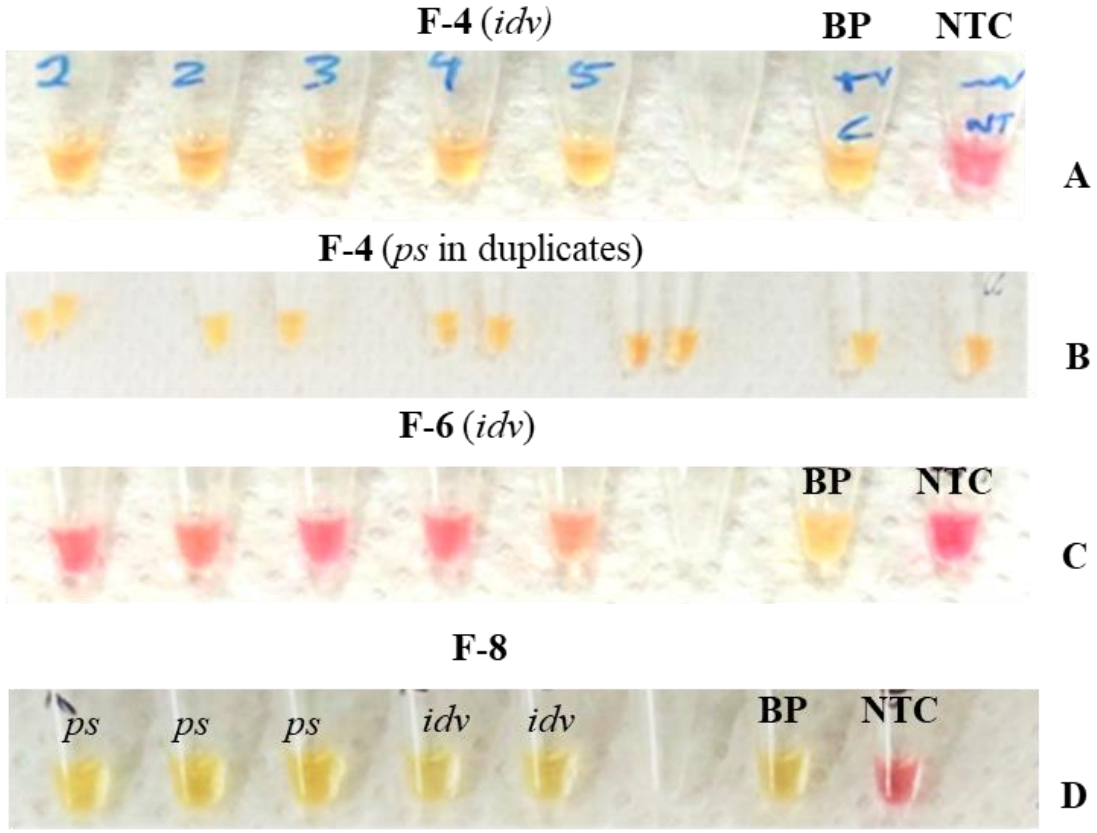

Figure 9: LAMP assay using the individual as well as pooled faecal samples. A: individual faecal sample DNA templates of F-4; B: pooled faecal sample DNA template of F-4; C: individual faecal sample DNA templates of F-6, which was used as negative control farm sample; D: individual and pooled faecal sample DNA templates of F-8; F-4 to F-8: farm gDNA; *idv*: individual sample; *ps*: pooled sample

4.3.3 *ITS2 single-species PCR validation*

Following the predicted detection of *H. contortus* in some farms mentioned above, ITS2 single-species PCR was performed to validate the LAMP assay and the result is shown in Figure 19. Farms F-1 to F5; F-7 to F-13; FD and FG were all recorded to have positive results while farms F-6 and F-14 recorded negative results in both the PCR and LAMP. None of the controls used showed false results. Briefly, it can be concluded from Figure 19 that there was 100% agreement between the two molecular-based assays.

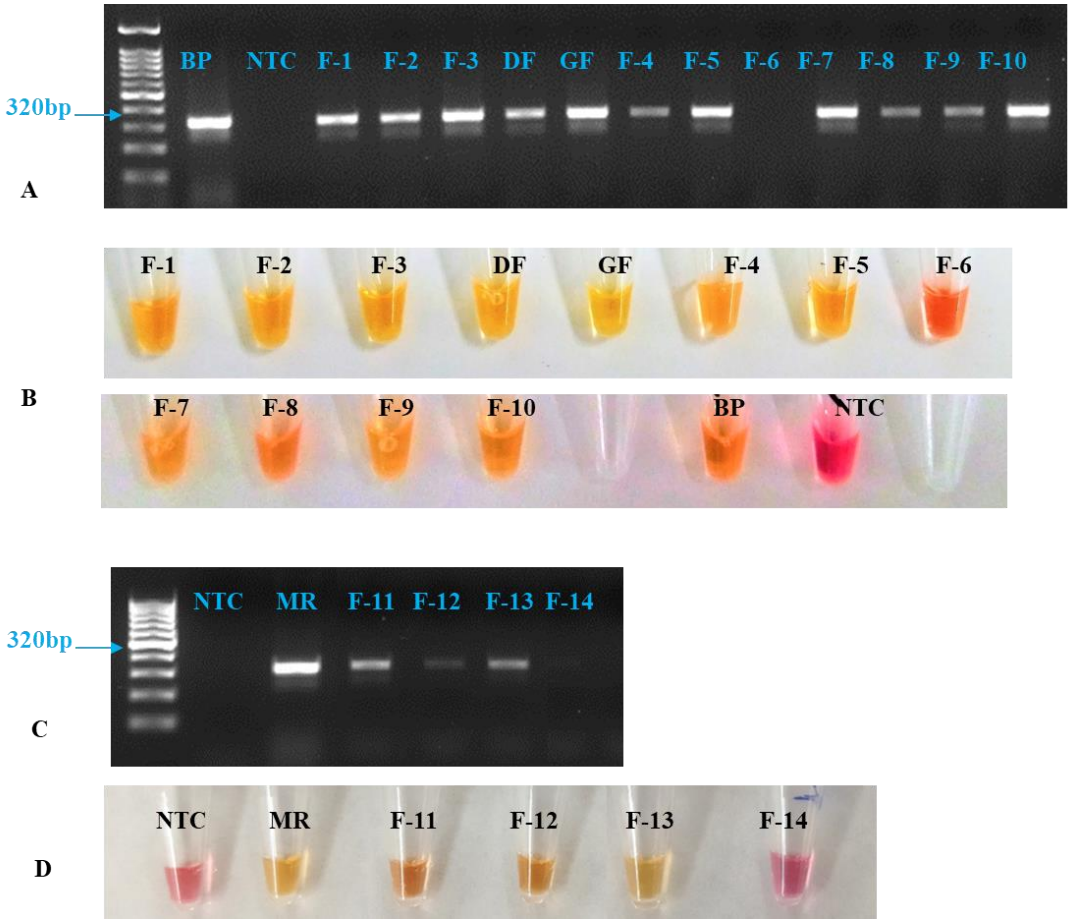

Figure 10: Single-species ITS2 PCR validation of the LAMP assay. A and C: ITS2 PCR result. 100bp ladder; B and D: LAMP assay using the gDNA from various farms; BP: *H.contortus* positive control template from Budapest; MR: *H.contortus* positive control template from Moredun; NTC: Non-template control; Pink/Purple = Negative; Yellow/Orange = Positive

4.3.4 *Recapitulation of the LAMP assay results*

Initial optimisation of the colourimetric LAMP assay was achieved using positive control gDNA samples from Slovakia and in Hungary (KS and BP, respectively) and later on expanded by utilizing positive control specimens from Scotland (MD). Once the optimised conditions were established, a validation of the assay on several farm template gDNA obtained from various farms in Eastern and South-Eastern Hungary (Figure 7) was also performed. The purpose of using these field samples was two-fold. Firstly, it was attempted to further validate the primers published in MELVILLE et al (2014) and to demonstrate that these primers were equally operational in a geographically and genetically distinct population of *H. contortus* from that tested in the original study. This was deemed necessary as this nematode parasite can display a high degree of both inter- and intra-isolate diversity (LAING et al., 2013; DOYLE et al., 2020).

Moreover, the results of the LAMP assay were in 100% agreement with those of the established ITS2 speciation PCR (Figure 19), showing the presence of *H. contortus* within those samples. It is also worth mentioning that farm F1 reportedly has a history of clinical haemonchosis and had been previously diagnosed by an independent veterinary laboratory. Subsequent analysis of the faecal samples by PNA fluorescence microscopy for F1 samples already detected *H. contortus* eggs. Also, farms F6 and F14 had a record of low EPG (Table 4) and the LAMP assay for both of these farms gave negative results which were also validated by the PCR (Figure 19). Subsequent tests of the optimised LAMP on DNA from individuals, as well as pooled samples, gave no false results (Figure 18-A and B). This was also true for F6 individual samples (Figure 18-C). It should be noted here that farm F2 had a significant number of eggs when counted by microscopy but only a few samples had suspected trichostrongyle eggs. Thus, two batches of pooled samples were prepared: one excluding the suspected trichostrongyle egg samples and another inclusive of all. LAMP assay showed negative and positive results, respectively for these two pooled samples.

It can be seen here that there was a difference in the shades of the colourimetric change of the results of the positive farms in the LAMP assay. It is worth noting that the colourimetric change could be largely affected by certain factors such as the lighting, the observer's point of view, the kit mechanism of action (the dye used, pH value etc) and the integrity of the starting DNA (MORI et al., 2013; DASKOU et al., 2019; LAI et al., 2020; PELTZER et al., 2021). For instance, F-12 and F-13 showed a weaker shade of pink (Figure 19-D) but this also corresponds to the weak band detected in the PCR result (Figure 19-C) which might be due to a low amount of DNA. Moreover, the LAMP assay here is

qualitative at this stage and a proof-of-concept for a probable farm-site molecular-based diagnostic system. However, the two independent observers' interpretation of the colourimetric changes showed no significant differences as a positive result was interpreted as orange-yellowish colour and a negative result as pink-reddish.

All the above evidence affirms that the assay can qualitatively predict the presence of *H. contortus*. If this qualitative detection is incorporated with FEC figures obtained on the spot, for instance by using Mini-FLOTAC® with a battery-operated portable microscope, it could aid in giving clinically relevant information to the farmers. The idea of minimal equipment usage was also the reason behind the adoption and use of the small-sized mini heat-blocks (VWR® Advanced Mini Dry Block Heaters) throughout all LAMP runs following the initial optimization. This yielded positive results and was indistinguishable from the use of a commercial thermocycler. Our minimal equipment set-up has thus been designed with the POC in mind, with each piece of equipment requiring low power input which could easily be supplied by a portable generator.

4.4. Crude DNA extraction trials

For the Chelex® reagent-based methods, no positive LAMP results were obtained. Also, the KS samples for Chelex® Method 1 could not yield any reading as the analyte was not clear enough for the absorbance reading.

The genesig®Easy DNA/RNA Extraction Kit (Primerdesign Ltd, UK) which utilises a magnetic bead extraction protocol gave inconsistent LAMP results. One replicate of the positive sample KS showed a negative result (Figure 20-A). Yet, both replicates from Farm F-4 showed positive results while that of Farm F-6 showed negative results, as expected (Figure 20-A).

For the bead-beating technique, the supernatant from the direct Fill-FLOTAC® solution did not yield any positive results by LAMP (Figure 20-B). However, the protocol was slightly modified by using the benchtop low *g* centrifuge machine. This led to an improvement in the detection of *H. contortus* DNA from the sample used as two out of three technical replicates gave positive LAMP results (Figure 20-C).

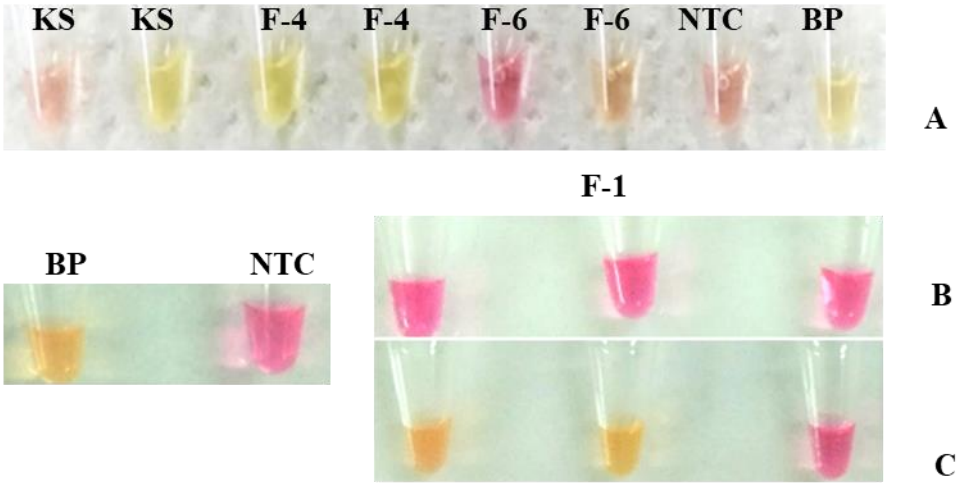

Figure 11: LAMP assay for crude DNA extraction. A: crude DNA templates obtained using magnetic bead extraction protocol; B: crude DNA templates obtained using bead-beating protocol and Fill-FLOTAC solution; C: crude DNA templates obtained using bead-beating protocol using Fill-FLOTAC solution with low *g* centrifuge; BP and KS: positive control template from Kosice and Budapest; F-1 to F-6: farm samples. NTC: Non-template control; Pink/Purple = Negative; Yellow/Orange = Positive

For the micropestle-crude DNA extraction method, microscopic analysis of the suspension after the application of the micro-pestle action showed the breaking of eggshells (Figure 21 – C) and PCR analysis of the subsequently extracted DNA yielded positive results (Figure 21-B).

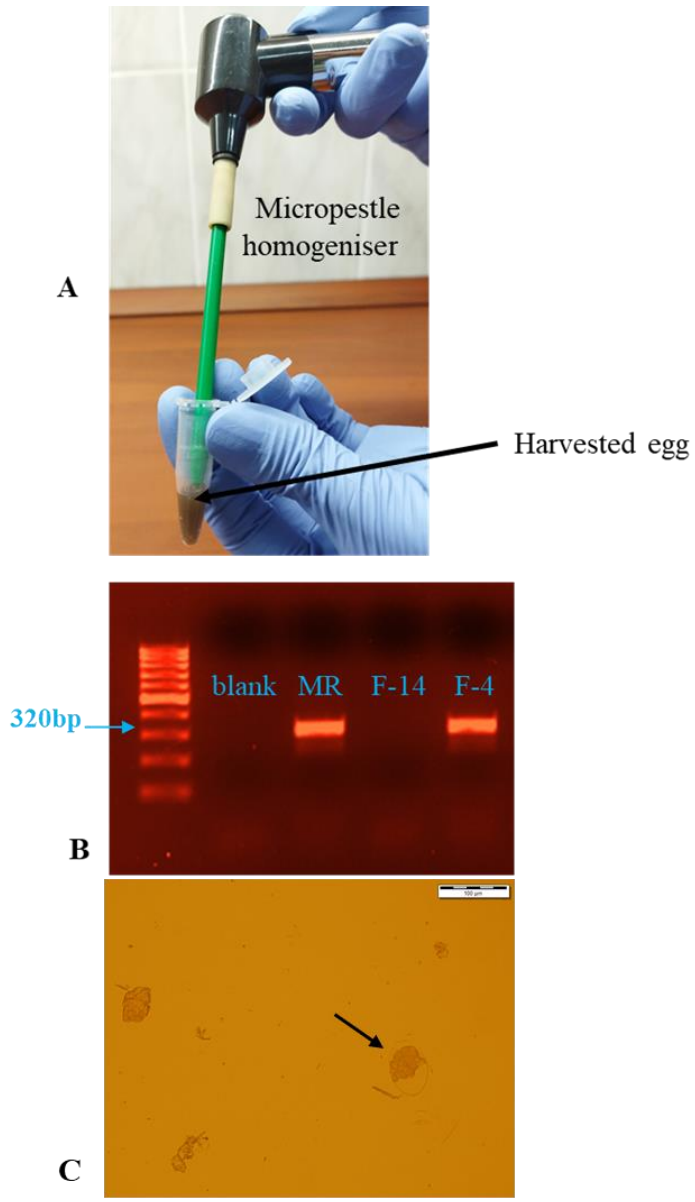

Figure 12:: Micropestle homogeniser crude DNA extraction. A: micropestle application.; B: ITS2 PCR; C: microscopy photograph of a broken eggshell (pointed with arrow) at 20x magnification; MR: positive control template; blank: control tube with no eggs in suspension; F-4:positive farm sample; F-14: negative farm sample

4.4.1 *Recapitulation of crude DNA extraction results*

All these various methods mentioned above were done to reduce the need for sophisticated laboratory equipment at the farm as well as to obtain DNA quickly as possible given the POC setting application. This is an important inclusion in the study as DNA extraction presents the current rate-limiting step, owing to the requirement of high-grade centrifugation equipment in most commercial kits. Proteinase K digestion is commonly used to produce crude lysates, and plenty of commercial kits use silica membrane-based technology for DNA isolation and elution. Both these techniques require relatively high-power centrifugation. Moreover, they are time-consuming in the sense that they generally demand long protein digestion and inactivation period. Although the Chelex® reagent-based DNA extraction was already shown to be effective in crude DNA lysis for other target samples (AWAWDEH et al., 2019; GUEVARA et al., 2018), a concrete result could not be obtained in this study. This might be attributed to the comparative difficulty in breaking the tough egg wall of the parasite in question.

Of the centrifuge-free DNA extraction methods tested, the genesig® Easy DNA/RNA Extraction Kit (Primerdesign Ltd, UK) yielded promising results. Comparing DNA yields, it was found that there was a lower yield obtained with magnetic bead extraction, although this is compensated by the ease of POC flexibility of this magnet-based kit. For the glass bead-beating lysis method, there was an inconsistent result as only two out of the three replicates yielded a positive result when combined with egg concentration steps. This inconsistency might be because of the scarce number of eggs in the pellets obtained due to the low-power vortexing (and centrifugation) ability of the portable centrifuge device used during egg concentration. This technique could be improved if a larger starting volume for the pellets was available and also by using a stronger centrifugation/vortexing device with adequate farm site adaptability.

Keeping this in mind, the motorised micro-pestle method was designed and tested. This resulted in a sufficient breaking of the egg wall at the same time eliminating the need for centrifugation and vortexing. When the magnet-based DNA kit was used along with this, the DNA extracted was sufficient enough despite it being crude. This provided a preliminary solution to the rate-limiting step encountered earlier for a true POC diagnostic. Mention can be made here that a farm site-friendly rapid DNA extraction technique using a Whatman filter paper-based was reported successful by AULA et al., (2021) for detecting the parasite *Schistosoma* spp. Thus, the importance of rapid and reliable DNA extraction is a must for IA-based diagnostics.

4.5. LAMP-LF Assay

4.5.1 *LAMP-LF optimisation*

The initial optimisation was done using two *H. contortus* positive control gDNA (BP and KS) and non-template controls. Results showed that the LF was capable of detecting these two positive control gDNA samples with no false-positive bands visible for the non-template control (Figure 22-A) when the amplicon was diluted at 1:9 ratio.

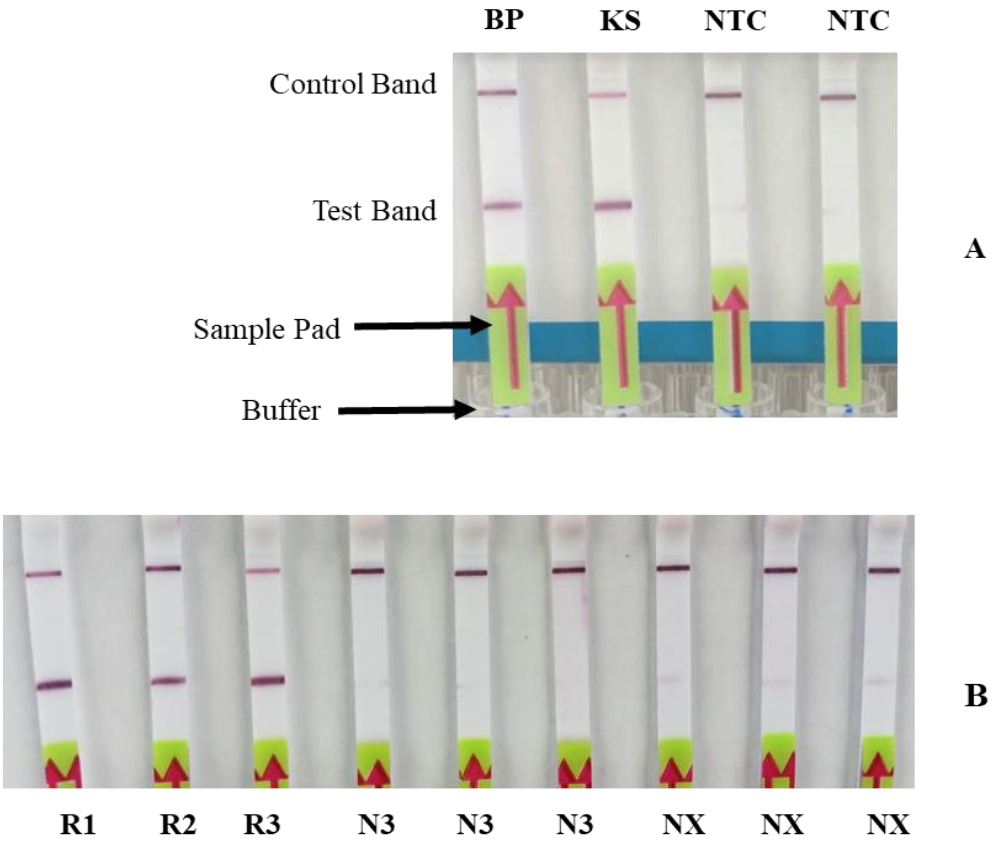

Figure 13: Optimisation of LAMP-LF assay. A: assay set-up showing the correct way to interpret the test result; B: optimisation of amplicon volume to prevent false positives. BP and KS: positive control templates; NTC: non-template control; R1-R3: LAMP-LF with a positive control template at various amplicon dilutions where R3 being optimised at 1:9 amplicon:ddH_20; N3: optimised non-template control amplicon dilution at time=5min; NX: non-template control corresponding to the dilutions of R1-R2 at time>5 min.

Initially, it was observed that NTC also recorded faintly visible bands (Figure 22-B; test-strip NX) and this could be interpreted as false positives. After an optimisation at 1:9 (amplicon to double-distilled water) and a time to result of 5min, this false positive could be solved as no bands were detected for the NTC test strip (N3, Figure 22-B) but a clear band for the positive control test strip (strip R3 Figure 22-B).

4.5.2 *LAMP-LF field trials*

Once optimised, the LAMP-LF was tested using DNA templates from randomly selected farm samples and the results are shown in Figure 23. All the positive detection of LAMP-LF (Figures 23 A and C) were also shown positive correspondingly in the LAMP assay (Figures 23 B and D). Weakly positive farm samples (due to low FEC) was also seen to show weaker bands and colouration on LAMP-LF (Figure 23 – C and LAMP assy (Figure 23 – D) respectively**.**

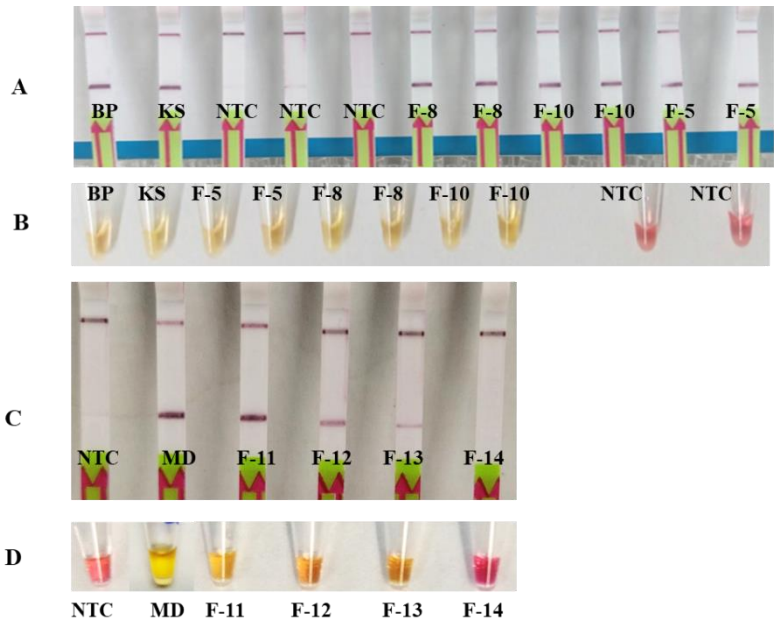

Figure 14: Field trial of some randomly selected farms for LAMP-LF assay. A: LAMP-LF assay using positive control from Kosice and Budapest. B: corresponding LAMP assay for farms F-5, F-8 and F-10; C: LAMP-LF assay using positive control from Moredun; D: corresponding LAMP assay for farms F-11 to F-14; NTC: Non-template control; Pink/Purple = Negative; Yellow/Orange = Positive

4.5.3 *Recapitulation of LAMP-LF assay results*

The LAMP-LF employed a commercially available and readily optimised lateral flow assay kit to optimise and demonstrate a proof of concept LAMP-LF or POC amenable confirmatory diagnostic test for *H. contortus*. At the time of publishing the finding of this LAMP and LAMP-LF study (KHANGEMBAM et al., 2021), this constitutes the first demonstration of a LAMP-LF assay for the species-specific colourimetric confirmatory diagnosis of *H. contortus*. The LAMP-LF was tested in field samples previously predicted to be positive for *H. contortus* by LAMP and confirmed by PCR. The study found 100% agreement between the results of our colourimetric LAMP assay and the LAMP-LF assay,

indicating the validity of either of the end-point detection methods for potential future POC confirmatory diagnosis of *H. contortus*.

However, this proof of concept LAMP-LF assay is still purely qualitative and thus cannot seek to replace quantitative microscopy and/or other molecular-based methods at present. Nevertheless, significant improvements have been made in recently published studies detailing the use of smartphone-based technologies demonstrating proof-of-concept point-of-care quantitative diagnosis using a colourimetric LAMP assay (ABDULLAHI et al., 2015; YIN et al., 2020). The applicability of membrane-based techniques for streamlined sample collection, storage or even diagnostic tools was already reviewed by ROGERS et al., (2021). This presents an important avenue for future research towards creating molecular assays that can replace traditional microscopy by delivering both species-specific identification and quantification.

4.6. RPA technique

4.6.1 *Optimisation: primer screening, betaine treatment, amplificon clean-up*

The RPA reaction time-temperature combination was optimised at 37ºC for 25 min amplification step and a final 85ºC for 5 min amplification termination step. Initially, three primer sets (Table 3) were tried to find out the best fit for the assay. The assay was performed using the BP positive control template. The result of the primer optimisation is shown in Figure 24 (A and B). It can be seen here that the best set of primers is P2 (Figure 24-A) with the least unwanted amplification bands while the other two sets (P1 and P3) gave some unwanted amplification despite the target amplification also being clearly visible. This optimal primer set was determined to be 'R_HC-2' in the text henceforth. The integrity of this screening could be verified as the kit-positive control bands were distinctly recorded in duplicates.

Once the primer set has been established, the study further aimed to investigate the effectiveness of betaine addition to the two post-amplification kits and the result can be seen in Figures 24-C and D. This post-amplification was recommended by the kit manual for better end-result visualisation. The ChargeSwitch™ PCR Clean-Up kit took longer to perform compared to the enzymatic-based clean-up principle of the VWR ExoCleanUP FAST kit (about 20-25 min and 8-15 min respectively for 8 reaction tubes) although the latter kit gave smearing. Thus, the choice of a post-amplification cleaning kit could also affect the quality of the resulting output and the overall result-output time. The non-specific amplifications observed previously were not detected following the addition of betaine (optimised at 0.8M concentration) in the RPA master mix, as shown in Figure 24-D. This indicates that betaine addition increased primer specificity as reported in many studies (LOBATO and O'SULLIVAN, 2018; LUO et al., 2019).

Keeping in view POC amenability, the study also attempted to eliminate this post-amplification clean-up and visualised the amplification result without this step using farm F-4 and F-14 as the negative control template and MD as the positive control template. There was no significant difference in the detection of the amplification bands apart from a faintly visible smear track, as shown in Figure 24-D. This could greatly reduce the time to result for future RPA techniques.

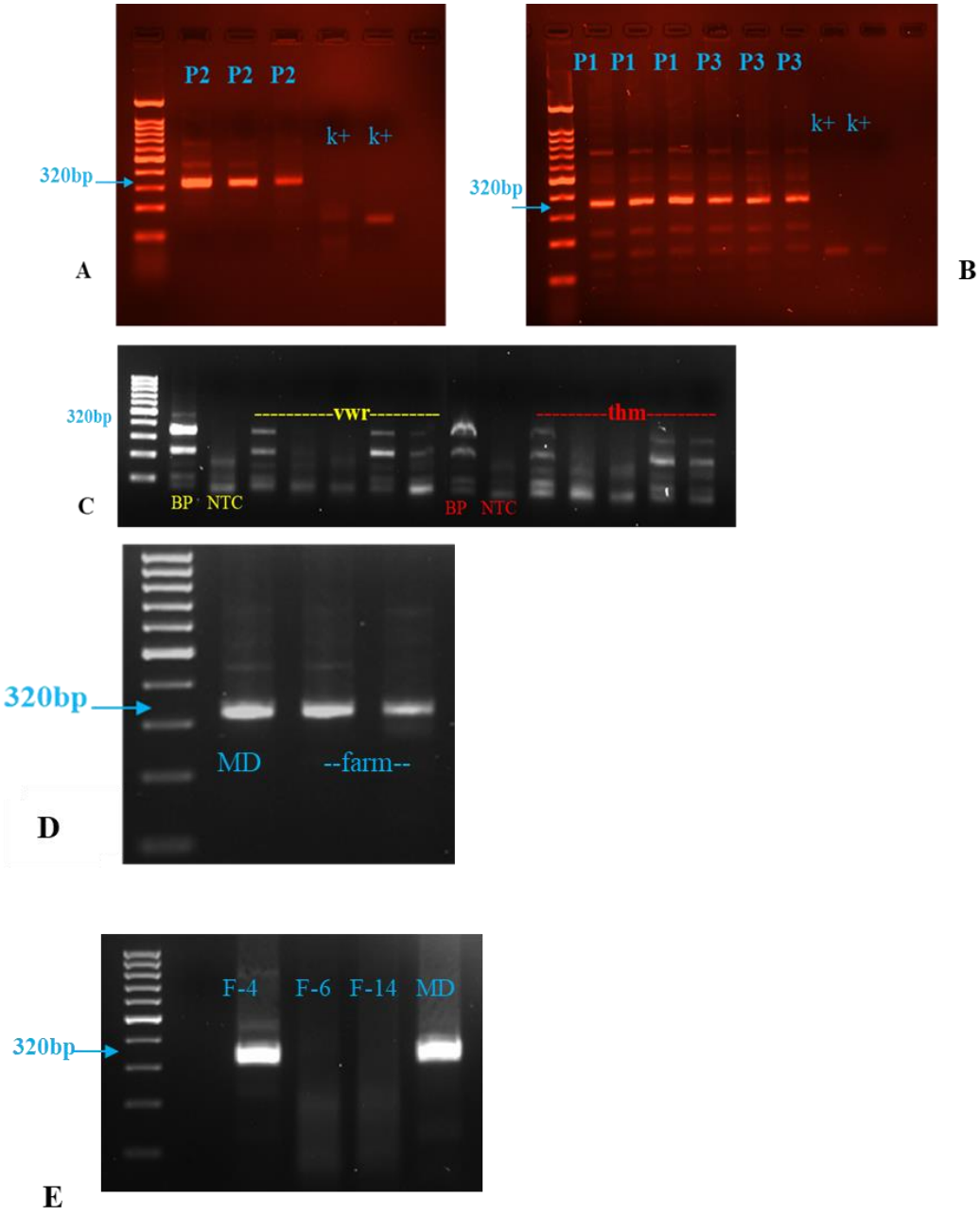

Figure 15: Agarose gel electrophoresis result of the optimisation of RPA technique. 100bp ladder used. A and B: primer screening where P1-P3 are the three primer sets listed in the table respectively where P2 = 'R_HC-2' primer set; C: post-amplification result of two different kits; D: betaine addition trial; E: amplification visualization without the post-amplification clean-up step; k+: kit positive control; thm: ChargeSwitch™ PCR Clean-Up kit (Thermo-Scientific); vwr: EXOCleanUp FAST kit (VWR); BP: positive control template; NTC: non-template control; F-4, F-6, F-14: farm samples

4.6.2 *Analytical specificity and sensitivity*

The *H. contortus* RPA technique was tested against the seven positive control specimens from Moredun. Amplification was detected at the expected size for *H. contortus* (Figure 25-A) of 320bp. No amplification was seen for any of the remaining species assayed. The specificity of the assay was also verified by the single species ITS2 PCR (Figure 25-B) to confirm species specificity. Only the *H. contortus* template gave a clear band at the expected amplicon size of 320bp for the PCR also. Thus, the RPA assay was in agreement with the result of the single species ITS2 PCR, with no amplification detected in any species other than *H. contortus.*

Following confirmation of species-specific amplification, the limit of detection of the assay was established by using a 10-fold serial dilution of positive control *H. contortus* DNA from Moredun. The limit of detection of the RPA assay for *H. contortus* was determined to be 0.1 ng/µl (Figure 25-C). This is lower than that reported for the previous LAMP study we built upon for this assay, where the limit of detection was between 1×10^{-5} ng/µl (MELVILLE et al., 2014) to 2.5×10^{-4} ng/µl (KHANGEMBAM et al., 2021). A previous RPA study also reported a limit of detection of 100 fg of *H. contortus* DNA (WU et al., 2021). However, the differences between these studies and our own are likely attributable to several factors and this is briefly discussed later on.

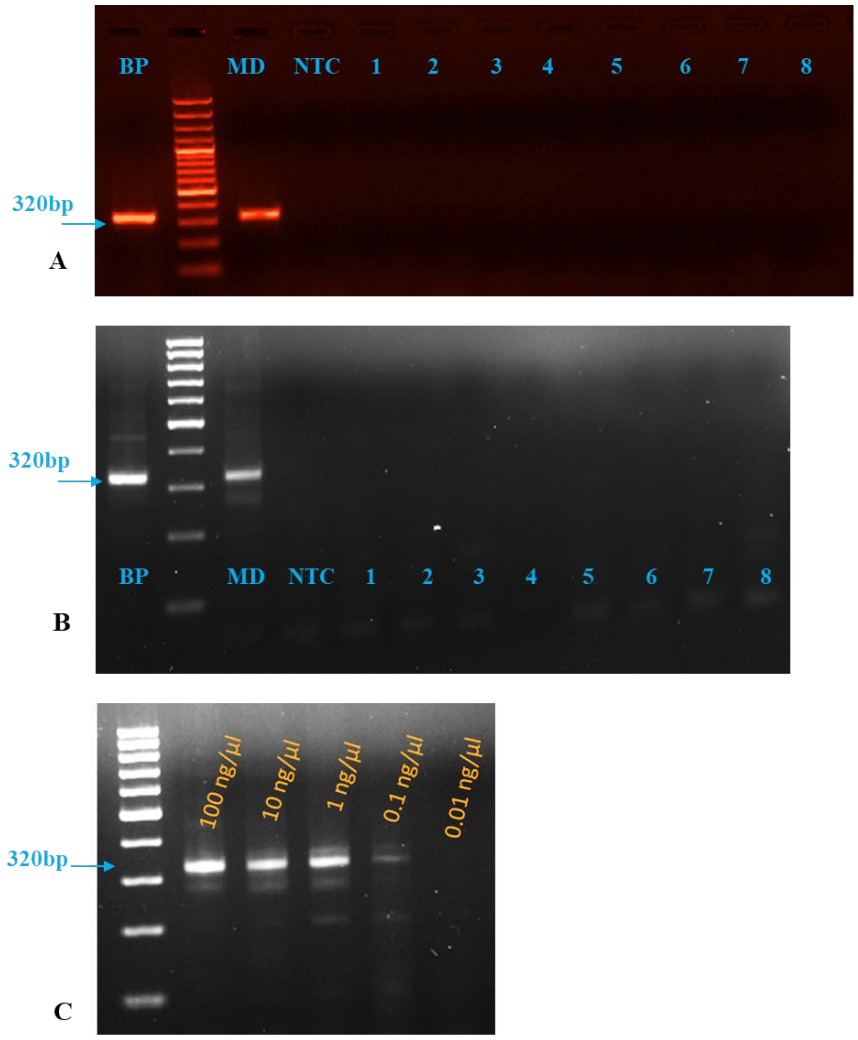

Figure 16: Agarose gel electrophoresis result of the RPA technique specificity and sensitivity. 100bp ladder used. A: single-species ITS2 PCR; B: RPA result; 1-8: positive control templates of the eight control specimen from Moredun; C: RPA analytical sensitivity test using a 10-fold serial dilution of MD control template. BP and MD: positive control from Budapest and Moredun respectively; NTC: non-template control

4.6.3 *Farm sample trial of RPA*

The *H. contortus* ITS2 RPA assay was then used to detect the presence of *H. contortus* DNA in five Hungarian field samples (Figure 26). Three out of the five farms, namely F-2, F-4 and F-5, gave positive results for the presence of *H. contortus* DNA, while the remaining two farms, F-6 and F-14 gave negative results (Figure 26-B). This was also confirmed by the ITS2 species identification PCR (Figure 26-A). It should be noted that farm F-6 reported a low EPG (mean EPG = 5.76) with insignificant trichostrongyle egg counts, while F14 had no detectable trichostrongyle egg counts. Besides, F2 and F5 farms had already been analysed with PNA fluorescence microscopy and confirmed positively (Appendix Table 1) the presence of the parasite. Furthermore, these results were in agreement with those obtained for the same farms with the ITS2 PCR (Figure 26 – A). This shows that the RPA assay is robust and can accurately and specifically detect *H. contortus* in farm isolates. Although the sensitivity is lower than that described by WU et al. (2021), this nevertheless demonstrates that the RPA assay developed herein offers a comparable detection accuracy to that of the ITS2 species identification PCR in practice for Hungarian field isolates.

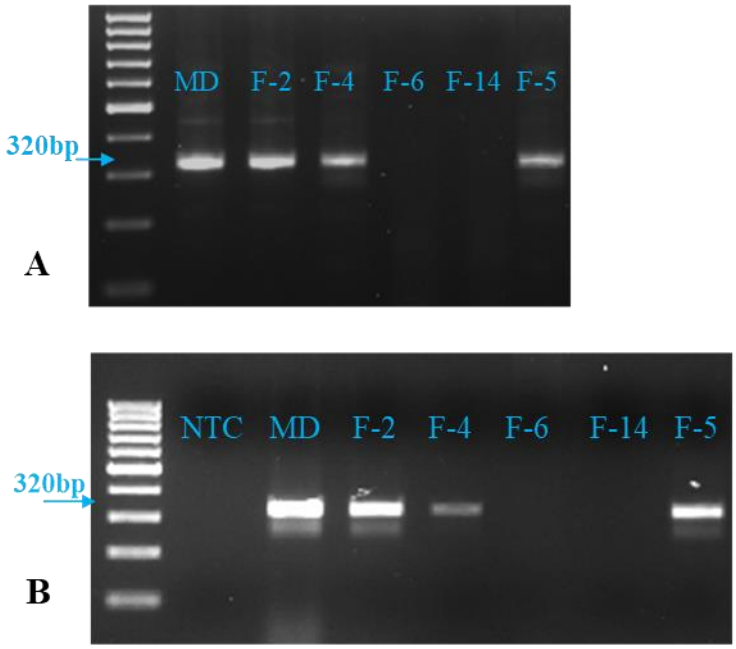

Figure 17: RPA farm trials. 100bp used. A: ITS2 PCR; B: RPA results using arbitrarily selected farm samples

4.6.4 *Recapitulation of RPA*

The unmodified ITS2 PCR primer set (R_HC-3) was tested but no significant amplification was observed. This was nonetheless an important aspect of the assay design trial as this would significantly speed up future development for RPA, a research point which the kit manufacturer encourages to report the findings. Had this been proven successful, this could have presented a significant advantage compared to LAMP which usually requires extensive primer design and optimisation with specialised software (TORRES et al., 2011). However, the results indicated that this approach is unlikely to yield optimal results for *H. contortus*. The R_HC-1 primer set yielded amplification but also showed some non-specific amplification, which was not improved by the addition of betaine (Figure 24). Single-species PCR and LAMP were performed after gel excision of non-specific amplicons resulting from the R_HC-1 assay, *H. contortus* DNA was not detected. It should also be noted that post-amplification clean-up steps did not result in any significant improvements to reduce this despite using two different kits. These non-specific amplicons could be due to primer binding at secondary loci.

The use of a relatively cheap thermal block (VWR^{TM} Advanced Mini Dry Block Heater) with low power requirements and a high degree of portability was chosen to improve the POC amenability of the assay. This simple thermal block was sufficient to provide the optimised time-temperature of 37ºC for 25 min amplification step and a final 85ºC for 5 min amplification termination step.

A previous RPA study also reported a limit of detection of 100 fg of *H. contortus* DNA (WU et al., 2021). However, the differences between these studies and this study are likely attributable to several factors including the divergence of Hungarian *H. contortus* isolates genetically, which is supported further by a lower limit of detection for the LAMP assay developed by MELVILLE et al. (2014) when applied by KHANGEMBAM et al. (2021) to Hungarian field isolates. Secondly, our assay approach prioritised the speed of development of a working proof-of-concept assay by modifying existing PCR primers to RPA. Hence, the principal aim of our assay was to demonstrate a rapid adaptation and adoption pipeline for researchers and clinicians within the field of veterinary parasitology, mainly of GIN parasites, to improve species-specific identification within specific local contexts. This is particularly important as current conventional diagnostics are no longer optimal, but also molecular assay development lags far behind other fields, such as human medicine. This requires a concerted effort from the research community to demonstrate effective proof-of-concept assays (KAPLAN et al., 2020).

4.6.5 *RPA detection using DNA-intercalating dye.*

For a true POC adaptable RPA assay, a minimal equipment requirement is a must. This remains impractical in conventional RPA assays, particularly if the post-amplification clean-up step and gel electrophoresis steps have to be performed. Initial attempts to eliminate the recommended post-amplification clean-up were done. The study found that RPA amplicons could still be detected albeit with some 'smearing' in the lane of the positive bands, while the negative templates showed no bands with relatively fainter smearing. This smearing has been explained by the kit manufacturer (TwistDx Ltd, FAQ Section) as possibly due to the interference by the crowding agent and proteins.

As a follow-up to this and in line with designing a true farm-site-friendly RPA diagnostic, the study also tested if the amplicons could be visualised either with UV illumination or by the naked eye in the presence of a DNA intercalating dye. The result is presented in Appendix Figure 2.

Of the many DNA intercalating dyes available, SYBR Green I is one of the most widely used dye-detection systems. Despite this, the main disadvantage is that SYBR Green I is expensive and often used for qualitative PCR systems that require expensive equipment unsuitable outside of a laboratory. Hence, we tested if the comparatively cheaper alternative dyes, EvaGreen® and GelRed™ dyes could replicate the results. Preliminary findings showed that after (dye: amplicon ratio of 4:1) optimisation, RPA amplicons could not be visualised under white light but could be easily detected using a UV light source (Appendix Figure 1-A). The EvaGreen® dye showed promising results in this preliminary trial as the change in colours of the tested RPA tubes was visualised clearly under UV illumination. Nevertheless, it should also be noted that the EvaGreen® dye used here was of a low concentration (5x) and this might have also contributed to the failure of any colourimetric change detection by unaided eyes. This low concentration proved practical in this trial as this was more readily accessible in a laboratory as well as cheaper in the market.

Yet, the use of a handheld UV lamp of decent quality can easily offset the need for UV illumination to detect any colourimetric change. GelRed™ dye showed inconsistent results; at a working concentration of 10x, the GelRed™ dye correctly illuminated two of three positive control templates under UV (Appendix Figure 2-B and C). This could be due to the mismatched dye-to-amplicon ratio or interference by the RPA reagents. Our attempts to rectify and improve this using various working dilutions (100x, 200x and 300x) proved unsuccessful (resulting in no change in the colour of the tubes either in white light or UV

illumination. For comparative purposes as per the original studies adapted from, the SYBR Green I dye resulted in better visualisation at 300x dilution (amplicon: dye = 4:1) as shown in Appendix Figure 2-C.

Hence, this preliminary finding of the dye detection system acknowledges further work is necessary for this detection system to be fully optimised for effective farm-side detection. Despite this setback, these results constitute an important first step towards developing naked-eye detection of RPA amplicons. The limited source of RPA kits and the detection system significantly complicate the development of new RPA tests hindering the design and optimisation of reaction conditions, custom-designed kit components are available but costly (LOBATO and SULLIVAN, 2018). This has slowed the development and adoption of RPA in the context of point-of-care diagnostics, with a majority of the current RPA development restricted to research settings. It is nonetheless necessary to demonstrate the potential of this technology, as it offers significant advantages over conventional PCR-based molecular tests without compromising the sensitivity and specificity, particularly for resource-limited settings such as a farm.

4.7. Gene sequencing and phylogenetic analysis: a brief report

The phylogenetic analysis was performed as an additional work to access a preliminary examination of the possible genetic diversity of the Hungarian isolates of the *H. contortus*. The evolutionary history was inferred using the Neighbor-Joining method (SAITOU and NEI, 1987). The optimal tree is shown in Figure 27, where F10, F11 and F13 were the isolates used in this preliminary study. The percentage of replicate trees (FELSENSTEIN, 1992) in which the associated taxa clustered together in the bootstrap test (1000 replicates) are shown next to the branches. The evolutionary distances were computed using the Maximum Composite Likelihood method (TAMURA et al., 2004) and are in the units of the number of base substitutions per site. The proportion of sites where at least 1 unambiguous base is present in at least 1 sequence for each descendent clade is shown next to each internal node in the tree. This analysis involved 15 nucleotide sequences. All ambiguous positions were removed for each sequence pair (pairwise deletion option). There were a total of 315 positions in the final dataset.

The tree presented here shows 4 clades and 1 outgroup (*H. placei*). Clade-1 (as read from the top-down sequence), consisted of two sequences from Nigeria and Australia with relatively very strong support (bootstrap =100%); clade-2 consisted of isolates from Hungary with good nodal support (bootstrap >50%). In the middle is a cluster comprising many isolates from various parts of the world (bootstrap >85%) while the last one consisted of sequences from Sweden, New Zealand and an *H. longistipes* sequence. The presented phylogenetic tree analysis showed that there is a distinctive haplotype of *H. contortus* isolates in the three farm locations (F10, F11 and F13) in Hungary. These were evidently at distant places from the outgroup *H. placei* in the tree which is the most closely related species. The finding also agrees with studies in Pakistan (QAMAR et al., 2022), Egypt (KANDIL et al., 2017) and Tunisia (AKKARI et al., 2013) targeting the ITS2 region of *H. contortus*. Closer to Hungary's perspective, a study in Sweden was conducted by TROELL (2006) by comparing the genetic differences in the ITS1 and ITS2 using the *Haemonchus* spp from Sweden and Kenya. It concluded that they could be of the same species but of a distinct population. The study here also presented a common root for the isolates in Kenya, India, Iran, Japan, the USA and China.

It should be noted here that the genetic sequence analysis results obtained showed some degree of mixed peaks in the chromatogram and unidentified bases (Appendix Figure 3). Because of this, manual editing and interpretation of the missing/unidentified bases had to be performed by taking into consideration the highest peak. However, a BLAST search

as recommended by HALL, (2013) and KUMAR et al., (2018) using these edited sequences gave positive hits on *H. contortus* ITS2 gene accession data, upon which the tree was built. The sequences used here in the analysis gave 92-95 % similarity in the BLAST search results. Nevertheless, the study acknowledges that a deeper study for the Hungarian isolates is needed, even by expanding the target gene to *nad4* as many other studies have shown pieces of evidence of diversity (or not) within and between the isolates from different parts of the world (TROELL et al., 2006; F. YIN et al., 2016) when genetic sequence analysis was performed targeting ITS2 as well as the *nad4* gene. For such a study, a more refined gene sequencing tool, and collection of more isolates from different locations as well as host animals inside Hungary is necessary.

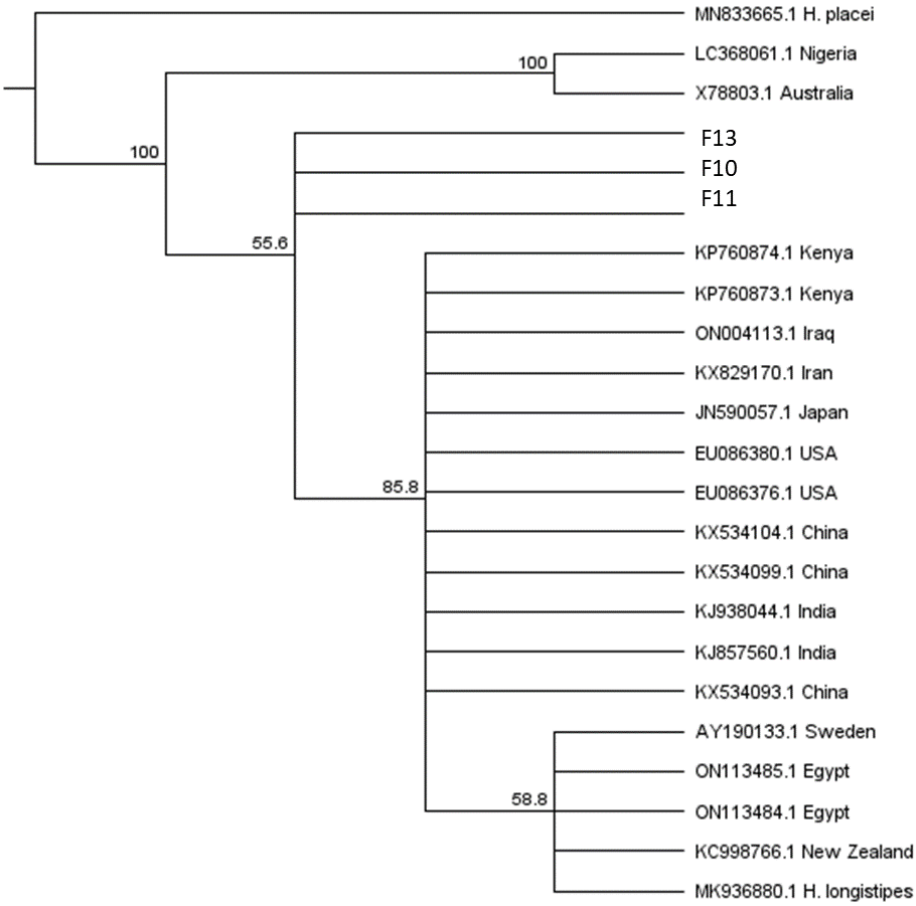

Figure 18: Phylogenetic tree of three *H. contortus* isolates from Hungary as deduced from the ITS2 target region. Bootstrap values >50% are displayed at the nodes. The accession number for the respective country's sequences used in the analysis are also given. *H. placei* (accession number MN833665) is used as an outgroup.

5. CONCLUSION

Despite the advancement in molecular-based diagnosis of haemonchosis, the main demerit is that most of these technologies are confined within the walls of a laboratory and require expensive pieces of equipment along with the trained staff. This bottleneck in reaching out the molecular techniques beyond a research laboratory can be reduced to some extent by adopting isothermal amplification techniques like LAMP and RPA. These two isothermal amplification-based techniques also satisfied the criteria (ROGERS et al., 2021) for reliable and trust worthy POC tests, defined by the World Health Organisation in 2015 as 'ASSURED' (Affordable, Sensitive, Specific, User-friendly, Rapid and robust, Equipment-free, and Deliverable to end-users).

In conclusion, this study was performed keeping in view the importance of the GIN parasite *Haemonchus contortus,* to design and test two proof of concept isothermal amplification assays for a POC diagnosis. In the course of this study, 14 sheep farms, 1 goat farm and 1 roe deer hunting location in Eastern and Central Hungary were covered. This study detected the presence of the parasite in 14 locations. The research work also outlined the necessity of an FEC examination as well as some of the challenges faced in copromicroscopy techniques. For instance, the study adopted the Mini-FLOTAC system for the initial FEC steps, which was very efficient and self-contained. Initial screening for the samples for a specific diagnosis was met by PNA fluorescence microscopy. Yet, the PNA staining was very time-consuming and difficult to enumerate the result. Hence, the PNA results were expressed as a percentage (Appendix Table 1).

During the course of the assay designs, the study also acknowledges that for a true POC diagnosis, the source of the starting DNA is of the foremost importance. Attempts to address this issue were done by modifying a few crude DNA extraction methods already established elsewhere and one designed in its entirety during the research work. The motorised micro-pestle-based DNA extraction proved promising. Coming to the isothermal assays, the optimised LAMP, LAMP-LF and RPA techniques are all qualitative but the robustness and integrity are maintained and well-tested by cross-examining the results with that of PCR. As one of the aims of true POC diagnostics, the equipment set-up of the optimised assays was done as shown in Figure 30. Here, it can be seen that the centrifugation was sufficient in a low *g* and highly portable table-top centrifuge, the self-contained Mini-FLOTAC was effectively incorporated for FEC and for a crude DNA extraction and finally, the heat source of the molecular reaction was also sufficiently provided by the portable heat-block. Besides, plenty of portable microscopes are available

in the market that is cheap but sufficient to serve a microscopic analysis along with the option of digital photography. Even though the study is mainly of qualitative, a collaboration to design a qLAMP is already underway.

Figure 19: A point-of-care (POC) friendly set-up of LAMP and RPA techniques involved in the study: the self-contained Mini-FLOTAC system for FEC as well as a source of faecal suspension; portable heat-block and the centrifuge can also be seen.

The study would also like to make some recommendations based on the findings of the study. Firstly, a detailed prevalence study in Hungary is highly recommended to give a clear picture of the overall epidemiology including the drug resistance status of this important parasite. This can be achieved by FECRT and adopting an appropriate nucleic acid amplification diagnostic tool. Secondly, a study on the genetic diversity of the parasite isolates of the country could also add to the control of the spread of drug-resistant isolates, if any. Attempts were made in the course of the study by including a Sanger sequencing analysis of three Hungarian isolates, with results showing a distinct cluster. Yet, this needs a more refined study with a better sequencing technique and a larger sample size to give a true picture. Last but not least, a general recommendation is to keep up the pace of designing and testing more isothermal-based diagnostics, especially those that can be adopted at the farm site. This is deemed necessary because most of the currently available

POC techniques for molecular diagnostics are confined mainly to those of human parasites and only to a few zoonotic helminths and protozoa. Closing the gap in this could transform the control and treatment of many parasites of veterinary importance, especially in poorer countries.

6. NEW SCIENTIFIC RESULTS

1. A centrifuge-free crude DNA extraction method was successfully adapted using the Fill-FLOTAC apparatus, a magnetic beads DNA extraction kit and a motorised micropestle for egg disintegration.
2. A LAMP and another LAMP-LF assay for the qualitative detection of *H. contortus* from the faecal samples of ruminant flocks were successfully designed. These two assays allow visual detection to the unaided eyes without compromising the specificity and sensitivity. The analytical sensitivity is determined to be 2.5×10^{-4} ng/µl of DNA template.
3. An RPA technique, another isothermal-based amplification tool, was also successfully designed for the detection of *H. contortus* with an analytical sensitivity of 0.1 ng/µl DNA template. This study also would like to register two preliminary findings: i) that the post-amplification clean-up for the RPA amplicons could be eliminated without any significant loss in analytical sensitivity, and ii) a colourimetric change detection using some commonly DNA intercalating dyes (such as Eva Green and SYBR Green dyes) is possible.
4. 12 sheep farms and 1 goat farm in 6 counties of Hungary were confirmed to have the *H. contortus* parasite. Recovery of adult worms from the abomasum of hunted roe deers (n>20) and the subsequent molecular-technique-based confirmation of *H. contortus* from the Biharugra village suggested a probable cross-contamination of pasture ground shared between the wild and domestic small ruminants in that area.

7. RESULTS APPLICABLE IN PRACTICE

1. Since a quick and reliable qualitative diagnosis of *H. contortus* can be made without compromising the integrity of the test, a more detailed epidemiological survey can be followed up after such a preliminary screening of selected/suspected farms. This screening can be done side by side with a detailed FEC examination of the farm to present more concise and meaningful data on the occurrence of the important GIT parasites in Hungary, of which the data is very limited at the moment.
2. Need for a study to determine the genetic makeup of the *H. contortus* isolates recovered from both domesticated flocks as well as wild ruminants can be done. This could contribute to reducing the knowledge gap on the genetic characteristics and the diversity of this parasite in Europe in general and Hungary in particular.
3. Mini-FLOTAC system can be effectively integrated into a farm site-friendly nucleic acid amplification detection diagnostic tool, starting from a crude DNA extraction to supplementation of reliable FEC data. Such a combination of the FEC tool and molecular detection of the parasite can be a step towards a clinically significant point-of-care diagnosis that can indirectly help in making an effective deworming decision.
4. Isothermal techniques like LAMP and RPA should be encouraged for veterinary helminth diagnosis considering that isothermal nucleic acid amplification has the advantage of a quick result time without compromising the sensitivity and specificity. Also, there are plenty of assays based on these techniques for the detection of various pathogens including parasites in human medicine either at the field level or in laboratory applications.
5. Currently, there is only a single kit manufacturer for the RPA technique and at the time of writing this, the kit that can use an LF detection system has been discontinued. Accordingly, using a DNA intercalating dye can, to some extent, facilitate a colourimetric detection of results without having to rely on the gel electrophoresis method.

8. SUMMARY

A study on the economic burden of major livestock parasitism involving 18 countries in Europe was published recently by CHARLIER et al., (2020). They reported a production loss of 81% and 19% to treatment out of the total € 1.8 billion annual expenditure. The study also reported that for GIN parasite controls, the cost of resistance against macrocyclic lactones class of anthelmintic drugs alone was estimated in the range of € 11–87 million annually. This sums up the picture of the importance of effectively controlling and preventing the spread of these endoparasites including the GIN parasitic nematodes. Among the many GIN parasites that can affect small ruminants, the family of Trichostrongylidae is very important and out of which *Haemonchus contortus* has established itself to be the most dangerous and clinically important species. A severely affected animal can harbour up to 5000 worms inside it and this can lead to the continual loss of about 250ml of blood daily, which is a fatal consequence.

Although *H. contortus* had its origin in the hot and tropical climates of Africa, the parasite has taken its foothold even in the temperate and colder regions of the globe most likely due to animal migration along with human intervention in terms of trade. Reports on its epidemiology, genetic diversity and drug resistance are increasingly available from varied climatic conditions in the world, including that of Europe. Yet, the data on this parasite is still very limited in Hungary. The present study analysed n=16 farms located in 5 different counties in Eastern and Central Hungary. Out of these farms, n=14 were sheep farms; 1 goat farm and a village where roe deers were hunted. Faecal samples were collected from individual animals and the FEC data were obtained from another larger study. The present study found out n=12 sheep farms, the goat farm as well as the roe deer all had a positive result for *H. contortus.* As summarized below, the preliminary analysis/screening was done through morphological examination of recovered adult worms, the FEC examination (along with PNA fluorescence microscopy) of faecal eggs and confirmation was followed up through ITS2 species-specific PCR along with custom-developed isothermal amplification assays summarised below.

The faecal egg examination under a microscope is termed a “copro-microscopic technique” and this can be done by adopting many recognised methods. Also, it is important to keep in mind that faecal egg copro-microscopic diagnosis of GIN parasite infections can be interpreted to be qualitative or quantitative in nature. For the first instance, the technique can provide a piece of general information on whether the flock/farm has the

parasite or not while the latter aspect gives the FEC data expressed as the number of eggs per gram of faeces.

The study here performed the copro-microscopic examination using the Mini-FLOTAC® system for the initial screening of the farms for the presence of GIT nematodes, although only the average FEC of the pooled faecal sample of the farms were presented here. The sheep farm F-4 recorded the highest FEC=1750 EPG of faeces (registered to be of "moderate intensity" of infection) while the F-6 recorded the least FEC=5.76 EPG (registered "light intensity" of infection). The goat farm did not have FEC data as the sample amount was not sufficient for the Mini- FLOTAC® protocol d further attempt to re-collect from the farm was unsuccessful due to unavoidable circumstances. It should also be noted that the correlation between FEC and the degree of infection is not definite and depends on many factors hence, the intensity of infection provided here was not treated as clinically significant but only as qualitative data. Moreover, the faecal samples from farms F-6 and F-14 were treated as negative control farms for the subsequent assays as there were no *H. contortus* eggs detected in them.

The parasite has a high fecundity; a single female can lay even upto 15000 eggs/day and it has a short pre-patent period of about 3-4 weeks. The eggs are voided in the faeces of the host animals and they aid in diagnosing the parasite by faecal egg examination or as a source of DNA template for nucleic acid detection techniques. Morphometric analysis of the eggs was also done in this study and the average dimension of the eggs was recorded to be 39-43µm in width and 68-89µm in length. However, in a few circumstances, the blastomeres could not be distinctly outlined and usually filled up the whole of the eggs.

The study also adopted PNA fluorescence microscopy for accurate microscopic identification of the *H. contortus* eggs. PNA is a lectin derived from peanut (*Arachis hypogaea*) that is proven to specifically bind to the eggshell of *H. contortus*. This binding can be visualised when PNA is conjugated with a fluorescence dye such as FITC. When observed under appropriate wavelength filters, a bright-green glow of the egg outline is seen. In this study, the PNA fluorescence microscopy was performed on those faecal samples suspected to have *H. contortus* eggs under normal light microscopy. To do this, the eggs in the faecal sample needed to be harvested/concentrated as much as possible for the lectin staining. For this egg concentration, the study managed to harvest the eggs from the faecal suspension without the centrifugation step as commonly approached by other protocols. This was made possible by using an inverted 200µl micropipette tip from multiple replicates of faecal suspension decantated from the Fill-FLOTAC device. Under

fluorescence microscopy, those eggs with clearly green stained egg outlines were interpreted as “positive” and those partially stained or unstained eggs were interpreted as “negative”. Interestingly, certain eggs which were interpreted to be non-*Haemonchus* were observed to take up the PNA-FITC stain and hence, counted to be *H. contortus*. The results were interpreted in the percentage of stained eggs and farm F-10 recorded the highest count (79.13%) while both the negative farms control F-6 and F-14 registered no stained eggs. Once the individual animals/farms confirmed a positive *H. contortus* result, the faecal samples were preserved for further downstream molecular tests.

Coming to the recovery and subsequent identification from the post-mortem of the hunted roe deers, it should be noted that the gross morphology of the adult females gives a typical red-white striped appearance and so the worm is also commonly known as “barber’s pole worm”. During the time of collection, certain numbers of worms (later identified to be females) were seen to have a reddish colouration with some showing a red-white stripe pattern. As per available literature, the length of adult males ranges from 10-20mm length and adult females can grow up to 18-30mm. Under the microscope, the adults present certain striking features such as linguiform vulval flap (in females), unequal bursal flaps having a barbed spicule (in males) and cervical papillae in both sexes. These features can aid in the identification of the parasite in a post-mortem examination. The present study also observed these features distinctly although a few specimens (n=8) had a knob-like vulval flap. This study also recorded the length of adult worms ranging from 9-18 mm (males) while those of identified adult females ranged from 15-27mm.

Although the copro-microscopy and FEC examination are still valuable tools, it should be noted here they have a main demerit of difficulty in accurate identification of the parasite to species level. For instance, among the members of the trichostrongyloid worms, only the eggs of *Nematodirus* spp can be easily differentiated under normal microscopy. The PNA fluorescence microscopy can somehow alleviate this drawback in the sense that only *H. contortus* can be visualized. Even then, the PNA technique is time-consuming owing to egg concentration plus staining and also requires a sophisticated microscope. Moreover, the quantification of the result is also a problem as no standardized counting chambers are available for the PNA technique. Thus, for a specific diagnosis, nucleic acid amplification and detection methods such as PCR are regarded as confirmatory.

Despite the advancement of the available molecular techniques such as PCR and its various forms for the specific detection and diagnosis of *H. contortus*, the majority of them are still confined to laboratories and require expertise. Nevertheless, there are an increasing

number of other isothermal amplification-based techniques. Out of these IA techniques, mention can be made of the LAMP and the RPA techniques. There are reports on their usage in other pathogens including parasites but it is quite limited for *H. contortus.* One of the aims of this study is to design and optimise these two isothermal amplification assays as a preliminary step/proof of concept towards a point-of-care diagnostic bringing the molecular tests to the doorstep of the farmers. All the results of the three assays were cross-checked and confirmed by the species-specific ITS2 PCR starting from the optimisation to that of farm trials (Table 5).

For the LAMP assay, the study utilised an already published primer but modified the end-result detection method. Here, a colourimetric LAMP kit was utilised and the optimised LAMP assay could detect the presence of the *H. contortus* amplicons in the reaction tubes by the change of colour from pink-red to orange-yellow. The optimised time-temperature condition was determined to be 62ºC for 30 min. Both individual faecal samples, as well as pooled faecal samples, were tested during the optimisation. The analytical sensitivity of this colourimetric LAMP assay was determined to be 2.5 x 10^{-4} ng/µl of DNA template and its specificity had been tested against the positive control DNA templates of other eight related nematode species (*C. curticei, N. battus, O. venulosum, T. axei, T. colubriformis, T. circumcincta, T. ovis* and *T. vitrines*). As a continuation of this LAMP assay, another POC-friendly assay was also optimised using the lateral flow application to detect the end result. This LAMP-LF assay adopted a lateral flow dipstick paper currently available commercially. The LAMP amplicons were tagged with BIO and FITC and when these tagged amplicons were allowed to migrate upwards the dipstick by capillary action, positive results were visualised when the 'Control band' and 'Test band' were stained. Optimisation of the LAMP-LF was achieved by diluting the amplicons with double distilled water to avoid false positives.

Coming to the RPA technique, the study designed two primer sets based on the ITS2 region, out of which one was found to be suitable. The time-temperature condition was determined to be at 37ºC for 25 min amplification step and a final 85ºC for 5 min amplification termination step. During optimisation, betaine was added at 0.8M to reduce unspecific amplification, a common finding in the RPA technique. Also, two different post-amplification clean-up kits were tested as the RPA manual defined the necessity of this step. The ChargeSwitch™ PCR Clean-Up kit (20-25 min for eight tubes) took longer to perform compared to the VWR ExoCleanUP FAST kit (8-15 min for eight tubes) although the latter kit gave smearing. Hence, the choice of a post-amplification cleaning kit could

also affect the quality of the resulting output and the overall result-output time. The results of the assay were detected by 2.5% AGE at the band size of 320 bp. The analytical sensitivity was determined to be 0.1 ng/µl of template DNA. The specificity was tested against the other nematode species as mentioned above and only the *H. contortus* gave positive amplification.

Initially, for the RPA technique, an attempt was made to utilise the lateral flow dipstick as the end-result detection method but this design had to be abandoned as the sole kit manufacturer in the market discontinued the lateral flow RPA kit. Nevertheless, the study tested and reproduced a modification of the end-result detection of amplicons using DNA intercalating dye. Also, the study tested the band detection eliminating the post-amplification cleaning step to move closer to a POC diagnostic. It was found that the positive amplicon bands could be visualised in the same 320 bp position albeit with some smearing effect. Besides, the use of DNA intercalating dyes like GelRed and EvaGreen allowed colourimetric detection eliminating the need for AGE. The GelRed was tested at various concentrations of 100x, 200x and 300x but gave inconsistent results while the EvaGreen dye gave purplish-green colouration for positive results under UV illumination.

For farm trials, pooled faecal sampling and subsequent DNA extraction were done from all the farms as well as DNA from the recovered adult worms. For the LAMP and LAMP-LF assays, farms F-1 to F-5 and F-7 to F-12 gave clear positive results; F-6 and F-4 showed a negative result; farms F-13 gave a weak positive colouration. This weak colourimetric change could be due to the low number of *H. contortus* eggs in the pooled faecal sample of the farm. For the LAMP-LF assay, farm trials agreed with the results of the LAMP although F-13 registered a normal positive interpretation by the LAMP-LF. Similarly, the RPA technique also gave corresponding results for both the negative and positive farms as the previous two assays although F-4 and F-13 registered weak bands.

During the course of the assay design and optimisation, it was realised that the source of the template DNA was the rate-limiting step if at all a true farm-site diagnostic was to be designed. Hence, the study also attempted three crude DNA extraction methods out of which i) the Chelex reagent-based methods were not successful; ii) the bead-beating gave inconsistent but promising results and iii) the micropestle plus magnetic kit technique for egg lysis genesig® Easy DNA/RNA Extraction Kit. The motorised micro-pestle allowed the breach of the tough egg cell (confirmed under a microscope) and the use of the magnetic kit (genesig® Easy DNA/RNA Extraction Kit) allowed a centrifugation-free crude DNA extraction. Also, the faecal suspension from the Fill-FLOTAC device was suitable as a

starting source for the template. Hence, the last technique was deemed the most farm-site-friendly crude DNA extraction method.

In conclusion, it should be noted here that these three IA assays presented here are qualitative and purely proof of concept at this level and thus, clinically important information should be provided only with other relevant data (such as FEC, body condition scoring, FAMACHA etc). For instance, if this qualitative detection is incorporated with FEC figures obtained on the spot, such as by using Mini-FLOTAC® with a battery-operated portable microscope, it could aid in giving clinically relevant information to the farmers. Also, the study proved the presence of the *H. contortus* parasite in Hungary with gene sequencing of three isolates showing their lineages. Nevertheless, a more detailed epidemiological study, an in-depth phylogenetic analysis using sequencing of both ITS2 and *nad4* genes and improvement in the isothermal assay by incorporating quantitative data are all highly recommended.

Table 5: Summary of the results of the three assays designed in the study validated against species-specific ITS2 PCR.

Farm ID	Average FEC (in EPG)	Result of Optimised Molecular Assay				Remarks
		LAMP	LAMP -LF	RPA	PCR	
F-1	600	☐	-NA-	☐	☐	
F-2	150*	☐	-NA-	☐	☐	*Only 3 animals had trichostrongyle eggs
F-3	276.4	☐	-NA-	☐	☐	
F-4	982.2	☐	☐	☐	☐	
F-5	1750	☐	☐	☐	☐	
F-6	5.7**	☐	☐	☐	☐	**Used as farm negative control
F-7	113.7	☐	☐	☐	☐	
F-8	767.2	☐	☐	☐	☐	
F-9	168.0	☐	☐	☐	☐	
F-10	159.7	☐	☐	☐	☐	
F-11	577.1	☐	☐	☐	☐	
F-12	754.2	☐	☐	☐	☐	
F-13	70.9	☐	☐	☐	☐	☐ = weak positive
F-14	22.2	☐	☐	☐	☐	No trichostrongyle eggs detected
FD	--	☐	☐	☐	☐	Adult worms collected
FG	--	☐	☐	☐	☐	FEC unavailable

☐: weak positive; ☐: positive; ☐: negative; NA: Not applicable

9. REFERENCES

1. ABBAS, I. and HILDRETH, M. (2019). Egg autofluorescence and options for detecting peanut agglutinin binding for the identification of Haemonchus contortus eggs in fecal samples. *Veterinary Parasitology*, *267*, 69–74. https://doi.org/10.1016/j.vetpar.2019.01.009
2. ABDULLAHI, U. F. – NAIM, R. – TAIB, W. R. W. – SALEH, A. – MUAZU, A. – ALIYU, S., and BAIG, A. A. (2015). Loop-mediated isothermal amplification (LAMP), an innovation in gene amplification: bridging the gap in molecular diagnostics; a review. *Indian Journal of Science and Technology*, *8*(17), 1.
3. AKKARI, H. – JEBALI, J. – GHARBI, M. – MHADHBI, M. – AWADI, S. and DARGHOUTH, M. A. (2013). Epidemiological study of sympatric Haemonchus species and genetic characterization of Haemonchus contortus in domestic ruminants in Tunisia. *Veterinary Parasitology*, *193*(1–3), 118–125.
4. AMARANTE, A. F. T. do. (2011). Why is it important to correctly identify Haemonchus species? *Revista Brasileira de Parasitologia Veterinária*, *20*, 263–268.
5. ANGULO-CUBILLÁN, F. J. – GARCÍA-COIRADAS, L. – CUQUERELLA, M. – DE LA FUENTE, C. and ALUNDA, J. M. (2007). Haemonchus contortus-sheep relationship: a review. *Revista Científica*, *17*(6), 577–587.
6. ANTONOPOULOS, A. – DOYLE, S. R. – BARTLEY, D. J. – MORRISON, A. A. – KAPLAN, R. – HOWELL, S. – NEVEU, C. – BUSIN, V. – DEVANEY, E. and LAING, R. (2022). Allele specific PCR for a major marker of levamisole resistance in Haemonchus contortus. *International Journal for Parasitology: Drugs and Drug Resistance*, *20*, 17–26. https://doi.org/10.1016/j.ijpddr.2022.08.001
7. ARSENOPOULOS, K. V. – FTHENAKIS, G. C. – KATSAROU, E. I. and PAPADOPOULOS, E. (2021). Haemonchosis: A challenging parasitic infection of sheep and goats. *Animals*, *11*(2), 1–29. https://doi.org/10.3390/ani11020363
8. AULA, O. P. – MCMANUS, D. P. – MASON, M. G. – BOTELLA, J. R. and GORDON, C. A. (2021). Rapid parasite detection utilizing a DNA dipstick. *Experimental Parasitology*, *224*, 108098.
9. AWAWDEH, L. – TURNI, C. – HENNING, J. – ALLAVENA, R. E. – COBBOLD, R. N. – MOLLINGER, J. L. – GIBSON, J. S. (2019). An optimized protocol for molecular screening of avian pathogenic Escherichia Coli from broiler chickens in South East Queensland, Australia. *Journal of Applied Poultry Research*, *28*(4), 1370–1381.
10. BABJÁK, M. – KÖNIGOVÁ, A. – URDA-DOLINSKÁ, M. – VÁRADY, M. (2017).

Gastrointestinal helminth infections of dairy goats in Slovakia. *Helminthologia*, *54*(3), 211–217.

11. BALTRUŠIS, P. – HALVARSSON, P. – HÖGLUND, J. (2020). Utilization of droplet digital PCR to survey resistance associated polymorphisms in the β tubulin gene of Haemonchus contortus in sheep flocks in Sweden. *Veterinary Parasitology*, *288*, 109278.
12. BARDA, B. D. – RINALDI, L. – IANNIELLO, D. – ZEPHERINE, H. – SALVO, F. – SADUTSHANG, T. – CRINGOLI, G. – CLEMENTI, M. – ALBONICO, M. (2013). Mini-FLOTAC, an innovative direct diagnostic technique for intestinal parasitic infections: experience from the field. *PLoS Neglected Tropical Diseases*, *7*(8), e2344.
13. BARGER, I. A. and COX, H. W. (1984). Wool production of sheep chronically infected with Haemonchus contortus. *Veterinary Parasitology*, *15*(2), 169–175.
14. BASSETTO, C. C. and AMARANTE, A. F. T. (2015). Vaccination of sheep and cattle against haemonchosis. *Journal of Helminthology*, *89*(5), 517–525.
15. BEH, K. J. – FOLEY, R. C. – GOODWIN, E. J. (1989). Restriction fragment length patterns of DNA from parasitic nematodes of sheep. *Research in Veterinary Science*, *46*(1), 127–128.
16. BENAVIDES, M. V. – SONSTEGARD, T. S. – KEMP, S. – MUGAMBI, J. M. – GIBSON, J. P. – BAKER, R. L. – HANOTTE, O. – MARSHALL, K., and VAN TASSELL, C. (2015). Identification of novel loci associated with gastrointestinal parasite resistance in a Red Maasai x Dorper backcross population. *PloS One*, *10*(4), e0122797.
17. BESIER, R. B. – KAHN, L. P. – SARGISON, N. D. and VAN WYK, J. A. (2016a). Diagnosis, Treatment and Management of Haemonchus contortus in Small Ruminants. *Advances in Parasitology*, *93*, 181–238. https://doi.org/10.1016/bs.apar.2016.02.024
18. BESIER, R. B. – KAHN, L. P. – SARGISON, N. D. and VAN WYK, J. A. (2016b). The Pathophysiology, Ecology and Epidemiology of Haemonchus contortus Infection in Small Ruminants. *Advances in Parasitology*, *93*, 95–143. https://doi.org/10.1016/bs.apar.2016.02.022
19. BHUNIA, A. K. – BISHA, B. – GEHRING, A. G. and BREHM-STECHER, B. F. (2020). *Advances in foodborne pathogen analysis* (Vol. 9, Issue 11, p. 1635). MDPI.
20. BLACKIE, S. (2014). A review of the epidemiology of gastrointestinal nematode infections in sheep and goats in Ghana. *Journal of Agricultural Science*, *6*(4), 109.
21. BLITZ, N., H (1972). Studies on the arrested development of Haemonchus contortus in

sheep—I. The induction of arrested development. *Elsevier*. Retrieved November 26, 2022, from https://www.sciencedirect.com/science/article/pii/0020751972900288

22. BOELOW, H. – KRÜCKEN, J. – THOMAS, E. – MIRAMS, G. – VON SAMSON-HIMMELSTJERNA, G. (2022). Comparison of FECPAKG2, a modified Mini-FLOTAC technique and combined sedimentation and flotation for the coproscopic examination of helminth eggs in horses. *Parasites & Vectors*, *15*(1), 1–18.
23. BORDES, L. – DUMONT, N. – LESPINE, A. – SOUIL, E. – SUTRA, J.-F. – PRÉVOT, F. – GRISEZ, C. – ROMANOS, L. – DAILLEDOUZE, A. and JACQUIET, P. (2020). First report of multiple resistance to eprinomectin and benzimidazole in Haemonchus contortus on a dairy goat farm in France. *Parasitology International*, *76*, 102063.
24. BORKOWSKI, E. A. – REDMAN, E. M. – CHANT, R. – AVULA, J. – MENZIES, P. I. – KARROW, N. A. – LILLIE, B. N. – SEARS, W. – GILLEARD, J. S. and PEREGRINE, A. S. (2020). Comparison of ITS-2 rDNA nemabiome sequencing with morphological identification to quantify gastrointestinal nematode community species composition in small ruminant feces. *Veterinary Parasitology*, *282*, 109104.
25. BOWMAN, D. D. (2020). *Georgis' Parasitology for Veterinarians E-Book*. Elsevier Health Sciences.
26. BURGESS, C. G. S. – BARTLEY, Y. – REDMAN, E. – SKUCE, P. J. – NATH, M. – WHITELAW, F. – TAIT, A. – GILLEARD, J. S. and JACKSON, F. (2012). A survey of the trichostrongylid nematode species present on UK sheep farms and associated anthelmintic control practices. *Veterinary Parasitology*, *189*(2–4), 299–307.
27. BURKE, J. M. and MILLER, J. E. (2006). Control of Haemonchus contortus in goats with a sustained-release multi-trace element/vitamin ruminal bolus containing copper. *Veterinary Parasitology*, *141*(1–2), 132–137.
28. CAMPBELL, B. E. – NISBET, A. J. – MULVENNA, J. – LOUKAS, A. and GASSER, R. B. (2008). Molecular and phylogenetic characterization of cytochromes c from Haemonchus contortus and Trichostrongylus vitrinus (Nematoda: Trichostrongylida). *Gene*, *424*(1–2), 121–129.
29. CASTELLANOS-GONZALEZ, A. – WHITE Jr, A. C. – MELBY, P. and TRAVI, B. (2018). Molecular diagnosis of protozoan parasites by Recombinase Polymerase Amplification. *Acta Tropica*, *182*, 4–11.
30. CAZAJOUS, T. – PREVOT, F. – KERBIRIOU, A. – MILHES, M. – GRISEZ, C. – TROPEE, A., GODART, C. – ARAGON, A. and JACQUIET, P. (2018). Multiple-resistance to ivermectin and benzimidazole of a Haemonchus contortus population in a

sheep flock from mainland France, first report. *Veterinary Parasitology: Regional Studies and Reports*, *14*, 103–105.

31. CHAOUCH, M. (2021). Loop-mediated isothermal amplification (LAMP): An effective molecular point-of-care technique for the rapid diagnosis of coronavirus SARS-CoV-2. *Reviews in Medical Virology*, *31*(6), e2215.
32. CHARLIER, J. – RINALDI, L. – MUSELLA, V. – PLOEGER, H. W. – CHARTIER, C. – VINEER, H. R. – Hinney, B. – von Samson-Himmelstjerna, G. – Băcescu, B. and Mickiewicz, M. (2020). Initial assessment of the economic burden of major parasitic helminth infections to the ruminant livestock industry in Europe. *Preventive Veterinary Medicine*, *182*, 105103.
33. CHAUDHRY, U. – REDMAN, E. M. – RAMAN, M. and GILLEARD, J. S. (2015). Genetic evidence for the spread of a benzimidazole resistance mutation across southern India from a single origin in the parasitic nematode Haemonchus contortus. *International Journal for Parasitology*, *45*(11), 721–728.
34. CHEN, Q. – ROBERTSON, L. – JONES, J. T. – BLOK, V. C. – PHILLIPS, M. S. and BROWN, D. J. F. (2001). Capture of nematodes using antiserum and lectin-coated magnetised beads. *Nematology*, *3*(6), 593–601.
35. CLARK, C. H. – KIESEL, G. K., and GOBY, C. H. (1962). Measurements of blood loss caused by Haemonchus contortus infection in sheep. *American Journal of Veterinary Research*, *23*(96), 977–980.
36. COADWELL, W. J. and WARD, P. F. V. (1982). The use of faecal egg counts for estimating worm burdens in sheep infected with Haemonchus contortus. *Parasitology*, *85*(2), 251–256.
37. COLDITZ, I. G. – Le JAMBRE, L. F. and HOSSE, R. (2002). Use of lectin binding characteristics to identify gastrointestinal parasite eggs in faeces. *Veterinary Parasitology*, *105*(3), 219–227.
38. COLES, G. C. – BAUER, C. – BORGSTEEDE, F. H. M. – GEERTS, S. – KLEI, T. R. – TAYLOR, M. A. and WALLER, P. J. (1992). World Association for the Advancement of Veterinary Parasitology (W.A.A.V.P.) methods for the detection of anthelmintic resistance in nematodes of veterinary importance. *Veterinary Parasitology*, *44*(1–2), 35–44. https://doi.org/10.1016/0304-4017(92)90141-U
39. COSTA-JUNIOR, L. M. – CHAUDHRY, U. N. – SILVA, C. R. – SOUSA, D. M. – SILVA, N. C. – Cutrim-Júnior, J. A. A. – Brito, D. R. B. and Sargison, N. D. (2021). Nemabiome metabarcoding reveals differences between gastrointestinal nematode

species infecting co-grazed sheep and goats. *Veterinary Parasitology*, *289*, 109339.

40. CRINGOLI, G. – AMADESI, A. – MAURELLI, M. P. – CELANO, B. – PIANTADOSI, G. – BOSCO, A. – CIUCA, L. – CESARELLI, M. – BIFULCO, P. – MONTRESOR, A. and RINALDI, L. (2021). The Kubic FLOTAC microscope (KFM): A new compact digital microscope for helminth egg counts. *Parasitology*, *148*(4), 427–434. https://doi.org/10.1017/S003118202000219X
41. CRINGOLI, G. – MAURELLI, M. P. – LEVECKE, B. – BOSCO, A. – VERCRUYSSE, J. – UTZINGER, J. and RINALDI, L. (2017). The Mini-FLOTAC technique for the diagnosis of helminth and protozoan infections in humans and animals. *Nature Protocols*, *12*(9), 1723–1732. https://doi.org/10.1038/nprot.2017.067
42. CRINGOLI, G. – RINALDI, L. – MAURELLI, M. P. and UTZINGER, J. (2010). FLOTAC: new multivalent techniques for qualitative and quantitative copromicroscopic diagnosis of parasites in animals and humans. *Nature Protocols*, *5*(3), 503–515.
43. CSIVINCSIK, Á. – NAGY, G. – HALÁSZ, T. and ZSOLNAI, A. (2017). Shared pastures and anthelmintic resistance in wildlife and livestock. *Agriculturae Conspectus Scientificus*, *82*(2 Special Issue 1), 189–191.
44. DAHER, R. K. – STEWART, G. – BOISSINOT, M. and BERGERON, M. G. (2016). Recombinase polymerase amplification for diagnostic applications. *Clinical Chemistry*, *62*(7), 947–958.
45. DARGIE, J. D. and ALLONBY, E. W. (1975). Pathophysiology of single and challenge infections of Haemonchus contortus in Merino sheep: Studies on red cell kinetics and the "self-cure" phenomenon. *International Journal for Parasitology*, *5*(2), 147–157. https://doi.org/10.1016/0020-7519(75)90021-1
46. DASKOU, M. – TSAKOGIANNIS, D. – DIMITRIOU, T. G. – AMOUTZIAS, G. D. – MOSSIALOS, D. – KOTTARIDI, C. – GARTZONIKA, C. and MARKOULATOS, P. (2019). WarmStart colorimetric LAMP for the specific and rapid detection of HPV16 and HPV18 DNA. *Journal of Virological Methods*, *270*, 87–94.
47. DE CLERCQ, P. – MASON, P. G. and BABENDREIER, D. (2011). Benefits and risks of exotic biological control agents. *BioControl*, *56*, 681–698.
48. DOMKE, A. V. M. – CHARTIER, C. – GJERDE, B. – LEINE, N. – VATN, S. and STUEN, S. (2013). Prevalence of gastrointestinal helminths, lungworms and liver fluke in sheep and goats in Norway. *Veterinary Parasitology*, *194*(1), 40–48.
49. DOUANNE, N. – WAGNER, V. – BÉLANGER, D. and FERNANDEZ-PRADA, C.

(2019). High-throughput identification and quantification of Haemonchus contortus in fecal samples. *Veterinary Parasitology*, *265*, 24–28.

50. DOYLE, S. R. – TRACEY, A. – LAING, R. – HOLROYD, N. – BARTLEY, D. – BAZANT, W. – BEASLEY, H. – BEECH, R. – BRITTON, C. – BROOKS, K. – CHAUDHRY, U. – MAITLAND, K. – MARTINELLI, A. – NOONAN, J. D. – PAULINI, M. – QUAIL, M. A. – REDMAN, E. – RODGERS, F. H. – SALLÉ, G., … COTTON, J. A. (2020). Genomic and transcriptomic variation defines the chromosome-scale assembly of Haemonchus contortus, a model gastrointestinal worm. *Communications Biology*, *3*(1), 656. https://doi.org/10.1038/s42003-020-01377-3
51. ECHEVARRIA, F. A. M. – GENNARI, S. M. and TAIT, A. (1992). Isoenzyme analysis of Haemonchus contortus resistant or susceptible to ivermectin. *Veterinary Parasitology*, *44*(1–2), 87–95.
52. ELGHRYANI, N. – CRISPELL, J. – EBRAHIMI, R. – KRIVORUCHKO, M. – LOBASKIN, V. – MCOWAN, T. – O'CONNOR, W. – POWER, E. – VOISIN, B. and SCHOLZ, D. (2020). Preliminary evaluation of a novel, fully automated, Telenostic device for rapid field-diagnosis of cattle parasites. *Parasitology*, *147*(11), 1249–1253.
53. ELMAHALAWY, S. T. – HALVARSSON, P. – SKARIN, M. and HÖGLUND, J. (2018). Droplet digital polymerase chain reaction (ddPCR) as a novel method for absolute quantification of major gastrointestinal nematodes in sheep. *Veterinary Parasitology*, *261*, 1–8.
54. EMERY, D. L. – HUNT, P. W. and LE JAMBRE, L. F. (2016). Haemonchus contortus: the then and now, and where to from here? *International Journal for Parasitology*, *46*(12), 755–769. https://doi.org/10.1016/j.ijpara.2016.07.001
55. FAKAE, B. B. (1990). Seasonal changes and hypobiosis in Haemonchus contortus infection in the West African Dwarf sheep and goats in the Nigerian derived savanna. *Veterinary Parasitology*, *36*(1–2), 123–130.
56. FALZON, L. C. – MENZIES, P. I. – VANLEEUWEN, J. – SHAKYA, K. P. – JONES-BITTON, A. – AVULA, J. – JANSEN, J. T. and PEREGRINE, A. S. (2014). Pilot project to investigate over-wintering of free-living gastrointestinal nematode larvae of sheep in Ontario, Canada. *The Canadian Veterinary Journal*, *55*(8), 749.
57. FÁVERO, F. C. – BUZZULINI, C. – CRUZ, B. C. – FELIPPELLI, G. – MACIEL, W. G. – SALATTA, B., TEIXEIRA, W. F. P. – SOARES, V. E. – DE OLIVEIRA, G. P. and LOPES, W. D. Z. (2016). Experimental infection of calves with Haemonchus placei and Haemonchus contortus: assessment of parasitological parameters. *Veterinary*

Parasitology, *217*, 25–28.

58. FELSENSTEIN, J. (1992). Phylogenies from restriction sites: a maximum-likelihood approach. *Evolution*, *46*(1), 159–173.
59. FLAY, K. J. – HILL, F. I. and MUGUIRO, D. H. (2022). A Review: Haemonchus contortus Infection in Pasture-Based Sheep Production Systems, with a Focus on the Pathogenesis of Anaemia and Changes in Haematological Parameters. *Animals*, *12*(10), 1238.
60. FRANCIS, E. K. and ŠLAPETA, J. (2022). A new diagnostic approach to fast-track and increase the accessibility of gastrointestinal nematode identification from faeces: FECPAKG2 egg nemabiome metabarcoding. *International Journal for Parasitology*, *52*(6), 331–342.
61. GARCÍA-BERNALT DIEGO, J. – FERNÁNDEZ-SOTO, P. – MÁRQUEZ-SÁNCHEZ, S. – SANTOS SANTOS, D. – FEBRER-SENDRA, B. – CREGO-VICENTE, B. – MUÑOZ-BELLIDO, J. L. – BELHASSEN-GARCÍA, M. – CORCHADO RODRÍGUEZ, J. M. and MURO, A. (2022). SMART-LAMP: A smartphone-operated handheld device for real-time colorimetric point-of-care diagnosis of infectious diseases via loop-mediated isothermal amplification. *Biosensors*, *12*(6), 424.
62. GAREH, A. – ELHAWARY, N. M. – TAHOUN, A. – RAMEZ, A. M. – EL-SHEWEHY, D. M. M., ELBAZ, E. – KHALIFA, M. I. – ALSHARIF, K. F. – KHALIFA, R. M. A. and DYAB, A. K. (2021). Epidemiological, morphological, and morphometric study on Haemonchus spp. Recovered from goats in Egypt. *Frontiers in Veterinary Science*, *8*, 705619.
63. GARG, N. – AHMAD, F. J. and KAR, S. (2022). Recent advances in loop-mediated isothermal amplification (LAMP) for rapid and efficient detection of pathogens. *Current Research in Microbial Sciences*, 100120.
64. GASSER, R. B. – BOTT, N. J. – CHILTON, N. B. – HUNT, P. and BEVERIDGE, I. (2008). Toward practical, DNA-based diagnostic methods for parasitic nematodes of livestock—bionomic and biotechnological implications. *Biotechnology Advances*, *26*(4), 325–334.
65. GASSER, R. B. – CHILTON, N. B. – HOSTE, H. and STEVENSON, L. A. (1994). Species identification of trichostrongyle nematodes by PCR-linked RFLP. *International Journal for Parasitology*, *24*(2), 291–293.
66. GATONGI, P. M. – PRICHARD, R. K. – RANJAN, S. – GATHUMA, J. M. –

MUNYUA, W. K. – CHERUIYOT, H. and SCOTT, M. E. (1998). Hypobiosis of Haemonchus contortus in natural infections of sheep and goats in a semi-arid area of Kenya. *Veterinary Parasitology*, *77*(1), 49–61.

67. GETACHEW, T. – DORCHIES, P. – JACQUIET, P. (2007). Trends and challenges in the effective and sustainable control of Haemonchus contortus infection in sheep. Review. *Parasite*, *14*(1), 3–14. https://doi.org/10.1051/parasite/2007141003
68. GHAFAR, A. – ABBAS, G. – KING, J. – JACOBSON, C. – HUGHES, K. J. – EL-HAGE, C. – BEASLEY, A. – BAUQUIER, J. – WILKES, E. J. A. and HURLEY, J. (2021). Comparative studies on faecal egg counting techniques used for the detection of gastrointestinal parasites of equines: A systematic review. *Current Research in Parasitology & Vector-Borne Diseases*, *1*, 100046.
69. GILLEARD, J. S. and REDMAN, E. (2016). Genetic Diversity and Population Structure of Haemonchus contortus. *Advances in Parasitology*, *93*, 31–68. https://doi.org/10.1016/bs.apar.2016.02.009
70. GORDON, H. M. and WHITLOCK, H. V. (1939). A new technique for counting nematode eggs in sheep faeces. *J Counc Sci Ind Res*, *12*(1), 50–52.
71. GOUŸ DE BELLOCQ, J. – FERTÉ, H. – DEPAQUIT, J. – JUSTINE, J. LOU, TILLIER, A. – DURETTE-DESSET, M. C. (2001). Phylogeny of the Trichostrongylina (Nematoda) inferred from 28S rDNA sequences. *Molecular Phylogenetics and Evolution*, *19*(3), 430–442. https://doi.org/10.1006/mpev.2001.0925
72. GUEVARA, E. E. – FRANKEL, D. C. – RANAIVONASY, J. – RICHARD, A. F. – RATSIRARSON, J. – LAWLER, R. R. and BRADLEY, B. J. (2018). A simple, economical protocol for DNA extraction and amplification where there is no lab. *Conservation Genetics Resources*, *10*(1), 119–125.
73. HALL, B. G. (2013). Building phylogenetic trees from molecular data with MEGA. *Molecular Biology and Evolution*, *30*(5), 1229–1235.
74. HEISE, M. – EPE, C. and SCHNIEDER, T. (1999). Differences in the second internal transcribed spacer (ITS-2) of eight species of gastrointestinal nematodes of ruminants. *The Journal of Parasitology*, 431–435.
75. HERTZBERG, H. – HUWYLER, U. and KOHLER, L. (2002). Kinetics of exsheathment of infective ovine and bovine strongylid larvae in vivo and in vitro. *Cambridge.Org*. https://doi.org/10.1017/S0031182002001816
76. HILLRICHS, K. – SCHNIEDER, T. – FORBES, A. B. – SIMCOCK, D. C. – PEDLEY, K. C. and SIMPSON, H. V. (2012). Use of fluorescent lectin binding to distinguish

Teladorsagia circumcincta and Haemonchus contortus eggs, third-stage larvae and adult worms. *Parasitology Research*, *110*(1), 449–458.

77. HOBERG, E. P. – LICHTENFELS, J. R. and GIBBONS, L. (2004). Phylogeny for species of Haemonchus (Nematoda: Trichostrongyloidea): Considerations of their evolutionary history and global biogeography among Camelidae and Pecora (Artiodactyla). *Journal of Parasitology*, *90*(5), 1085–1102. https://doi.org/10.1645/GE-3309
78. HOBERG, E. P. and ZARLENGA, D. S. (2016). Evolution and biogeography of Haemonchus contortus: linking faunal dynamics in space and time. *Advances in Parasitology*, *93*, 1–30.
79. HÖGLUND, J. – GUSTAFSSON, K. – LJUNGSTRÖM, B.-L. – ENGSTRÖM, A. – DONNAN, A. and SKUCE, P. (2009). Anthelmintic resistance in Swedish sheep flocks based on a comparison of the results from the faecal egg count reduction test and resistant allele frequencies of the β-tubulin gene. *Veterinary Parasitology*, *161*(1–2), 60–68.
80. JACKSON, P. G. G. and COCKCROFT, P. D. (2002). Appendix 2: Laboratory Reference Values: Haematology. *Clinical Examination of Farm Animals*, 302.
81. JURASEK, M. E. – BISHOP-STEWART, J. K. – STOREY, B. E. – KAPLAN, R. M. – KENT, M. L. (2010). Modification and further evaluation of a fluorescein-labeled peanut agglutinin test for identification of Haemonchus contortus eggs. *Veterinary Parasitology*, *169*(1–2), 209–213. https://doi.org/10.1016/j.vetpar.2009.12.003
82. KANDIL, O. M.. – ABDELRAHMAN, K. A. – FAHMY, H. A. – MAHMOUD, M. S. – EL NAMAKY, A. H. and MILLER, J. E. (2017). Phylogenetic patterns of Haemonchus contortus and related trichostrongylid nematodes isolated from Egyptian sheep. *Journal of Helminthology*, *91*(5), 583–588.
83. KAO, R. R. – LEATHWICK, D. M. – ROBERTS, M. G., & SUTHERLAND, I. A. (2000). Nematode parasites of sheep: a survey of epidemiological parameters and their application in a simple model. *Parasitology*, *121*(1), 85–103.
84. KASSAI, T – FÉSÜS, L – HENDRIKX, W. M. L – TAKATS, C – FOK, É – REDL, P – TAKACS, E – NILSSON, P. R – VAN LEEUWEN, M. A. W and JANSEN, J. (1990). Is there a relationship between haemoglobin genotype and the innate resistance to experimental Haemonchus contortus infection in Merino lambs? *Veterinary Parasitology*, *37*(1), 61–77.
85. KEARNEY, P. E – MURRAY, P. J – HOY, J. M – HOHENHAUS, M. and KOTZE,

A. (2016). The “Toolbox” of strategies for managing Haemonchus contortus in goats: What’s in and what’s out. *Veterinary Parasitology*, *220*, 93–107. https://doi.org/10.1016/j.vetpar.2016.02.028

86. KENYON, F – GREER, A. W – COLES, G. C – CRINGOLI, G – PAPADOPOULOS, E – CABARET, J – BERRAG, B – VARADY, M – VAN WYK, J. A. and THOMAS, E. (2009). The role of targeted selective treatments in the development of refugia-based approaches to the control of gastrointestinal nematodes of small ruminants. *Veterinary Parasitology*, *164*(1), 3–11.
87. KENYON, F – RINALDI, L – MCBEAN, D – PEPE, P – BOSCO, A – MELVILLE, L – DEVIN, L – MITCHELL, G – IANNIELLO, D. and CHARLIER, J. (2016). Pooling sheep faecal samples for the assessment of anthelmintic drug efficacy using McMaster and Mini-FLOTAC in gastrointestinal strongyle and Nematodirus infection. *Veterinary Parasitology*, *225*, 53–60.
88. KHANGEMBAM, R. – TÓTH, M. – VASS, N. – VÁRADY, M. – CZEGLÉDI, L. – FARKAS, R. and ANTONOPOULOS, A. (2021). Point of care colourimetric and lateral flow LAMP assay for the detection of Haemonchus contortus in ruminant faecal samples. *Parasite*, *28*. https://doi.org/10.1051/parasite/2021078
89. KIM, E.-M – JEON, H.-S – KIM, J.-J – SHIN, Y.-K – LEE, Y.-J – YEO, S.-G. and PARK, C.-K. (2016). Uracil-DNA glycosylase-treated reverse transcription loop-mediated isothermal amplification for rapid detection of avian influenza virus preventing carry-over contamination. *Journal of Veterinary Science*, *17*(3), 421–425.
90. KOTZE, A. C – COWLING, K – BAGNALL, N. H – HINES, B. M – RUFFELL, A. P – HUNT, P. W. and COLEMAN, G. T. (2012). Relative level of thiabendazole resistance associated with the E198A and F200Y SNPs in larvae of a multi-drug resistant isolate of Haemonchus contortus. *International Journal for Parasitology: Drugs and Drug Resistance*, *2*, 92–97.
91. KOWAL, J – WYROBISZ, A – NOSAL, P – KUCHARSKI, M – KACZOR, U – SKALSKA, M. and SENDOR, P. (2016). Benzimidazole resistance in the ovine Haemonchus contortus from southern Poland-coproscopical and molecular findings. *Annals of Parasitology*, *62*(2).
92. KUMAR, S – STECHER, G – Li, M – KNYAZ, C. and TAMURA, K. (2018). MEGA X: molecular evolutionary genetics analysis across computing platforms. *Molecular Biology and Evolution*, *35*(6), 1547.
93. KUNZE, A – DILCHER, M – ABD El WAHED, A – HUFERT, F – NIESSNER, R.

and SEIDEL, M. (2016). On-chip isothermal nucleic acid amplification on flow-based chemiluminescence microarray analysis platform for the detection of viruses and bacteria. *Analytical Chemistry*, *88*(1), 898–905.

94. LAFONTAINE, D. L. J. and TOLLERVEY, D. (2001). The function and synthesis of ribosomes. *Nature Reviews Molecular Cell Biology*, *2*(7), 514–520.
95. LAI, M. Y. – Ooi, C. H. – JAIMIN, J. J. and Lau, Y. L. (2020). Evaluation of WarmStart colorimetric loop-mediated isothermal amplification assay for diagnosis of malaria. *The American Journal of Tropical Medicine and Hygiene*, *102*(6), 1370.
96. LAING, R. – KIKUCHI, T. – MARTINELLI, A. – TSAI, I. J. – BEECH, R. N. – REDMAN, E. – HOLROYD, N. – BARTLEY, D. J. – BEASLEY, H. – BRITTON, C. – CURRAN, D. – DEVANEY, E. – GILABERT, A. – HUNT, M. – JACKSON, F. – JOHNSTON, S. L. – KRYUKOV, I. – LI, K. – MORRISON, A. A. – … COTTON, J. A. (2013). The genome and transcriptome of Haemonchus contortus, a key model parasite for drug and vaccine discovery. *Genome Biology*, *14*(8), 1–16. https://doi.org/10.1186/gb-2013-14-8-r88
97. LE JAMBRE, L. F. (1995). Relationship of blood loss to worm numbers, biomass and egg production in Haemonchus infected sheep. *International Journal for Parasitology*, *25*(3), 269–273. https://doi.org/10.1016/0020-7519(94)00118-8
98. LEHRTER, V. – JOUET, D. – LIÉNARD, E. – DECORS, A. – . and PATRELLE, C. (2016). Ashworthius sidemi Schulz, 1933 and Haemonchus contortus (Rudolphi, 1803) in cervids in France: integrative approach for species identification. *Infection, Genetics and Evolution*, *46*, 94–101. https://doi.org/10.1016/j.meegid.2016.10.027
99. LEVECKE, B. – DOBSON, R. J. – Speybroeck, N. – Vercruysse, J. and Charlier, J. (2012). Novel insights in the faecal egg count reduction test for monitoring drug efficacy against gastrointestinal nematodes of veterinary importance. *Veterinary Parasitology*, *188*(3–4), 391–396.
100. LJUNGSTRÖM, S. – MELVILLE, L. – SKUCE, P. J. and HÖGLUND, J. (2018). Comparison of four diagnostic methods for detection and relative quantification of Haemonchus contortus eggs in feces samples. *Frontiers in Veterinary Science*, *4*(JAN), 239. https://doi.org/10.3389/fvets.2017.00239
101. LOBATO, I. M. and O'SULLIVAN, C. K. (2018). Recombinase polymerase amplification: Basics, applications and recent advances. *TrAC - Trends in Analytical Chemistry*, *98*, 19–35. https://doi.org/10.1016/j.trac.2017.10.015
102. LOVE, S. C. J. . and HUTCHINSON, G. W. (2003). Pathology and diagnosis of

internal parasites in ruminants. *Gross Pathology of Ruminants, Proceedings*, *350*, 309–338.

103. LUO, G.-C. – Yi, T.-T. – JIANG, B. – GUO, X.. and Zhang, G.-Y. (2019). Betaine-assisted recombinase polymerase assay with enhanced specificity. *Analytical Biochemistry*, *575*, 36–39.
104. MCKENNA, P. B. (1987). The estimation of gastrointestinal strongyle worm burdens in young sheep flocks: a new approach to the interpretation of faecal egg counts. *New Zealand Veterinary Journal*, *35*(6), 94–97.
105. *McMaster egg counting technique: Principle*. (n.d.). Retrieved December 6, 2022, from https://www.rvc.ac.uk/review/parasitology/eggcount/Principle.htm
106. MCNALLY, J. – CALLAN, D. – ANDRONICOS, N. – BOTT, N. and HUNT, P. W. (2013). DNA-based methodology for the quantification of gastrointestinal nematode eggs in sheep faeces. *Veterinary Parasitology*, *198*(3–4), 325–335.
107. MELVILLE, L. – KENYON, F. – JAVED, S. – MCELARNEY, I. – DEMELER, J. and SKUCE, P. (2014). Development of a loop-mediated isothermal amplification (LAMP) assay for the sensitive detection of Haemonchus contortus eggs in ovine faecal samples. *Veterinary Parasitology*, *206*(3–4), 308–312. https://doi.org/10.1016/j.vetpar.2014.10.022
108. MES, T. H. M. – EYSKER, M. and PLOEGER, H. W. (2007). A simple, robust and semi-automated parasite egg isolation protocol. *Nature Protocols*, *2*(3), 486–489.
109. MICKIEWICZ, M. – CZOPOWICZ, M. – KAWECKA-GROCHOCKA, E. – MOROZ, A. – SZALUŚ-Jordanow, O. – Várady, M. – Königová, A. – Spinu, M. – Górski, P. and Bagnicka, E. (2020). The first report of multidrug resistance in gastrointestinal nematodes in goat population in Poland. *BMC Veterinary Research*, *16*, 1–12.
110. MORI, Y. – KANDA, H. and NOTOMI, T. (2013). Loop-mediated isothermal amplification (LAMP): recent progress in research and development. *Journal of Infection and Chemotherapy*, *19*(3), 404–411.
111. MULLIS, K. – FALOONA, F. – SCHARF, S. – SAIKI, R. – HORN, G. and ERLICH, H. (1986). Specific enzymatic amplification of DNA in vitro: the polymerase chain reaction. *Cold Spring Harbor Symposia on Quantitative Biology*, *51*, 263–273.
112. NABAVI, R. – SHAYAN, P. – SHOKRANI, H. R. – ESLAMI, A. and BOKAIE, S. (2011). Evaluation of benzimidazole resistance in Haemonchus contortus using comparative PCR-RFLP methods. *Iranian Journal of Parasitology*, *6*(2), 45.

113. NAEEM, M. – IQBAL, Z. and ROOHI, N. (2021). Ovine haemonchosis: a review. *Tropical Animal Health and Production*, *53*(1), 1–11. https://doi.org/10.1007/s11250-020-02439-8

114. NAGAMORI, Y. – SEDLAK, R. H. – DEROSA, A. – PULLINS, A. – CREE, T. – LOENSER, M. – LARSON, B. S. – SMITH, R. B. – PENN, C. and GOLDSTEIN, R. (2021). Further evaluation and validation of the VETSCAN IMAGYST: in-clinic feline and canine fecal parasite detection system integrated with a deep learning algorithm. *Parasites & Vectors*, *14*(1), 1–12.

115. NAGY, G. – CSIVINCSIK, Á. – SUGÁR, L. and ZSOLNAI, A. (2017). Benzimidazole resistance within red deer, roe deer and sheep populations within a joint habitat in Hungary. *Small Ruminant Research*, *149*, 172–175. https://doi.org/10.1016/j.smallrumres.2017.02.012

116. NAGY, G. – CSIVINCSIK, Á. – ZSOLNAI, A. and SUGÁR, L. (2016). Benzimidazole resistance in Haemonchus contortus recovered from farmed red deer. *Parasitology Research*, *115*(9), 3643–3647. https://doi.org/10.1007/s00436-016-5155-6

117. NDAMUKONG, K. J. N. and NGONE, M. M. (1996). Development and survival of Haemonchus contortus and Trichostrongylus sp. on pasture in Cameroon. *Tropical Animal Health and Production*, *28*(3), 193–198. https://doi.org/10.1007/BF02240933

118. NDAO, M. (2009). Diagnosis of parasitic diseases: old and new approaches. *Interdisciplinary Perspectives on Infectious Diseases*, *2009*.

119. NEWTON, S. E. and MEEUSEN, E. N. T. (2003). Progress and new technologies for developing vaccines against gastrointestinal nematode parasites of sheep. *Parasite Immunology*, *25*(5), 283–296.

120. NICHOLLS, J. and OBENDORF, D. L. (1994). Application of a composite faecal egg count procedure in diagnostic parasitology. *Veterinary Parasitology*, *52*(3–4), 337–342. https://doi.org/10.1016/0304-4017(94)90125-2

121. NIELSEN, M. K. (2021). What makes a good fecal egg count technique? *Veterinary Parasitology*, *296*, 109509. https://doi.org/10.1016/j.vetpar.2021.109509

122. NNADI, P. A. – KAMALU, T. N. and ONAH, D. N. (2009). The effect of dietary protein on the productivity of West African Dwarf (WAD) goats infected with Haemonchus contortus. *Veterinary Parasitology*, *161*(3–4), 232–238.

123. NOTOMI, T. – OKAYAMA, H. – MASUBUCHI, H. – YONEKAWA, T. – WATANABE, K. – AMINO, N. and HASE, T. (2000). Loop-mediated isothermal

amplification of DNA. *Nucleic Acids Research*, *28*(12), e63–e63.

124. O'CONNOR, L. J. – WALKDEN-BROWN, S. W. and KAHN, L. P. (2006). Ecology of the free-living stages of major trichostrongylid parasites of sheep. *Veterinary Parasitology*, *142*(1–2), 1–15. https://doi.org/10.1016/j.vetpar.2006.08.035
125. OLIVEIRA, B. B. – VEIGAS, B. and BAPTISTA, P. V. (2021). Isothermal amplification of nucleic acids: the race for the next "gold standard." *Frontiers in Sensors*, *2*, 752600.
126. PALMER, D. G. and MCCOMBE, I. L. (1996). Lectin staining of trichostrongylid nematode eggs of sheep: rapid identification of Haemonchus contortus eggs with peanut agglutinin. *International Journal for Parasitology*, *26*(4), 447–450.
127. PAPADAKIS, G. – PANTAZIS, A. K. – FIKAS, N. – CHATZIIOANNIDOU, S. – TSIAKALOU, V. – MICHAELIDOU, K. – POGKA, V. – MEGARITI, M. – VARDAKI, M. and GIARENTIS, K. (2022). Portable real-time colorimetric LAMP-device for rapid quantitative detection of nucleic acids in crude samples. *Scientific Reports*, *12*(1), 1–15.
128. PARAS, K. L. – GEORGE, M. M. – VIDYASHANKAR, A. N. and KAPLAN, R. M. (2018). Comparison of fecal egg counting methods in four livestock species. *Veterinary Parasitology*, *257*, 21–27.
129. PARK, J. S. – HSIEH, K. – CHEN, L. – KAUSHIK, A. – TRICK, A. Y. and WANG, T. (2021). Digital CRISPR/Cas-Assisted assay for rapid and sensitive detection of SARS-CoV-2. *Advanced Science*, *8*(5), 2003564.
130. PELTZER, D. – TOBLER, K. – FRAEFEL, C. – MALEY, M. and BACHOFEN, C. (2021). Rapid and simple colorimetric loop-mediated isothermal amplification (LAMP) assay for the detection of Bovine alphaherpesvirus 1. *Journal of Virological Methods*, *289*, 114041.
131. PENA-ESPINOZA, M. – THAMSBORG, S. M. – DEMELER, J. and ENEMARK, H. L. (2014). Field efficacy of four anthelmintics and confirmation of drug-resistant nematodes by controlled efficacy test and pyrosequencing on a sheep and goat farm in Denmark. *Veterinary Parasitology*, *206*(3–4), 208–215.
132. PIEPENBURG, O. – WILLIAMS, C. H. – STEMPLE, D. L. and ARMES, N. A. (2006). DNA detection using recombination proteins. *PLoS Biology*, *4*(7), e204.
133. PITAKSAKULRAT, O. – CHAIYASAENG, M. – ARTCHAYASAWAT, A. – EAMUDOMKARN, C. – Boonmars, T. – Kopolrat, K. Y. – Prasopdee, S. – Petney, T. N. – Blair, D. and Sithithaworn, P. (2021). Genetic diversity and population structure of

Haemonchus contortus in goats from Thailand. *Infection, Genetics and Evolution*, *95*, 105021.

134. PRESLAND, S. L. – MORGAN, E. R. and COLES, G. C. (2005). Counting nematode eggs in equine faecal samples. *Veterinary Record*, *156*(7), 208–210. https://doi.org/10.1136/vr.156.7.208

135. PRICHARD, R. K. (2001). Genetic variability following selection of Haemonchus contortus with anthelmintics. *Trends in Parasitology*, *17*(9), 445–453. https://doi.org/10.1016/S1471-4922(01)01983-3

136. QAMAR, W. – ZAMAN, M. A. – FAHEEM, M. – AHMED, I. – ALI, K. – QAMAR, M. F. – ISHAQ, H. M. and ATIF, F. A. (2022). Molecular Confirmation and Genetic characterization of Haemonchus contortus Isolates at the Nuclear Ribosomal ITS2 Region: First Update from Jhang Region of Pakistan. *Pakistan Veterinary Journal*, *42*(2).

137. QUEIROZ, C. – LEVY, M. – AVRAMENKO, R. – REDMAN, E. – KEARNS, K. – SWAIN, L. – Silas, H. – UEHLINGER, F. and GILLEARD, J. S. (2020). The use of ITS-2 rDNA nemabiome metabarcoding to enhance anthelmintic resistance diagnosis and surveillance of ovine gastrointestinal nematodes. *International Journal for Parasitology: Drugs and Drug Resistance*, *14*, 105–117.

138. RAMÜNKE, S. – MELVILLE, L. – RINALDI, L. – HERTZBERG, H. – DE WAAL, T. – VON SAMSON-HIMMELSTJERNA, G. – CRINGOLI, G. – MAVROT, F. – SKUCE, P. and KRÜCKEN, J. (2016). Benzimidazole resistance survey for Haemonchus, Teladorsagia and Trichostrongylus in three European countries using pyrosequencing including the development of new assays for Trichostrongylus. *International Journal for Parasitology: Drugs and Drug Resistance*, *6*(3), 230–240.

139. REDMAN, E. – PACKARD, E. – GRILLO, V. – SMITH, J. – JACKSON, F. and GILLEARD, J. S. (2008). Microsatellite analysis reveals marked genetic differentiation between Haemonchus contortus laboratory isolates and provides a rapid system of genetic fingerprinting. *International Journal for Parasitology*, *38*(1), 111–122. https://doi.org/10.1016/j.ijpara.2007.06.008

140. REDMAN, E. – QUEIROZ, C. – BARTLEY, D. J. – LEVY, M. – AVRAMENKO, R. W. and GILLEARD, J. S. (2019). Validation of ITS-2 rDNA nemabiome sequencing for ovine gastrointestinal nematodes and its application to a large scale survey of UK sheep farms. *Veterinary Parasitology*, *275*, 108933.

141. RESLOVA, N. – SKORPIKOVA, L. – KYRIANOVA, I. A. – VADLEJCH, J. –

HÖGLUND, J. – SKUCE, P. . and KASNY, M. (2021). The identification and semi-quantitative assessment of gastrointestinal nematodes in faecal samples using multiplex real-time PCR assays. *Parasites & Vectors*, *14*(1), 1–12.

142. RINALDI, L. (2014). *The coprological diagnosis of gastrointestinal nematode infections in small ruminants*. Ghent University.
143. RINALDI, L. – AMADESI, A. – DUFOURD, E. – BOSCO, A. – GADANHO, M. – LEHEBEL, A. – MAURELLI, M. P. – CHAUVIN, A. – CHARLIER, J. and CRINGOLI, G. (2019). Rapid assessment of faecal egg count and faecal egg count reduction through composite sampling in cattle. *Parasites & Vectors*, *12*(1), 1–8.
144. RINALDI, L. – CATELAN, D. – MUSELLA, V. – CECCONI, L. – HERTZBERG, H. – TORGERSON, P. R. – MAVROT, F. – de WAAL, T. – SELEMETAS, N. – COLL, T. – BOSCO, A. – BIGGERI, A. and CRINGOLI, G. (2015). Haemonchus contortus: Spatial risk distribution for infection in sheep in Europe. *Geospatial Health*, *9*(2), 325–331. https://doi.org/10.4081/gh.2015.355
145. RINALDI, L. – KRÜCKEN, J. – MARTINEZ-VALLADARES, M. – PEPE, P. – MAURELLI, M. P. – de QUEIROZ, C. – WANG, T. – CRINGOLI, G. – CHARLIER, J. and GILLEARD, J. S. (2022). Advances in diagnosis of gastrointestinal nematodes in livestock and companion animals. *Advances in Parasitology*, *118*, 85–176.
146. ROEBER, F. – JEX, A. R. and GASSER, R. B. (2013). Impact of gastrointestinal parasitic nematodes of sheep, and the role of advanced molecular tools for exploring epidemiology and drug resistance - An Australian perspective. *Parasites and Vectors*, *6*(1), 1–13. https://doi.org/10.1186/1756-3305-6-153
147. ROGERS, M. J. – MCMANUS, D. P. – MUHI, S. and GORDON, C. A. (2021). Membrane technology for rapid point-of-care diagnostics for parasitic neglected tropical diseases. *Clinical Microbiology Reviews*, *34*(4), e00329-20.
148. ROSE, H. – CAMINADE, C. – BOLAJOKO, M. B. – PHELAN, P. – VAN DIJK, J. – BAYLIS, M. – WILLIAMS, D. and MORGAN, E. R. (2016). Climate-driven changes to the spatio-temporal distribution of the parasitic nematode, Haemonchus contortus, in sheep in Europe. *Global Change Biology*, *22*(3), 1271–1285. https://doi.org/10.1111/gcb.13132
149. ROSE VINEER, H. – MORGAN, E. R. – HERTZBERG, H. – BARTLEY, D. J. – BOSCO, A. – CHARLIER, J. – Chartier, C. – Claerebout, E. – De Waal, T. – Hendrickx, G. – Hinney, B. – Höglund, J. – Jez Ek, J. I. – Kašný, M. – Keane, O. M. – Martínez-Valladares, M. – Mateus, T. L. – McIntyre, J. – Mickiewicz, M. – … Rinaldi, L. (2020).

Increasing importance of anthelmintic resistance in European livestock: Creation and meta-analysis of an open database. *Parasite*, *27*, 69. https://doi.org/10.1051/parasite/2020062

150. SACCAREAU, M. – SALLÉ, G. – ROBERT-GRANIÉ, C. – DUCHEMIN, T. – JACQUIET, P. – BLANCHARD, A. – CABARET, J. and MORENO, C. R. (2017). Meta-analysis of the parasitic phase traits of Haemonchus contortus infection in sheep. *Parasites and Vectors*, *10*(1), 1–14. https://doi.org/10.1186/s13071-017-2131-7
151. SAITOU, N. and NEI, M. (1987). The neighbor-joining method: a new method for reconstructing phylogenetic trees. *Molecular Biology and Evolution*, *4*(4), 406–425.
152. SALLÉ, G. – DOYLE, S. R. – CORTET, J. – CABARET, J. – BERRIMAN, M. – HOLROYD, N. and COTTON, J. A. (2019). The global diversity of Haemonchus contortus is shaped by human intervention and climate. *Nature Communications*, *10*(1), 4811. https://doi.org/10.1038/s41467-019-12695-4
153. SCHWARZ, E. M. – KORHONEN, P. K. – CAMPBELL, B. E. – YOUNG, N. D. – JEX, A. R. – JABBAR, A. – HALL, R. S. – MONDAL, A. – HOWE, A. C. and PELL, J. (2013). The genome and developmental transcriptome of the strongylid nematode Haemonchus contortus. *Genome Biology*, *14*(8), 1–18.
154. SHEN, D. D. – WANG, J. F. – ZHANG, D. Y. – PENG, Z. W. – YANG, T. Y. – WANG, Z. D. – BOWMAN, D. D. – HOU, Z. J. and LIU, Z. S. (2017). Genetic diversity of Haemonchus contortus isolated from sympatric wild blue sheep (Pseudois nayaur) and sheep in Helan Mountains, China. *Parasites and Vectors*, *10*(1), 1–10. https://doi.org/10.1186/s13071-017-2377-0
155. SIMPSON, H. V. (2000). Pathophysiology of abomasal parasitism: is the host or parasite responsible? *The Veterinary Journal*, *160*(3), 177–191.
156. SISSAY, M. M. – UGGLA, A. and WALLER, P. J. (2007). Epidemiology and seasonal dynamics of gastrointestinal nematode infections of sheep in a semi-arid region of eastern Ethiopia. *Veterinary Parasitology*, *143*(3–4), 311–321.
157. SLUSAREWICZ, P. – SLUSAREWICZ, J. H. and NIELSEN, M. K. (2021). Development and performance of an automated fecal egg count system for small ruminant strongylids. *Veterinary Parasitology*, *295*, 109442.
158. SOULSBY, E. J. L. (1968). Helminths, arthropods and protozoa of domesticated animals. *Helminths, Arthropods and Protozoa of Domesticated Animals.*
159. SPANGLER, G. L. – ROSEN, B. D. – ILORI, M. B. – HANOTTE, O. – KIM, E.-S. – SONSTEGARD, T. S. – BURKE, J. M. – MORGAN, J. L. M. – NOTTER, D. R. and

VAN TASSELL, C. P. (2017). Whole genome structural analysis of Caribbean hair sheep reveals quantitative link to West African ancestry. *PLoS One*, *12*(6), e0179021.

160. SRISRATTAKARN, A. – TIPPAYAWAT, P. – CHANAWONG, A. – TAVICHAKORNTRAKOOL, R. – DADUANG, J. – WONGLAKORN, L. – SOOKSONGSOONTORN, P. and LULITANOND, A. (2020). Direct detection of methicillin-resistant in Staphylococcus spp. in positive blood culture by isothermal recombinase polymerase amplification combined with lateral flow dipstick assay. *World Journal of Microbiology and Biotechnology*, *36*(11), 1–11. https://doi.org/10.1007/s11274-020-02938-8
161. STENBERG, J. A. – SUNDH, I. – BECHER, P. G. – BJÖRKMAN, C. – DUBEY, M. – EGAN, P. A. – FRIBERG, H. – GIL, J. F. – JENSEN, D. F. and JONSSON, M. (2021). When is it biological control? A framework of definitions, mechanisms, and classifications. *Journal of Pest Science*, *94*(3), 665–676.
162. STEVENSON, L. A. – CHILTON, N. B. and GASSER, R. B. (1995). Differentiation of Haemonchus placei from H. contortus (Nematoda: Trichostrongylidae) by the ribosomal DNA second internal transcribed spacer. *International Journal for Parasitology*, *25*(4), 483–488.
163. TAMURA, K. – NEI, M. and KUMAR, S. (2004). Prospects for inferring very large phylogenies by using the neighbor-joining method. *Proceedings of the National Academy of Sciences*, *101*(30), 11030–11035.
164. TAN, M. – LIAO, C. – LIANG, L. – YI, X. – ZHOU, Z. and WEI, G. (2022). Recent advances in recombinase polymerase amplification: Principle, advantages, disadvantages and applications. *Frontiers in Cellular and Infection Microbiology*, *12*, 1744.
165. TAYLOR, M. A. – COOP, R. L. and WALL, R. L. (2015). *Veterinary parasitology*. John Wiley & Sons.
166. TAYLOR, M.A. (2010). Parasitological examinations in sheep health management. *Small Ruminant Research*, *92*(1–3), 120–125.
167. TEIXEIRA, M. – MATOS, A. F. I. M. – ALBUQUERQUE, F. H. – BASSETTO, C. C. – SMITH, W. D. and MONTEIRO, J. P. (2019). Strategic vaccination of hair sheep against Haemonchus contortus. *Parasitology Research*, *118*(8), 2383–2388.
168. TROELL, K. (2006). *Genotypic and phenotypic characterization of Haemonchus contortus in Sweden* (Vol. 2006, Issue 2006: 36).
169. TROELL, K. – ENGSTRÖM, A. – MORRISON, D. A. – MATTSSON, J. G. and

HÖGLUND, J. (2006). Global patterns reveal strong population structure in Haemonchus contortus, a nematode parasite of domesticated ruminants. *International Journal for Parasitology*, *36*(12), 1305–1316.

170. UMAIR, S. – MCMURTRY, L. W. – KNIGHT, J. S. and SIMPSON, H. V. (2016). Use of fluorescent lectin binding to distinguish eggs of gastrointestinal nematode parasites of sheep. *Veterinary Parasitology*, *217*, 76–80.
171. UNTERSWEG, F. – FERNER, V. – WIEDERMANN, S. – GÖLLER, M. – HÖRL-RANNEGGER, M. – KAISER, W. – JOACHIM, A. – RINALDI, L. – KRÜCKEN, J. and HINNEY, B. (2021). Multispecific resistance of sheep trichostrongylids in Austria. *Parasite*, *28*.
172. URQUHART, G. M. – ARMOUR, J. – DUNCAN, J. L. – DUNN, A. M. and JENNINGS, F. W. (1996). Veterinary Parasitology, Blackwell Science. *United Kingdom*, *307*.
173. VADLEJCH, J. – KYRIÁNOVÁ, I. A. – VÁRADY, M. and CHARLIER, J. (2021). Resistance of strongylid nematodes to anthelmintic drugs and driving factors at Czech goat farms. *BMC Veterinary Research*, *17*(1), 1–11.
174. VAN WYK, J. A. – HOSTE, H. – KAPLAN, R. M. and BESIER, R. B. (2006). Targeted selective treatment for worm management—how do we sell rational programs to farmers? *Veterinary Parasitology*, *139*(4), 336–346.
175. VAN WYK, J. A. and MAYHEW, E. (2013). Morphological identification of parasitic nematode infective larvae of small ruminants and cattle: A practical lab guide. *Onderstepoort Journal of Veterinary Research*, *80*(1), 1–14.
176. VERÍSSIMO, C. J. – NICIURA, S. C. M. – ALBERTI, A. L. L. – RODRIGUES, C. F. C. – BARBOSA, C. M. P. – CHIEBAO, D. P. – CARDOSO, D. – DA SILVA, G. S. – PEREIRA, J. R. – MARGATHO, L. F. F. – DA COSTA, R. L. D. – NARDON, R. F. – UENO, T. E. H. – CURCI, V. C. L. M. and MOLENTO, M. B. (2012). Multidrug and multispecies resistance in sheep flocks from São Paulo state, Brazil. *Veterinary Parasitology*, *187*(1–2), 209–216. https://doi.org/10.1016/j.vetpar.2012.01.013
177. WALLER, P. J. and THAMSBORG, S. M. (2004). Nematode control in ‘green’ruminant production systems. *Trends in Parasitology*, *20*(10), 493–497.
178. WIDIARSO, B. P. – KURNIASIH, K. – PRASTOWO, J. and NURCAHYO, W. (2018). Morphology and morphometry of Haemonchus contortus exposed to Gigantochloa apus crude aqueous extract. *Veterinary World*, *11*(7), 921.
179. WU, Y. D. – WANG, Q. Q. – WANG, M. – ELSHEIKHA, H. M. – YANG, X. – HU,

M. – ZHU, X. Q. and XU, M. J. (2021). Development of a lateral flow strip-based recombinase polymerase amplification assay for the detection of haemonchus contortus in goat feces. *Korean Journal of Parasitology*, *59*(2), 167–171. https://doi.org/10.3347/kjp.2021.59.2.167

180. YIN, F. – GASSER, R. B. – LI, F. – BAO, M. – HUANG, W. – ZOU, F. – ZHAO, G. – WANG, C. – Yang, X. – Zhou, Y. – Zhao, J. – Fang, R. and Hu, M. (2016). Population structure of Haemonchus contortus from seven geographical regions in China, determined on the basis of microsatellite markers. *Parasites and Vectors*, *9*(1), 1–9. https://doi.org/10.1186/s13071-016-1864-z
181. YIN, K. – PANDIAN, V. – KADIMISETTY, K. – ZHANG, X. – RUIZ, C. – COOPER, K. and LIU, C. (2020). Real-time colorimetric quantitative molecular detection of infectious diseases on smartphone-based diagnostic platform. *Scientific Reports*, *10*(1), 1–9.
182. ZARLENGA, D. S., HOBERG, E. P. and TUO, W. (2016). The identification of Haemonchus species and diagnosis of haemonchosis. *Advances in parasitology*, *93*, 145-180.
183. ZARLENGA, D. S. – CHUTE, M. B. – GASBARRE, L. C. and BOYD, P. C. (2001). A multiplex PCR assay for differentiating economically important gastrointestinal nematodes of cattle. *Veterinary Parasitology*, *97*(3), 201–211.
184. ZARLENGA, D. S. – STRINGFELLOW, F. – NOBARY, M. and LICHTENFELS, J. R. (1994). Cloning and characterization of ribosomal RNA genes from three species of Haemonchus (Nematoda: Trichostrongyloidea) and identification of PCR primers for rapid differentiation. *Experimental Parasitology*, *78*(1), 28–36.

10. PUBLICATIONS ON THE TOPIC OF THE DISSERTATION

UNIVERSITY of DEBRECEN

UNIVERSITY AND NATIONAL LIBRARY
UNIVERSITY OF DEBRECEN
H-4002 Egyetem tér 1, Debrecen
Phone: +3652/410-443, email: publikaciok@lib.unideb.hu

Registry number: DEENK/276/2023.PL
Subject: PhD Publication List

Candidate: Rojesh Khangembam
Doctoral School: Doctoral School of Animal Husbandry
MTMT ID: 10065283

List of publications related to the dissertation

Foreign language scientific articles in Hungarian journals (2)

1. **Khangembam, R.**, Tóth, M., Gulyás, G., Czeglédi, L., Vass, N.: Recovery and confirmation of Haemonchus contortus from abomasal contents of roe deer (Capreolus capreolus) in Eastern-Hungary (Biharugra): A diagnostic case study.
   Acta agraria Debreceniensis. 1, 59-62, 2023. ISSN: 1587-1282.
   DOI: https://doi.org/10.34101/ACTAAGRAR/1/12058

2. **Khangembam, R.**, Czeglédi, L., Vass, N.: Routine microscopy examination of faecal samples as a tool for detection of common gastrointestinal parasites: a preliminary report from two Hungarian farms.
   Acta agraria Debreceniensis. 1, 63-66, 2023. ISSN: 1587-1282.
   DOI: http://dx.doi.org/https://doi.org/10.34101/actaagrar/1/12059

Foreign language scientific articles in international journals (3)

3. **Khangembam, R.**, Vass, N., Morrison, A., Melville, L. A., Antonopoulos, A., Czeglédi, L.: Preliminary Results of the Recombinase Polymerase Amplification Technique for the Detection of Haemonchus contortus from Hungarian Field Samples.
   Vet. Parasitol. Epub, 1-20, 2023. ISSN: 0304-4017.
   DOI: https://doi.org/10.1016/j.vetpar.2023.109974
   IF: 2.821 (2021)

4. **Khangembam, R.**, Tóth, M., Vass, N., Várady, M., Czeglédi, L., Farkas, R., Antonopoulos, A.: Point of care colourimetric and lateral flow LAMP assay for the detection of Haemonchus contortus in ruminant faecal samples.
   Parasite. 28, 1-12, 2021. ISSN: 1252-607X.
   DOI: http://dx.doi.org/10.1051/parasite/2021078
   IF: 3.02

5. Tóth, M., **Khangembam, R.**, Farkas, R., Oláh, J., Vass, N., Monori, I.: A case report: sheep endoparasitism dynamics under semi-dry continental climate of Karcag, Hungary.
   Biol. Tvarin. 21 (2), 66-69, 2019. ISSN: 1681-0015.
   DOI: http://dx.doi.org/10.15407/animbiol21.02.066

Foreign language conference proceedings (1)

6. **Khangembam, R.**, Czeglédi, L., Vass, N.: Detection of Haemonchus contortus eggs using peanut agglutinin (PNA) fluorescence microcopy.
In: XXX Jubilee International Congress of the Hungarian Association for Buiatrics. Proceedings, Magyar Buiatrikusok Társasága / Hungarian Association for Buiatrics, Budapest, 221-224, 2023. ISBN: 9786158141321

Foreign language abstracts (3)

7. **Khangembam, R.**, Czeglédi, L., Vass, N., Antonopoulos, A.: Proof of concept recombinase polymerase assay (RPA) for the detection of Haemonchus contortus in ruminants.
In: ICOPA 2022 International Congress of Parasitology Online Abstracts, World Federation of Parasitologists, Copenhagen, 1269, 2022.

8. **Khangembam, R.**, Vass, N.: Loop-mediated Isothermal Amplification (LAMP) as a tool for diagnosis of parasitism: Why it is gaining popularity.
In: XXIV. Tavaszi Szél Konferencia 2021 : Absztraktkötet. Szerk.: Molnár Dániel, Molnár Dóra, Doktoranduszok Országos Szövetsége, Budapest, 87-88, 2021. ISBN: 9786155586996

9. **Khangembam, R.**, Tóth, M., Vass, N., Várady, M., Farkas, R., Antonopoulos, A.: Point of care colourimetric and Lateral Flow-LAMP Assay for the detection of Haemonchus contortus from ruminant faecal samples.
In: 28th International Conference of the World Association for the Advancement of Veterinary Parasitology WAAVP 2021 : Book of Abstracts. Ed.: Grace Mulcahy, World Association for the Advancement of Veterinary Parasitology, Dublin, 178-179, 2021.

List of other publications

Foreign language scientific articles in international journals (1)

10. Xayalath, S., Mujitaba, M. A., Ortega, A. D. S. V., **Khangembam, R.**, Novotniné Dankó, G., Rátky, J.: Effects of birth weight on puberty and the reproductive performance of crossbred Moo Lath x Duroc gilts = A születési súly hatása az ivarérésre és a szaporodásbiológiai teljesítményre keresztezett Moo Lath x Duroc kocasüldőknél.
J. Cent. Eur. Agric. "Accepted by Publisher" (-), 1-11, 2023. ISSN: 1332-9049.

UNIVERSITY AND NATIONAL LIBRARY
UNIVERSITY OF DEBRECEN
H-4002 Egyetem tér 1, Debrecen
Phone: +3652/410-443, email: publikaciok@lib.unideb.hu

Informational/educational articles (1)

11. Oláh, J., Tóth, M., Molnár, A., Jávor, A., **Khangembam, R.**, Egerszegi, I.: Korszerű módszerek alkalmazása cigája tenyészkos jelöltek hústermelő képességének javítására. *Magyar juhászat + kecsketenyésztés. 28* (9), 2-4, 2019. ISSN: 0025-018X.

Total IF of journals (all publications): 5,841
Total IF of journals (publications related to the dissertation): 5,841

The Candidate's publication data submitted to the iDEa Tudóstér have been validated by DEENK on the basis of the Journal Citation Report (Impact Factor) database.

26 June, 2023

DEBRECENI EGYETEM Egyetemi és Nemzeti Könyvtár

11. ACKNOWLEDGEMENT

Though this dissertation bears only my name as the author, it is a product of many individuals who contributed directly or indirectly to make it complete. I pay my sincere gratitude to all those who have made this possible and my coursework a worthwhile experience.

It is my pleasure to express my deepest gratitude firstly to my advisor, **Dr. Nóra Pálfyné Vass** (Assistant Professor, Institute of Animal Science, Biotechnology and Nature Conservation, University of Debrecen) for her advice, feedback, sampling and overall moral support. Her guidance and affection showed to me right from the beginning of my application to this PhD course way back in 2018 till the end of drafting this manuscript are irreplaceable. I would also like to convey special gratitude to **Dr. Levente Czeglédi** (Head of Department of Animal Science, University of Debrecen) for being my mentor and a guide for my molecular-based works and advising on my dissertation manuscript.

I am also very thankful to **Dr. István Komlósi** (Head of Doctoral School of Animal Science, University of Debrecen) for his constructive criticism, insightful lectures and other support beyond the faculty room. A particular instance outside of the normal lectures for which I remain forever grateful is his kind action in trying to sort out my accommodation when I had to be quarantined during the covid-19 lockdown. Sincere gratitude to **Korcsmáros Marianna Varga** (Secretary of Doctoral School of Animal Science, University of Debrecen) for giving her best support, especially with all the paperwork I needed. I am also thankful to other members of the Department of Animal Science, University of Debrecen for their warmest kind support. My gratitude to **Mariann Tóth** and **István Monori** for their help in sampling visits and sharing the FEC data**.** I owe a big thanks to my colleagues in the faculty, especially **Dr. Brigitta Csernus, Dr. Gabriella Gulyás and Xénia Erika Ozsváth** for providing me with a helping hand whenever I asked in the molecular laboratory.

Much appreciation and gratitude to all my friends, especially **Dr. Andualem Tonamo**, for not being just a friend but also my flatmate and office mate. I am also grateful to my other friends in the department, **Somsy Xayalath**, **Arth David Sol Ortega**, **Malam Abubashar Mujtaba**, **Klein Renáta** and **Eszter Angyal** for their enthusiasm in and outside my PhD work.

I will also remain grateful to **Dr. Alistair Antonopoulos** (Kreavet, Belgium) who is not just a friend but also a colleague full of collaborative passion for any molecular laboratory work. My gratitude reaches out to **Dr. Lynsey Melville** (Moredun Research Institute, Scotland) for kindly helping me with all those valuable positive control specimens as well as for advice on the RPA manuscript. I am also thankful to **Dr. Róbert Farkas** (Professor, Department of Zoology and Parasitology, University of Veterinary Medicine, Budapest) for his valuable advice and worm samples.

A huge appreciation to the **Stipendium Hungaricum Scholarship Programme** (Tempus Public Foundation) for funding my PhD as well as the **EFOP-3.6.3-VEKOP-16-2017-00008** (European Union and European Social Fund) for all the other necessary funding and equipment.

Last but not least, I have heartfelt gratitude to my partner **Kata Juhász** for being there next to me for the past years and providing me with moral support to overcome my weakness and stress. I will forever remain grateful for her help in proofing/typesetting and also in 'debugging' my chromatogram data. Words fail me to express my appreciation and whole-hearted respect to my loving **mother Hemabati Yumnam**, and my caring **aunt Niengboi Haokip**, who have all been providing me with moral strength and prayers throughout.

All may not have been mentioned but none is forgotten.

12. APPENDIX

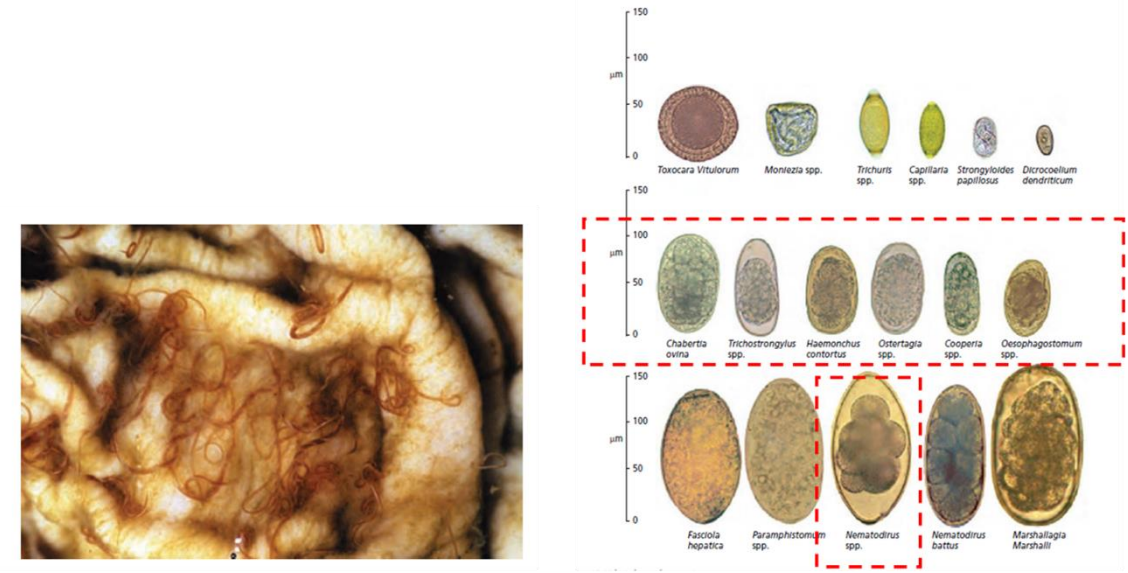

A B

Appendix Figure 1:

A: Adult *H. contortus* attached to the abomasal mucosa

B: Common helminth parasite eggs of small ruminants. The red-dotted box shows similar eggs which are difficult to differentiate under normal microscopy.

Adapted from TAYLOR et al., (2015)

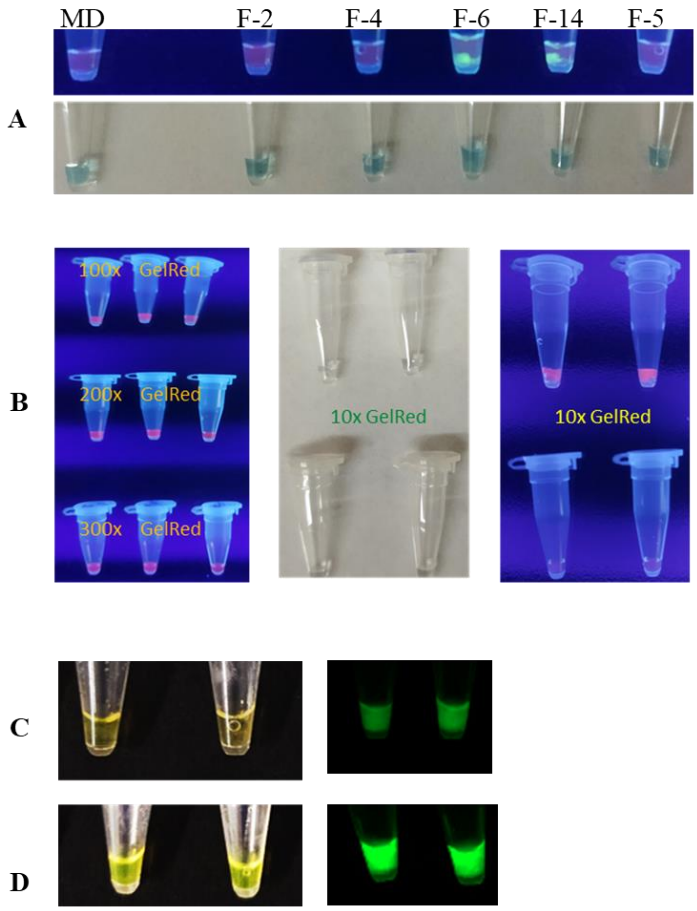

Appendix Figure 2:

Colourimetric detection of RPA assay results using various DNA intercalating dyes. A: Results of various farms as observed under UV-illumination (upper panel; positive results=purplish-green colour) and white light (lower panel) using EvaGreen dye; B: Results detected using various concentrations of GelRed dye. The middle panel shows results under white light with no significant colourimetric change. Positive result= purple glow; C: Negative control results using 300x SYBR Green II dye. The right side panel shows the same tubes under UV illumination; D: Positive control results using 300x SYBR Green II dye showing bright green colouration under white light (left panel) as well as stronger fluorescence under UV illumination. MD= positive control; F-2, F-4, F-5, F-6 and F-14 = farm samples

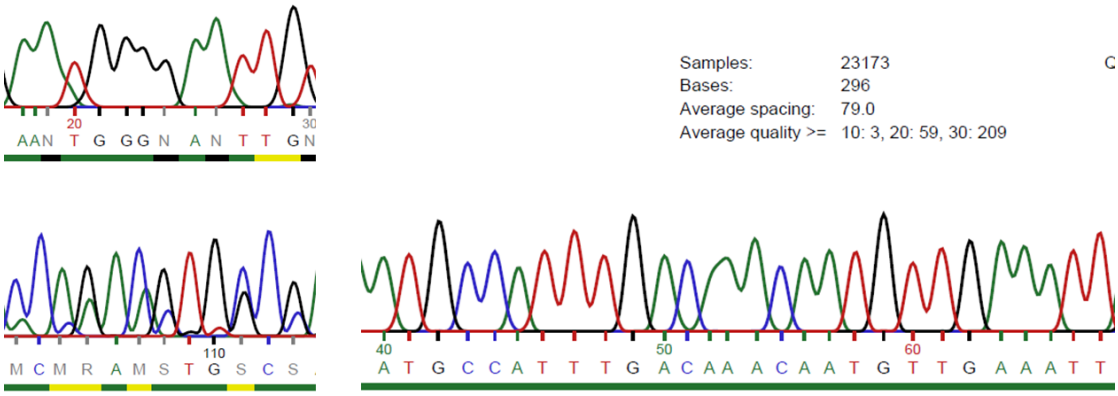

A **B**

Appendix Figure 3:

Screenshot of the Sanger sequencing chromatogram of one of the three isolates of *H. contortus* from Hungary.

A: Weak and/or mixed signal peaks resulting in misinterpreted nucleotide sequence;

B: Clean and uniform peaks and the corresponding nucleotide sequence.

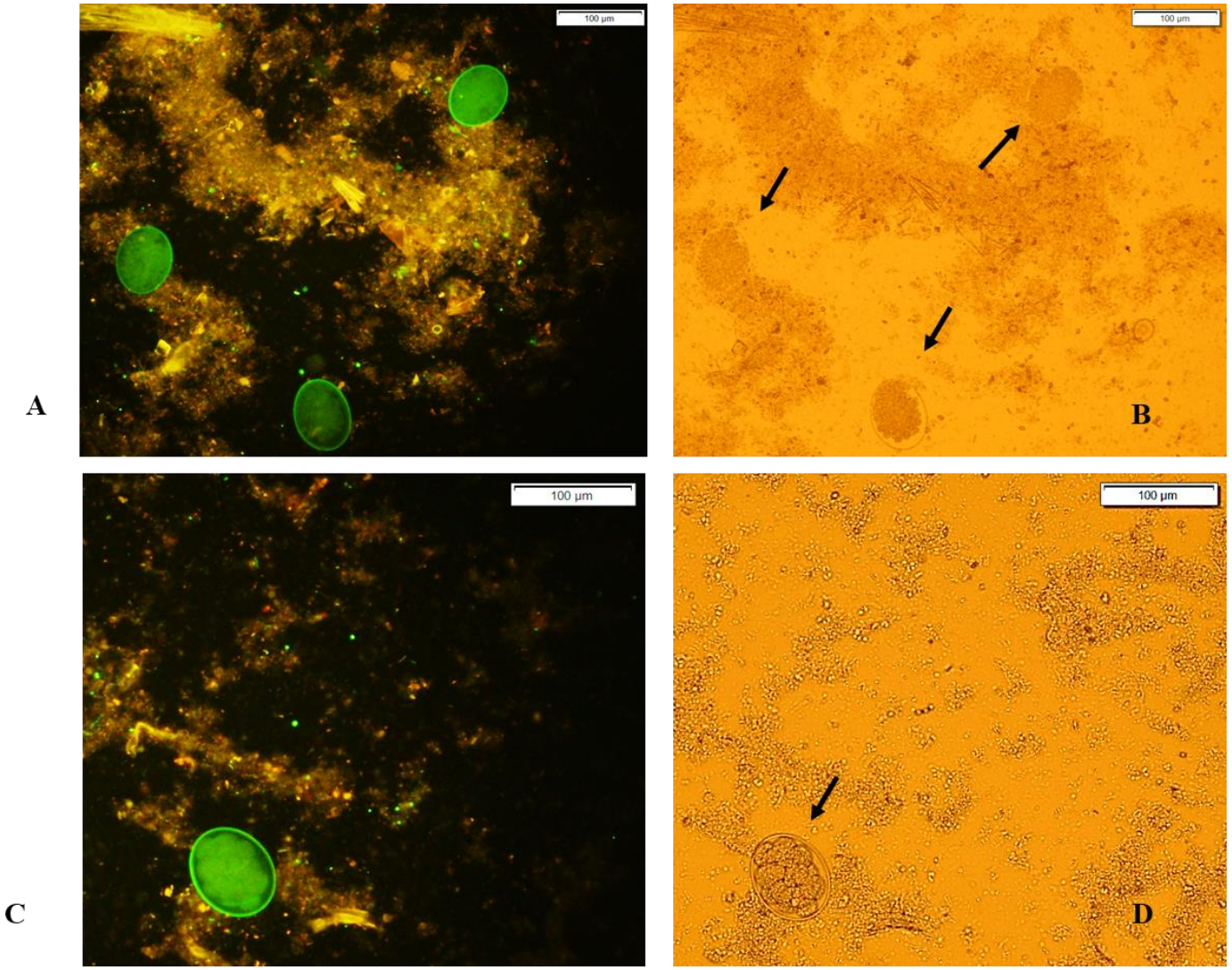

Appendix Figure 4:
A magnified image from Figure 13 showing the PNA staining of *H. contortus* egg.

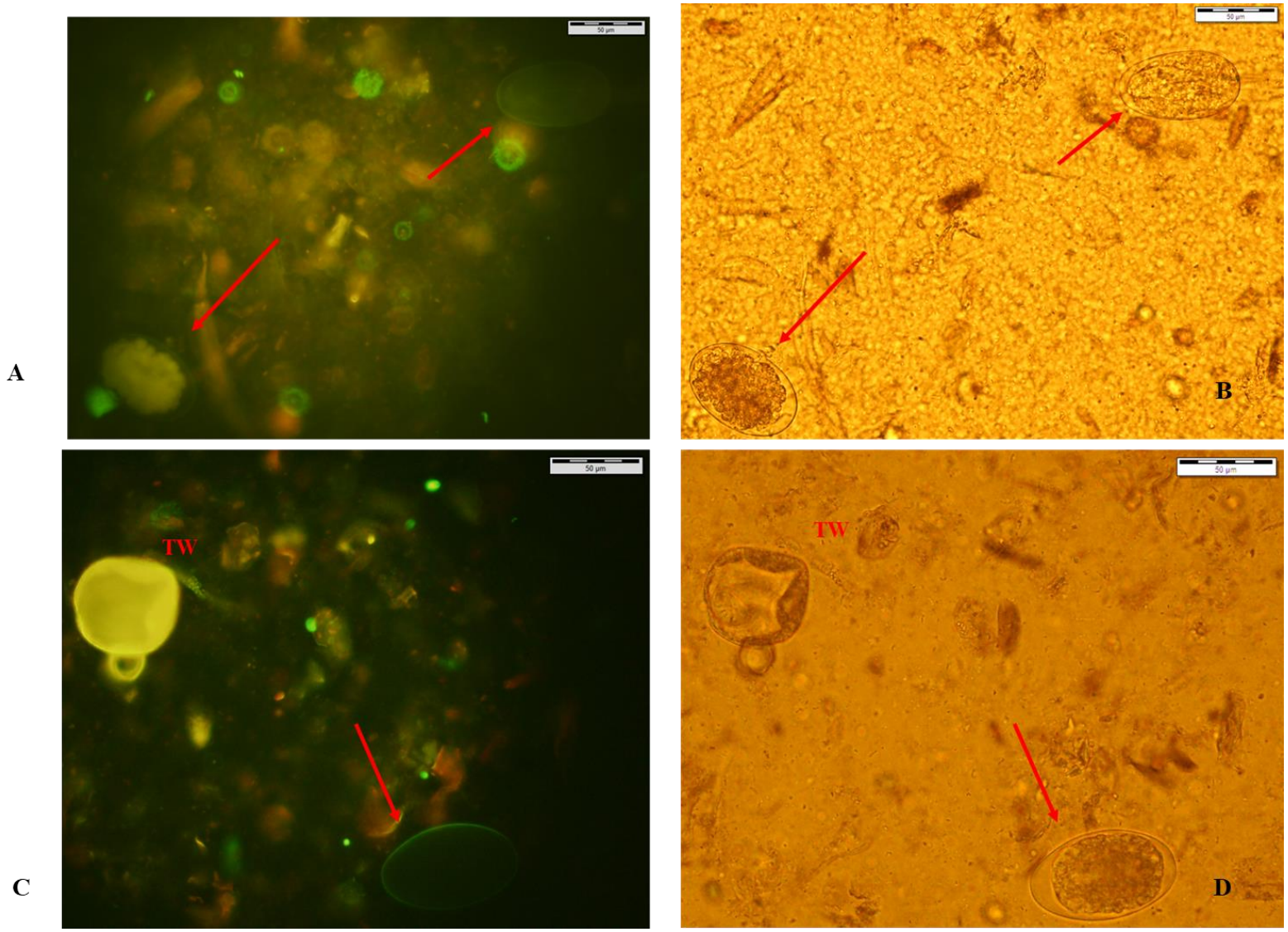

Appendix Figure 5:
A magnified image from Figure 14, showing the different PNA staining behaviours of parasite eggs.

Appendix Table 1:

Average egg counts of PNA fluorescence microscopy following JURASEK et al., (2010)

Farm ID	Avg FEC harvested egg	Stained Egg	Unstained Or Partially stained	Percentage of *H. contortus* eggs
F-1	420	241	179	57.3%
F-2	75	53	22	70.6%
F-3	157	103	54	65.6%
F-4	892	554	338	62.1%
F-5	1583	780	803	49.2%
F-6	3	0	0	0.0%
F-7	56	36	20	64.2%
F-8	530	109	421	20.5%
F-9	157	58	99	36.9%
F-10	139	110	29	79.1%
F-11	680	483	197	71.0%
F-12	604	428	176	70.8%
F-13	102	9	83	18.62%
F-14	57	0	15	0.0%

Appendix Table 2:

Meteorological data of F-1 to F-9 collected during the 2019 winter-spring season. NA: not available.

Farm ID and its corresponding Met Station		2019 (Winter-Spring)		
		Avg. Temp (°C)	Cumulative Rainfall (mm)	Avg. RH (%)
F-1	Szerep	5.9	209	68.8
F-2	Eger	6.1	230	64.3
F-3	Békéscsaba	6.1	220	69.8
F-4	Szerep	5.9	209	68.8
F-5	Felcsút	5.8	254	72.2
F-6	Csenger	5.7	244	68.3
F-7	Tarcal	6.2	248	NA*
F-8	Poroszló	5.6	227	67.3
F-9	Körös-ladány	6.2	231	71.5